

2  
m-1

X-621-73-33

PREPRINT

NASA TM X-66194

**VERTICAL DISTRIBUTION  
OF VIBRATIONAL ENERGY  
OF MOLECULAR NITROGEN IN A STABLE  
AURORAL RED ARC AND ITS EFFECT  
ON IONOSPHERIC ELECTRON DENSITIES**

**GEORGE P. NEWTON**

(NASA-TM-X-66194) VERTICAL DISTRIBUTION  
OF VIBRATIONAL ENERGY OF MOLECULAR  
NITROGEN IN A STABLE AURORAL RED ARC AND  
ITS EFFECT ON IONOSPHERIC ELECTRON (NASA)  
161 p HC \$10.25

N73-18390

CSCI 04A

G3/13

Unclas  
63935

JANUARY 1973

**GSFC**

**GODDARD SPACE FLIGHT CENTER**

**GREENBELT, MARYLAND**

THE CATHOLIC UNIVERSITY OF AMERICA

Vertical Distribution of Vibrational Energy of  
Molecular Nitrogen in a Stable Auroral Red Arc  
and its Effect on Ionospheric Electron Densities

A Dissertation Submitted to  
The Faculty of The Graduate School of Arts and Sciences  
of The Catholic University of America  
In Partial Fulfillment of the Requirements  
For the Degree  
Doctor of Philosophy

by

George P. Newton

Washington, D. C.

1972

i

This dissertation was approved by Paul H. E. Meyer

as director and by Robert L. Hannon and

Tomoyasu Tanaka as readers.

## ACKNOWLEDGEMENTS

I want to gratefully acknowledge the guidance and help received from Professor J. C. G. Walker of Yale University, during the formulation and solution of this problem. I also acknowledge and thank Professors P. H. E. Meijer and T. Tanaka of Catholic University for their guidance and the many informative and heuristic discussions concerning this problem.

VERTICAL DISTRIBUTION OF VIBRATIONAL ENERGY OF  
MOLECULAR NITROGEN IN A STABLE AURORAL RED ARC  
AND ITS EFFECT ON IONOSPHERIC ELECTRON DENSITIES

by

George P. Newton

ABSTRACT

Previous solutions of the problem of the distribution of vibrationally excited molecular nitrogen in the thermosphere have either assumed a Boltzmann distribution and considered diffusion as one of the loss processes or solved for the energy level populations and neglected diffusion. This work combines both of the previous approaches by solving the time dependent continuity equations, including the diffusion process, for the first six energy levels of molecular nitrogen for conditions in the thermosphere corresponding to a stable auroral red arc. The primary source of molecular nitrogen excitation was subexcitation, inelastic, collisions between thermal electrons and molecular nitrogen. The reaction rates for this process were calculated from published cross section calculations. The loss processes for vibrational energy were electron and atomic oxygen quenching and vibrational energy exchange. The coupled sets of non-linear, partial differential equations were solved numerically by employing finite difference equations. The results show that molecular nitrogen is excited vibrationally to the degree that the rate constant for the rate limiting ionospheric loss process  $O^+ + N_2 \rightarrow NO^+ + N$  is increased by as much as a factor of eight at  $F_2$  region altitudes. It was found that deviations from a Boltzmann distribution caused the reaction rate constant to be as much as 1.7 times the reaction rate constant calculated for the energetically equivalent Boltzmann distributed densities.

The time constant for loss of ionospheric electrons was calculated using the enhanced reaction rates. It was found that, for altitudes where the normal loss time constant is less than one day, the loss time constant was decreased in the arc by factors of 1.6 to 5 depending, on altitude. It is concluded that the observed decrease of electron density in the  $F_2$  region in stable auroral red arcs can be explained by enhanced reaction rates for ion-atom interchange between  $O^+$  and  $N_2$  caused by vibrational excitation of molecular nitrogen through electronic collisions.

# TABLE OF CONTENTS

	<u>Page</u>
Chapter 1. Introduction . . . . .	1
1.1 Description of stable auroral red arcs . . . . .	1
1.2 Cause of SAR-Arcs . . . . .	1
1.3 Ionospheric behavior in a SAR-arc . . . . .	2
1.4 Objective of this work . . . . .	3
Chapter 2. Formulation of the Problem . . . . .	8
2.1 Previous calculations of the distribution of vibrationally excited nitrogen . . . . .	8
2.2 Differences between this and previous works . . . . .	10
2.3 The equations of continuity . . . . .	10
2.4 The coefficients in the equations of continuity . . . . .	15
2.5 Boundary conditions . . . . .	19
2.6 Simplification of equations and technique of solution . . . . .	20
2.7 Finite difference equations and solutions . . . . .	25
Chapter 3. Application to SAR-Arc . . . . .	30
3.1 Solution for the Boltzmann part . . . . .	32
3.2 Solutions for the deviation parts . . . . .	34
3.3 Reaction rate constant for reaction (1-1) and ionospheric loss time constant . . . . .	37
3.4 The effects of: neglect of $\epsilon_j/n$ ; boundary conditions; and atomic oxygen loss process . . . . .	58

# TABLE OF CONTENTS--(continued)

	<u>Page</u>
Chapter 4. Summary and Conclusions . . . . .	61
References . . . . .	64

## LIST OF TABLES

Table 1. Chen cross sections used for this work . . . . .	68
Table 2. Parameters for reaction rate constants for production and loss of vibrational excitation by electron collisions . . . . .	69
Table 3. Reaction rates for vibrational levels . . . . .	70

## LIST OF ILLUSTRATIONS

Figure 1-1. Observed ionospheric electron densities and observed and calculated electron temperatures for a 500 R SAR-arc . . .	4
Figure 1-2. Model neutral atmosphere and ionospheric electron densities . . . . .	5
Figure 1-3. Neutral atmosphere kinetic and electron temperature models . . . . .	6
Figure 2-1. Rates of production and loss of vibrational energy and diffusion . . . . .	29
Figure 3-1. Comparison of $\sum_{i=0} i \epsilon_i$ and the number density of vibra- tional quanta . . . . .	31
Figure 3-2. $\sum_{i=0} \epsilon_i / \epsilon_i$ for energy levels 0 through 5 . . . . .	33
Figure 3-3. Vibrational temperatures calculated from the $\psi$ equation solutions versus altitude for five time steps . . . . .	35



# TABLE OF CONTENTS--(continued)

	<u>Page</u>
Figure 3-4. Vibrational temperatures calculated from the $\psi$ equation versus time for several altitudes . . . . .	36
Figure 3-5. $ \phi_0 $ versus altitude for 3 time steps . . . . .	38
Figure 3-6. $ \phi_1 $ versus altitude for 3 time steps . . . . .	39
Figure 3-7. $ \phi_2 $ versus altitude for 3 time steps . . . . .	40
Figure 3-8. $ \phi_3 $ versus altitude for 3 time steps . . . . .	41
Figure 3-9. $\phi_4$ versus altitude for 3 time steps . . . . .	42
Figure 3-10. $\phi_5$ versus altitude for 3 time steps . . . . .	43
Figure 3-11. $ \phi_0 $ versus time for several altitudes . . . . .	44
Figure 3-12. $ \phi_1 $ versus time for several altitudes . . . . .	45
Figure 3-13. $ \phi_2 $ versus time for several altitudes . . . . .	46
Figure 3-14. $ \phi_3 $ versus time for several altitudes . . . . .	47
Figure 3-15. $\phi_4$ versus time for several altitudes . . . . .	48
Figure 3-16. $\phi_5$ versus time for several altitudes . . . . .	49
Figure 3-17. Ratio of the effective to the energetically equivalent reac- tion constant, $k_e/k_B$ , versus time for several altitudes . . .	50
Figure 3-18. Ratio of the effective to the energetically equivalent reac- tion constant, $k_e/k_B$ , versus altitude for five time steps . .	52
Figure 3-19. Effective reaction rate constant versus time for several altitudes . . . . .	53
Figure 3-20. Effective reaction rate constant versus altitude for five time steps . . . . .	54

# TABLE OF CONTENTS—(continued)

	<u>Page</u>
Figure 3-21. Ionospheric loss time constant versus altitude for four time steps . . . . .	56
Figure 3-22. Ionospheric loss time constant versus time for altitudes where the time constant is 24 hours or less . . . . .	57
Figure A1-1. Reaction rate constant calculated from $\sigma_{10}$ . . . . .	90
Figure A1-2. Reaction rate constant calculated from $\sigma_{20}$ . . . . .	91
Figure A1-3. Reaction rate constant calculated from $\sigma_{03}$ . . . . .	92
Figure A1-4. Reaction rate constant calculated from $\sigma_{04}$ . . . . .	93
Figure A1-5. Reaction rate constant calculated from $\sigma_{50}$ . . . . .	94
Figure A1-6. Reaction rate constant calculated from $\sigma_{12}$ . . . . .	95
Figure A1-7. Reaction rate constant calculated from $\sigma_{13}$ . . . . .	96
Figure A1-8. Reaction rate constant calculated from $\sigma_{14}$ . . . . .	97
Figure A1-9. Reaction rate constant calculated from $\sigma_{51}$ . . . . .	98
Figure A1-10. Reaction rate constant calculated from $\sigma_{23}$ . . . . .	99
Figure A1-11. Reaction rate constant calculated from $\sigma_{24}$ . . . . .	100
Figure A1-12. Reaction rate constant calculated from $\sigma_{52}$ . . . . .	101
Figure A1-13. Reaction rate constant calculated from $\sigma_{34}$ . . . . .	102
Figure A1-14. Reaction rate constant calculated from $\sigma_{53}$ . . . . .	103
Figure A1-15. Reaction rate constant calculated from $\sigma_{54}$ . . . . .	104

TABLE OF CONTENTS—(continued)

LIST OF APPENDICES

	<u>Page</u>
Appendix I. Electronic production and loss of vibrational exciation . . .	71
Appendix II. Simplification of the continuity equations . . . . .	106
Appendix III. Construction of finite difference equations . . . . .	123
Appendix IV. Computer program listings . . . . .	128

## CHAPTER I. INTRODUCTION

### 1.1 Description of Stable Auroral Red Arcs

Stable Auroral Red Arcs (SAR-Arcs) are photometrically observed enhancements of air-glow at  $6300 \text{ \AA}$  and  $6364 \text{ \AA}$  wavelengths occurring during geomagnetically active times. They were first observed by Barbier (1) in 1957. The emissions are from the forbidden red lines of atomic oxygen OI ( $^1D-^3P$ ). Peak intensities of emissions are located at altitudes near 400 km. and vary from a few hundred rayleighs<sup>1</sup> to tens of kilorayleighs. The arcs generally occur near midlatitudes and are distinct in location from usual auroral phenomena. They extend over spatial dimensions of approximately 1000 km. horizontally in a meridional direction and globally in a longitudinal direction. The arcs are magnetically controlled as evidenced by their alignment in geomagnetic, rather than geographic latitude, and by their simultaneous occurrence at magnetically conjugate points. Once the SAR-arc is formed it generally persists for ten hours or longer. The frequency of observation appears to follow the solar cycle. Reviews of the general properties of SAR-arcs and citations to the literature are contained in Reference (2) and more recently Reference (3).

### 1.2 Cause of SAR-Arcs

The absence of the atomic oxygen green line OI ( $^1S-^1D$ ) in the air glow enhancements during SAR-arcs, implies that a low energy source must exist for the excitation of the OI( $^1D$ ) state. Several mechanisms have been proposed for selectively exciting  $^1D$  level and their implications studied (see (3) for summary)

---

<sup>1</sup> a rayleigh is  $10^6 \text{ photons cm}^{-2} \text{ sec}^{-1}$

but one proposal has recently gained prominence. In this proposal (4) energy originating in the solar wind is transferred through the ring current in the magnetosphere to the ambient plasma, from which it is conducted down magnetic field lines into the ionosphere where it heats ambient electrons. These heated electrons collisionally excite the atomic oxygen  $^1D$  level, but lack sufficient energy to excite the  $^1S$  level. This proposal was utilized together with in-situ measurements of electron temperatures and densities by Roble et al. (5), (6) who found it to be consistent with all observations. Other proposals have been excluded by in-situ measurements (see (3) for discussion of the proposals and (7), (8) for observations).

### 1.3 Ionospheric Behavior in a SAR-ARC

From ground based (see (3) for review) and more importantly from satellite obtained data (9), (6), (7), (8), the following behavior of the ionosphere in the vicinity of SAR-arc has been determined.

At the satellites where the electron temperatures, and in some instances the ion temperatures, were measured a general enhancement of the charged particle temperatures was observed on the geomagnetic field lines intersecting the SAR-arcs. The electron densities at these satellite attitudes (usually greater than 1000 km.) showed for different SAR-arc occurrences both increases, decreases and no change in the electron densities, apparently depending on the altitude of measurement. However, corresponding topside sounder data always showed electron density depressions in the lower  $F_2$  regions (near 300-800 km altitude) in the corresponding region of enhanced electron temperature. The electron density scale heights often are less in the red arc region, reflecting changes in the ion composition (7), (6). The more complex electron density behavior at the

higher altitudes (1000 km and greater) may in part be explained by a combination of the ion composition changes and the increased plasma temperature. A typical observation of the electron density and temperature in the vicinity of a SAR-arc is shown in Figure 1-1.

#### 1.4 Objective of this work

One of the primary loss processes for ionization in the  $F_2$  region, where atomic oxygen ions are the dominate ion species, is



followed by



where  $k$  and  $\alpha$  are the ion-atom interchange and dissociative recombination reaction rates, respectively. Typically  $\alpha$  is about four orders of magnitude greater than  $k$ , (11), so that the rate determining process for ionization loss is reaction (1-1). However,  $k$  in reaction (1-1) is known to be a strong function of the vibrational temperature of molecular nitrogen (12), (13). This is why knowledge of the energy distribution of the excited levels plays a crucial role in the understanding of the electron loss rates in the SAR-arc. Thus, as suggested earlier, (12), the loss of ionospheric ionization may be considerably enhanced by the presence of vibrationally excited nitrogen. The source of the vibrationally excited nitrogen molecules is sub-excitation,<sup>2</sup> inelastic, collisions between the

---

<sup>2</sup>Subexcitation means that the final state of the  $N_2$  is neither electronically excited nor ionized.

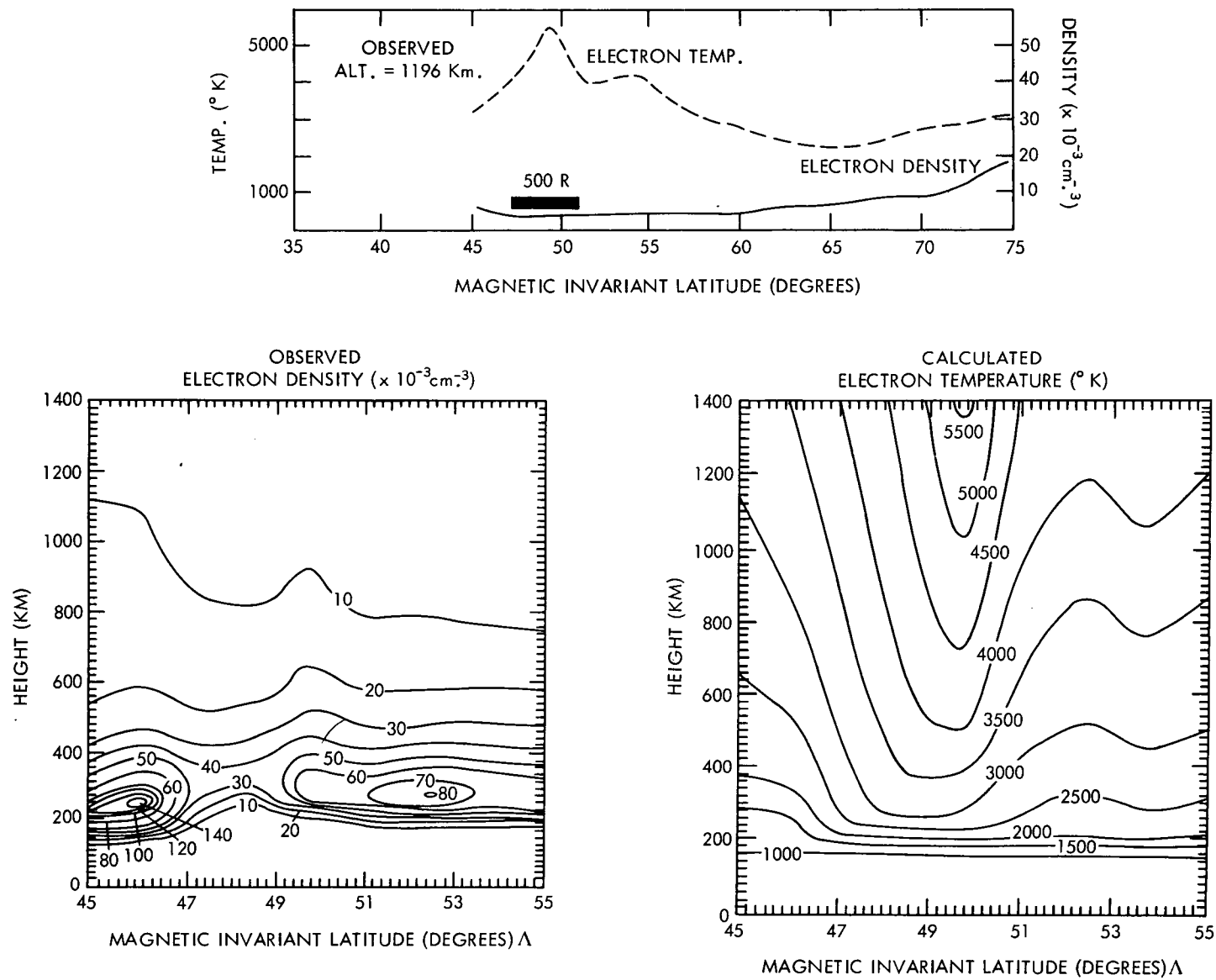


Figure 1-1. Observed ionospheric electron densities and observed and calculated electron temperatures for a 500 R SAR-arc

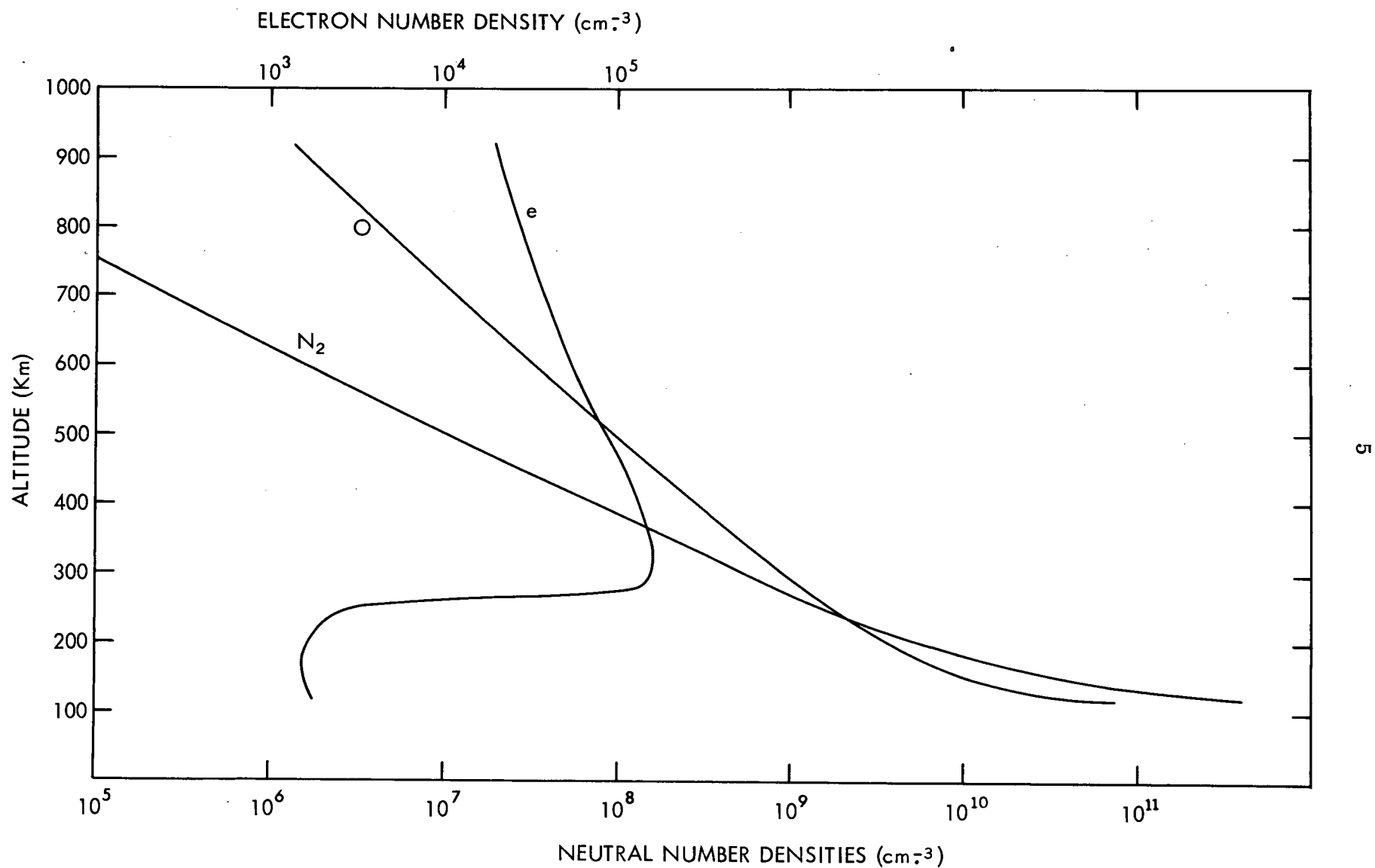


Figure 1-2. Model neutral atmosphere and ionospheric electron densities



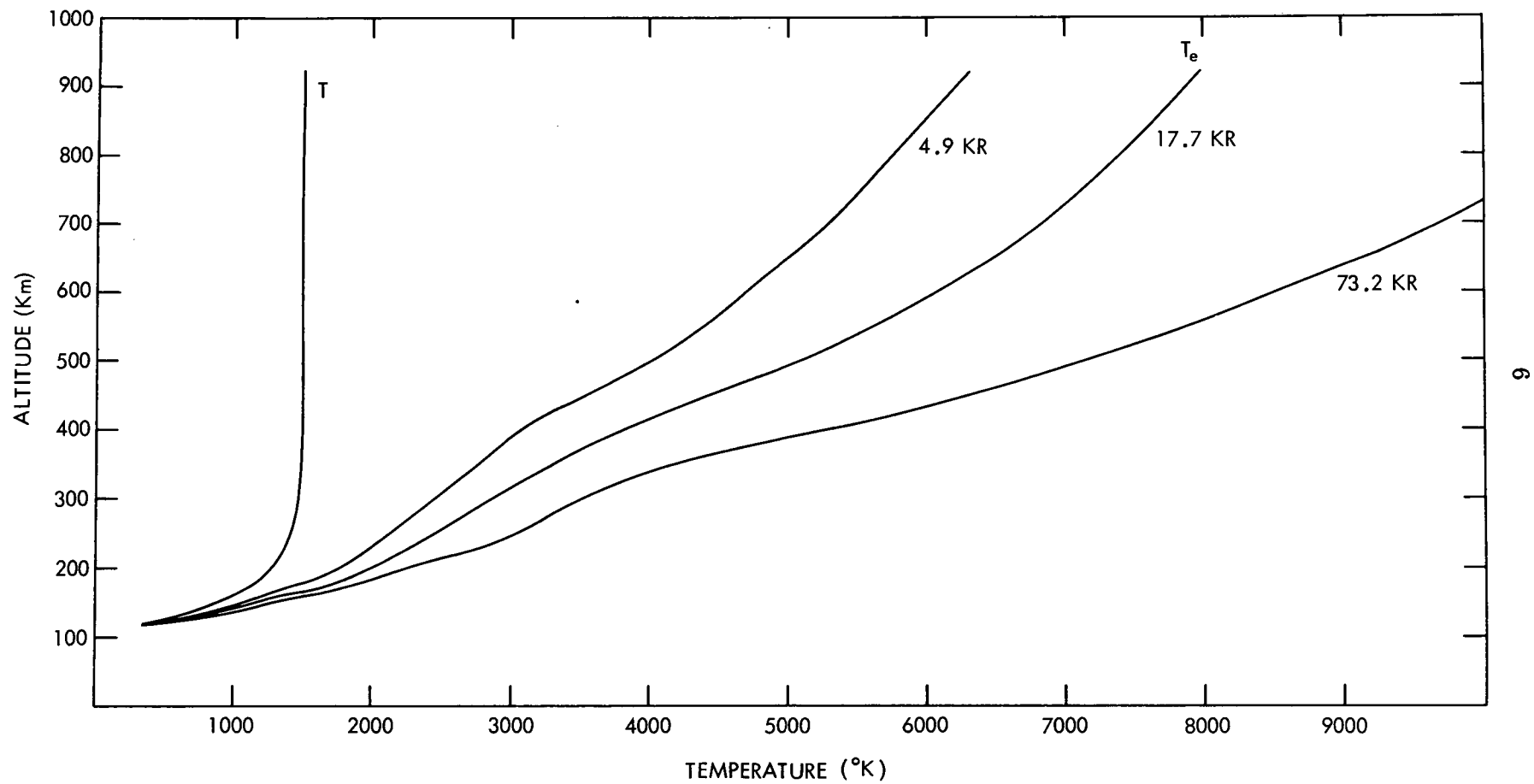


Figure 1-3. Neutral atmosphere kinetic and electron temperature models

ambient molecular nitrogen and the thermal ionospheric electrons, the same mechanism that excites the  $\text{OI}(^1\text{D})$ . The cross section for this type of process is important to this study (Appendix I).

The objective of this work is to investigate the distribution of vibrationally excited molecular nitrogen under conditions corresponding to a SAR-ARC to determine if the presence of vibrationally excited nitrogen can account for the observed decrease in the electron density in the  $\text{F}_2$  region. For this study we used the same electron density profiles that Roble (10) used to calculate the temperature profiles for SAR-arcs, and we used his calculated electron temperatures. The electron density profile and model atmosphere used for this work are shown in Figure 1-2. The neutral atmospheric model used for this work is the 1965 Jacchia model (14) with an exospheric temperature of  $1500^\circ\text{K}$ . We did not include minor constituents. The neutral atmosphere temperature profile is shown in Figure 1-3, together with several of Roble's, (10), electron temperature profiles corresponding to different SAR-ARC intensities.

## 2.1 Previous Calculations of the Distribution of Vibrationally Excited Nitrogen

Several authors have suggested that vibrationally excited nitrogen may influence the excitation of atmospheric radiations, chemical reactions, and the ionospheric temperature (15), (16), (17), (18), (12), (19). Walker et. al. (20) were the first to calculate the altitudinal distribution and diurnal variation of the vibrating molecules assuming a Boltzmann distribution. The diurnal calculations assumed an unperturbed atmosphere and ionosphere. They considered diffusion of the vibrationally excited nitrogen vertically and limited their calculation to altitudes between 100 km and 300 km altitude. They found that vibrational energy exchange with  $\text{CO}_2$  was the dominant loss process for vibrational quanta below 125 km altitude. The principal sources of vibrational quanta in the lower thermosphere (100 km and 600 km) were found to be: (1) the reaction between atomic nitrogen and nitric oxide; (2) the collisions of photoelectrons and nitrogen molecules; and (3) possibly the quenching of metastable oxygen atoms,  $\text{OI} (^1\text{D})$ , by nitrogen, although the vibrational yield of the last process is unknown.

Recently, McNeal, et. al. (21) measured the reaction rate for vibrational-translation energy exchange between atomic oxygen and vibrationally excited molecular nitrogen at 300°K and found the rate to be considerably larger than extrapolated values (which were used by Walker et. al. (20).) obtained from experiments at higher temperatures. The quenching of vibrationally excited molecular nitrogen by atomic oxygen, which was ignored in the calculations of Walker et. al. (20), has been included in the calculations of Breig, et. al (22) who used the recently determined reaction rate. They essentially repeated the calculations

of Walker, et. al. (19) and found that inclusion of the loss of vibrational excitation by nitrogen molecules to atomic oxygen significantly decreased (by factors of 2 to 4) the vibrational temperatures in the lower thermosphere.

Schunk and Hays (23) solved the continuity equations for the first eleven energy levels of molecular nitrogen for altitudes above 150 km. under conditions corresponding to an aurora. Diffusion processes were not included in their calculations. The source of vibrational excitation was non-thermal electrons and the only loss process included for each level was vibrational energy exchange between nitrogen molecules. They found that when the non-thermal electron source was acting, the  $N_2$  vibrational distribution was non-Boltzmann and that the deviation from the Boltzmann distribution increased with increasing altitude. They found that the loss rate for  $O^+$  due to reaction (1-1) was increased by a factor of 1.5 when allowance was made for the non-Boltzmann distribution. The non-thermal electron source was allowed to operate for 15 min. and they found that the enhanced loss rate persisted for 1000-2000 sec. after the auroral bombardment commenced.

Walker (24) discussed the result of Schunk and Hays (23) and included in his discussion the effects of diffusion. He starts with the steady state continuity equation for each level and ignores quenching processes for the vibrationally excited nitrogen molecules. Under these conditions, the source of vibrational excitation and diffusion are the only terms which can cause departures from a Boltzmann distribution. By comparing the production term for a given vibrational level with the production at that level due to vibrational exchange, he concluded that departures for vibrational levels containing a significant fraction of the nitrogen molecules will not exist at altitudes below 300 km. By comparing the diffusive

flux term with the loss due to vibrational energy exchange he concludes that diffusion is less important than vibrational energy exchange at altitudes below 370 km. These conclusions were based on conditions of an undisturbed atmosphere and source terms similar to those used by Walker, et al. (20).

## 2.2 Differences between this and previous works.

The source of vibrational excitation for this work is the thermal electrons in SAR-arcs. This source extends to higher altitudes than the sources used by Walker, et. al. (20), Breig et. al., (22) and Schunk and Hays (23). As a result, the molecular excitation occurs in a region of the thermosphere where vibrational energy exchange is slow in comparison with the diffusion process. Thus, because the source is non-Boltzmann in its energy distribution and because the excited molecules diffuse to lower altitudes where vibrational energy exchange is the dominant process, the assumptions of a Boltzmann distribution and negligible diffusion loss are no longer tenable. This work differs from that of Walker, et. al., (20) and Breig, et. al. (22), by not assuming a Boltzmann distribution, and from that of Schunk and Hays (23) by including diffusion of the excited molecules.

## 2.3 The equations of continuity.

The continuity equation for each energy level of vibrationally excited molecular nitrogen,  $N_2^*$ , governs the level population and its altitudinal distribution. For the  $i$ th level the equation is

$$\frac{\partial}{\partial t} n_i + \nabla \cdot (n_i \vec{v}_i) = Q_i - L_i \quad (2-1)$$

where  $n_i$  is the number density of molecular nitrogen in energy level  $i$

$\vec{v}_i$  is the vector velocity of transport of  $n_i$

$Q_i$  is the production rate of  $n_i$

$L_i$  is the loss rate of  $n_i$ .

In principal the production and loss rate terms contain all sources and sinks for the  $i$ th level. However, we are interested in solutions of (2-1) corresponding to SAR-arc conditions where the electron temperature is unusually large. In addition we are interested in a process which, to first order, can be considered as an additional source to those ordinarily present in the thermosphere.

Figure 2-1 shows the rates of the dominant processes for equation (2-1). Also included in Figure 2-1, for comparison purposes, are the total vibrational quanta production rates between 120 and 300 km. calculated from the work of Walker et. al. (20) and Kummeler and Bortner (25) and shown as squares and circles, respectively. Shown as triangles in Figure 2-1 are the  $\text{CO}_2$  quenching rates for vibrationally excited nitrogen at 120 km. taken from references (20), (22) and (25).

The atomic oxygen quenching curve shown in Figure 2-1 was calculated using the reaction rate of  $3.5 \times 10^{-15} \text{ cm}^3 \text{ sec}^{-1}$ , (21), and the atomic oxygen number density shown in Figure 1-2. The curve of atomic oxygen production of  $\text{N}_2^*$  (translational-vibrational energy exchange process) was calculated from the quenching curve using detailed balance considerations. These curves correspond to  $1 \rightarrow 0$  and  $0 \rightarrow 1$  transitions of  $\text{N}_2$  respectively.

The vibrational energy exchange curve was calculated for the  $0 \rightarrow 1$ ,  $1 \rightarrow 0$  transitions using the exact resonance case of the Schwartz-Slawsky-Herzfeld,

(SSH), theory, (27) page 330, and the molecular nitrogen number density profile of Figure 1-2.

The rate for diffusion was calculated from the diffusion coefficient,  $D$ , and the density scale height,  $H$ , for molecular nitrogen by

$$\text{rate} = \frac{D}{H^2} \quad (2-2)$$

This rate may be regarded as the inverse of the time for a nitrogen molecule to diffuse to an altitude where there is an appreciably greater density (by a factor of  $e$ ) of molecular nitrogen.

The electronic production curve was calculated using the reaction rates for inelastic collisions between thermal electrons and molecular nitrogen discussed in Appendix I and the electron and molecular nitrogen densities and electron temperatures in Figures 1-2 and 1-3, respectively. The electron temperature used is that for a 17.7 KR SAR-arc. For the calculation it was assumed that the vibrational temperature was zero.

From Figure 2-1 it is seen that the source of vibrational energy from thermal electrons, under the SAR-ARC condition, is larger over most of the altitude range of interest than the source of vibrational energy from ordinary ionospheric processes (20), (25). Because of the uncertainty in the yield of vibrational energy from  $O(^1D)$  quenching by molecular nitrogen (20), (25), and because the  $O(^1D)$  density during SAR-arcs is enhanced and its spatial distribution is complex, we have ignored this potential source term. Thus, the source term,  $Q_1$ , in equation (2-1) will only include production of vibrationally excited nitrogen by collisions between nitrogen molecules and thermal electrons (and only

coincidentally by atomic oxygen) and vibrational energy exchange between nitrogen molecules. These approximations should underestimate the source terms and hence the calculated temperatures would tend to be a lower bound for this reason.

The dominant loss processes for vibrationally excited molecular nitrogen at higher altitudes is electron quenching at altitudes above 400 km. (20, 25), and diffusion above 320 km. (see Figure 2-1). At low altitudes the dominant loss processes are quenching by atomic oxygen for altitudes between 120 and 300 km (Walker et. al., (20), found that quenching by other minor constituents in the lower thermosphere through translational-vibration energy exchange was negligible) and vibrational energy exchange with  $\text{CO}_2$  (20), (22), at 120 km. Thus, the loss term,  $L_i$ , in equation (2-1) will include loss by electron and atomic oxygen quenching and vibrational energy exchange with molecular nitrogen. The vibrational energy loss by molecular nitrogen to carbon dioxide will be included through a lower boundary condition on the vibrational temperature for the following reasons. The abundance of carbon dioxide at 120 km is somewhat uncertain and depends on the altitude of the turbopause. The turbopause of the atmosphere is below 120 km altitude. Thus, in the altitude region of interest, carbon dioxide could be expected to approach diffusive equilibrium. Because of its relatively large mass, the density of carbon dioxide should decrease rapidly above 120 km. and increase rapidly below 120 km. altitude, thus creating a loss process significant only at the lower boundary.



The source and loss terms for equation (2-1) are therefore given by

$$\begin{aligned}
 Q_i = & \sum_{j=0}^{\prime} A_{ij} n_j + \sum_{j=0} P_{i,j;i-1,j+1} \nu_{j+1,i-1} n_{j+1} \\
 & + \sum_{j=1} P_{i,j;i+1,j-1} \nu_{j-1,i+1} n_{j-1} + C_{i,i-1} \nu_{i-1,[0]} n_{i-1} \\
 & + C_{i,i+1} \nu_{i+1,[0]} n_{i+1}
 \end{aligned} \tag{2-3}$$

$$\begin{aligned}
 L_i = & \sum_{j=0}^{\prime} A_{ji} n_i + \sum_{j=0} P_{i-1,j+1:i,j} \nu_{ij} n_i \\
 & + \sum_{j=1} P_{i+1,j-1:i,j} \nu_{ij} n_i \\
 & + C_{i-1,i} \nu_{i,[0]} + C_{i+1,i} \nu_{i,[0]} n_i
 \end{aligned} \tag{2-4}$$

where a prime on the summation excludes  $j = i$ , and

$P_{i,j;i-1,j+1}$  is the exchange transition probability for a nitrogen molecule in level  $i - 1$  going to level  $i$  while the collisional partner molecule goes from level  $j + 1$  to level  $j$ .

$\nu_{i,j}$  is the collision frequency of a nitrogen molecule in level  $j$  with a molecule in level  $i$ .

$C_{i,j}$  is the probability for collisional transitions from level  $j$  to level  $i$  where the collision is with atomic oxygen atoms.

$A_{ij}$  is the reaction rate, from Appendix I, for the transition from level  $j$  to level  $i$  due to collisions between thermal electrons and molecular nitrogen molecules in level  $j$ .

$\nu_{i,[0]}$  is the collision frequency of a molecule in level  $i$  with an atomic oxygen atom.

#### 2.4 The coefficients in the equations of continuity.

The cross sections for the subexcitation, inelastic, scattering of electrons by molecular nitrogen (28), (29), (30) are only available for the first five energy levels. These cross-section calculations and the calculation of reaction rates from the cross-sections are discussed in Appendix 1.

We will assume that molecular nitrogen can be represented by a harmonic oscillator. Thus, only transitions between adjacent levels will be considered. This assumption is appropriate for the moderate vibrational temperatures of this problem where only the lower lying energy levels are important and where anharmonic effects are small (31), (32), (33). It is also implicit to this calculation that the first five excited levels of molecular nitrogen will be considered as the totality of excited levels.

The above assumption and the theory for exact resonance vibrational-vibrational energy exchange of SSH, (27), allow us to write the vibrational-vibrational energy exchange probability in terms of the  $0 \rightarrow 1$ ,  $1 \rightarrow 0$  transitions of molecular nitrogen as

$$P_{i,j:i-1,j+1} = i(j+1) P_{1,0:0,1} \quad (2-5)$$

From detailed balance considerations

$$P_{i-1,j+1:i,j} = P_{i,j:i-1,j+1} \quad (2-6)$$

Setting the steric factor in the SSH theory to three, and using the Lennard-Jones potential parameters for  $N_2$  from table 66-1 of (27), and table 66-5 of (27) for the characteristic  $\ell$  of the theory, we have

$$P_{i,j:i-1,j+1} = 2.600322 \times 10^{-6} i(j+1) T e^{91.5/T} \quad (2-7)$$

where  $T$  is the kinetic gas temperature.

It is assumed that

$$C_{i+1,i} = (i+1) C_{1,0} \quad (2-8)$$

for the translational-vibrational energy exchange probability, the reason will become apparent later. Thus, (2-8) is consistent with SSH theory,<sup>3</sup> but  $C_{1,0}$  will not be determined from this theory (see reference (21)). Detailed balance gives

$$C_{i,i-1} = C_{i-1,i} e^{-\theta/T} \quad (2-9)$$

where  $\theta$  is the characteristic temperature of  $N_2$  ( $\theta = 3380^\circ K$ ).

We assume that the vibrational level in which the nitrogen molecule resides does not effect its collision cross section for both molecules and atoms. Thus we write

$$\nu_{ji} = \nu n_i \quad (2-10)$$

$$\nu_{i,[0]} = \nu' n[0], \quad (2-11)$$

Equations (2-3) and (2-4) become respectively

$$Q_i = \sum_{j=0} A_{ij} n_j + P_{1,0:0,1} \nu \sum_{j=0} i(j+1) n_{i-1} n_{j+1} + P_{1,0:0,1} \nu \sum_{j=1} j(i+1) n_{i+1} n_{j-1} + C_{1,0} \nu' n[0] [i n_{i-1} + (i+1) e^{\theta/T} n_{i+1}] \quad (2-12)$$

---

<sup>3</sup> The measured reaction rate for  $C_{0,1}$  is several orders of magnitude larger than would be calculated using SSH theory. The reason for the discrepancy may be that chemical interactions are responsible for the anomalous quenching, whereas SSH theory attributes the interaction as being due to short range repulsive potentials.

$$L_i = \sum_{j=0} A_{ji} n_i + P_{1,0:0,1} \nu \sum_{j=0} i(j+1) n_i n_j + P_{1,0:0,1} \nu \sum_{j=i} j(i+1) n_j n_i + C_{1,0} \nu' n [0] [i e^{\theta/T} + (i+1)] n_i \quad (2-13)$$

The quantity  $\nu$  in equations (2-10), (2-12) and (2-13) is calculated from equation (36-3) of reference (27)

$$\nu = \frac{1.271 p}{\eta_{N_2} n} \quad (2-14)$$

where

$p$  is the gas pressure

$N_2$  is the viscosity for molecular nitrogen

$n$  is the total number density of molecular nitrogen

Using the ideal gas law, we have

$$\nu = \frac{1.271 k T}{\eta_{N_2}} \quad (2-15)$$

where  $k$  is Boltzmann's constant. Using (8.2-18) of reference (34), and average values of the appropriate parameters for temperatures of 355°K and 1500°K, we obtain for  $\nu$

$$\nu = 1.482094 \times 10^{-11} \sqrt{T} \quad (2-16)$$

The quantity  $C_{1,0} \nu'$  occurring in equations (2-12) and (2-13) is calculated from  $C_{01} \nu'$  by equation (2-9), where  $C_{01} \nu'$  is considered to be a "lumped" constant equal to the reaction rate constant reported by McNeal, et. al., (21) and is considered constant with altitude.

It will be assumed that the neutral atmosphere is static, and uniform horizontally in all of its parameters. The transport velocity,  $\vec{v}_i$ , is then the diffusion

velocity for molecular nitrogen through the atmosphere, and is given by (35), page 244,

$$\vec{v}_i = -D \left[ \frac{1}{p_i} (\nabla p_i - \rho_i \vec{g}) + k_T \frac{1}{T} \nabla T \right] \quad (2-17)$$

where

$D$  is the binary diffusion coefficient for molecular nitrogen, assumed to be independent of vibrational excitation.

$p_i$  is the pressure of the molecular nitrogen in energy level  $i$ .

$\rho_i$  is the mass density of molecular nitrogen

$k_T$  is the thermal diffusion ratio

$\vec{g}$  is the acceleration of gravity.

Using the ideal gas law in (2-17) we have

$$\vec{v}_i = -D \left[ \frac{1}{n_i} \nabla n_i + (k_T + 1) \frac{1}{T} \nabla T + \frac{mg}{kT} \hat{k} \right] \quad (2-18)$$

where  $\hat{k}$  is a unit vector in the vertical direction

$m$  is the mass of molecular nitrogen.

Rewriting (2-18) we have

$$\vec{v}_i = -D \left[ \frac{1}{n_i} \nabla n_i + \frac{1}{H} \hat{k} \right] \quad (2-19)$$

where

$$\frac{1}{H} = (k_T + 1) \frac{1}{T} \frac{\partial T}{\partial z} + \frac{mg}{kT}, \quad (2-20)$$

and  $z$  is the vertical coordinate, positive upward and  $H$  is the density scale height.

Thermal diffusion for molecular nitrogen is small, and therefore  $k_T$  will be set to zero. The flux term in equation (2-1) becomes

$$\vec{F}_i = n_i \vec{v}_i = -D \left[ \nabla n_i + \frac{n_i}{H} \hat{k} \right] \quad (2-21)$$

It will be assumed that the magnetic field line is vertical, so that the SAR-arc is symmetrical about the vertical. Under this assumption the horizontal flux at the arc center vanishes. If, in addition, the divergence of the horizontal flux is ignored, equation (2-1) can be reduced to one spatial dimension corresponding to conditions at the arc center.

Under the above assumptions and using (2-21), (2-12) and (2-13), equation (2-1) becomes

$$\begin{aligned}
 \frac{\partial n_i}{\partial t} + \frac{\partial}{\partial z} (\vec{F}_i)_z = & \sum_{j=0} \{A_{ij} n_j - A_{ji} n_i\} + P_{1,0:0,1} \nu_i \sum_{j=0} (j+1) [n_{i-1} n_{j+1} \\
 & - n_i n_j] + P_{1,0:0,1} \nu (i+1) \sum_{j=1} j [n_{i+1} n_{j-1} - n_i n_j] \\
 & + C_{1,0} \nu' n[0] [i n_{i-1} + (i+1) e^{\theta/T} n_{i+1} \\
 & - (i e^{\theta/T} + i+1) n_i]
 \end{aligned} \tag{2-22}$$

## 2.5 Boundary conditions.

Two sets of boundary conditions will be used for equation (2-22).

For the first set we have

Initial condition:  $n_i(z, 0) = 0$  for all  $i > 0$

$$= n \text{ for } i = 0$$

Lower boundary:  $n_i(120, t) = 0$  for all  $i > 0$

$$= n(120) \text{ for } i = 0$$

Upper Boundary:

$$\left. \frac{\partial n_i}{\partial z} \right|_{z=\infty} = - \frac{n_i(\infty, t)}{H} \text{ for all } i.$$

The initial and lower boundary conditions correspond to all molecular nitrogen being in the ground state. This would correspond to total quenching by  $\text{CO}_2$  at the lower boundary, and no excitation initially. The upper boundary condition insures zero flux, for all excited levels, at the top of the atmosphere.

For the second set of boundary conditions,

$$\text{Initial Condition } n_i(z, 0) = \frac{n}{1 - e^{-\theta/355}} e^{-i\theta/355} \text{ for all } i$$

$$\text{Lower Boundary } n_i(120, t) = \frac{n}{1 - e^{-\theta/355}} e^{-i\theta/355} \text{ for all } i$$

$$\text{Upper boundary } \left. \frac{\partial n_i}{\partial z} \right|_{z=\infty} = - \frac{n_i(\infty, t)}{H} \text{ for all } i$$

The initial and lower boundary conditions in this case correspond to assuming the vibrationally excited nitrogen to be Boltzmann distributed corresponding to a vibrational temperature of 355°K, the kinetic temperature at the lower boundary.

## 2.6 Simplification of equations and technique of solution.

In Appendix II the set of six, coupled, non-linear, partial differential equations (2-22) are replaced by seven equations in which the essential coupling is more

readily observed. This simplification is achieved by expressing the solutions of equation (2-22) as a sum of a Boltzmann distributed part and a part representing a deviation from a Boltzmann distribution, that is

$$n_i = n'_i + \epsilon_i \quad (\text{A2-1})$$

It is then required that the Boltzmann distributed part,  $n'_i$ , possess the total vibrational energy and number density of molecular nitrogen for the problem (see equations (A2-2) and (A2-3)). The deviation part,  $\epsilon_i$ , is then a measure of the departure, at each altitude, of the solution from the energetically equivalent Boltzmann solution part. The differential equation to be solved for the Boltzmann part of the solution is

$$\begin{aligned} \frac{\partial \psi}{\partial t} - \frac{1}{n} \frac{\partial D n}{\partial z} \frac{\partial \psi}{\partial z} - D \frac{\partial^2 \psi}{\partial z^2} \\ = \sum_{j=0} \sum_{i=0} \left[ \frac{1}{\psi + 1} \left( \frac{\psi}{\psi + 1} \right)^j + \frac{\epsilon_j}{n} \right] (i - j) A_{ij} \\ + C_{1,0} \nu' n [0] \cdot [\psi + 1 - e^{\theta/T} \psi] \end{aligned} \quad (\text{A2-30})$$

where  $\psi$  is related to the partition function,  $Z_p$ , for the vibrationally excited nitrogen by

$$\psi = (Z_p - 1) \quad (\text{A2-27})$$

The differential equation for the deviation part of the solution is



$$\begin{aligned}
& \frac{\partial}{\partial t} \varphi_i - D \frac{\partial^2}{\partial z^2} \varphi_i - \left[ \frac{\partial D}{\partial z} + D \left( -\frac{1}{H} + 2 \left\{ \frac{i}{\psi} - \frac{i+1}{\psi+1} \right\} \frac{\partial \psi}{\partial z} \right) \right] \frac{\partial \varphi_i}{\partial z} \\
& + \left[ \left\{ \frac{i}{\psi} - \frac{i+1}{\psi+1} \right\} \frac{\partial \psi}{\partial t} - \frac{\partial \psi}{\partial z} \left\{ \frac{i}{\psi} - \frac{i+1}{\psi+1} \right\} \left\{ \frac{\partial D}{\partial z} + D \left( -\frac{1}{H} \right. \right. \right. \\
& + \left. \left. \left\{ \frac{i}{\psi} - \frac{i+1}{\psi+1} \right\} \frac{\partial \psi}{\partial z} \right) \right\} - D \left\{ \frac{i}{\psi} - \frac{i+1}{\psi+1} \right\} \frac{\partial^2 \psi}{\partial z^2} - D \left( \frac{\partial \psi}{\partial z} \right)^2 \left\{ -\frac{i}{\psi^2} \right. \right. \\
& + \left. \left. \frac{(i+1)}{(\psi+1)^2} \right\} + \sum_{j=0}^n A_{ji} (1 - \delta_{ij}) + P_{1,0:0,1} \nu n \{ (2i+1) \psi + i \} \right. \\
& + C_{1,0} \nu' n [0] (i e^{\theta/T} + i + 1) \left. \right] \varphi_i = \sum_{j=0} \left\{ A_{ij} (1 + \varphi_j) e^{-(j-1)\theta/T_v} \right\} (1 - \delta_{ij}) \\
& - \left[ \left( \frac{i}{\psi} - \frac{i+1}{\psi+1} \right) \frac{\partial \psi}{\partial t} - \frac{\partial \psi}{\partial z} \left\{ \frac{i}{\psi} - \frac{i+1}{\psi+1} \right\} \left\{ \frac{\partial D}{\partial z} + D \left\{ -\frac{1}{H} \right. \right. \right. \\
& + \left. \left. \left\{ \frac{i}{\psi} - \frac{i+1}{\psi+1} \right\} \frac{\partial \psi}{\partial z} \right\} + \sum_{j=0} A_{ji} (1 - \delta_{ij}) - D \left\{ \frac{i}{\psi} - \frac{i+1}{\psi+1} \right\} \frac{\partial^2 \psi}{\partial z^2} \right. \\
& - D \left( \frac{\partial \psi}{\partial z} \right)^2 \left\{ -\frac{i}{\psi^2} + \frac{i+1}{(\psi+1)^2} \right\} + P_{1,0:0,1} \nu n \{ (2i+1) \psi + i \} \\
& + C_{1,0} \nu' n [0] (i e^{\theta/T} + i + 1) \left. \right] + P_{1,0:0,1} \nu n \{ (2i+1) \psi + i \} \\
& + C_{1,0} \nu' n [0] \left[ i e^{\theta/T_v} + (i+1) e^{\theta/T - \theta/T_v} \right] + \varphi_{i-1} e^{\theta/T_v} \left[ P_{1,0:0,1} \nu n_i \psi \right. \\
& + C_{1,0} \nu' n [0] i \left. \right] + \varphi_{i+1} e^{-\theta/T_v} \left[ P_{1,0:0,1} \nu n(i+1) (\psi+1) \right. \\
& + C_{1,0} \nu' n [0] e^{\theta/T} (i+1) \left. \right]
\end{aligned}$$

where

$$\varphi_i = \frac{\epsilon_i}{n'_i} \quad (\text{A2-39})$$

The boundary conditions are

set 1:

Initial condition  $\psi(z, 0) = 0$

Lower boundary  $\psi(120, t) = 0$

Upper boundary  $\left. \frac{\partial \psi}{\partial z} \right|_{z=\infty} = 0 \quad (\text{A2-31})$

set 2:

Initial condition  $\psi(z, 0) = 7.329241 \times 10^{-5}$

Lower boundary  $\psi(120, t) = 7.329241 \times 10^{-5}$

Upper boundary  $\left. \frac{\partial \psi}{\partial z} \right|_{z=\infty} = 0 \quad (\text{A2-32})$

set 1 and set 2

Initial condition  $\varphi_i(z, 0) = 0 \quad \text{for all } i$

Lower boundary  $\varphi_i(120, t) = 0 \quad \text{for all } i$

Upper boundary  $\left. \frac{\partial \varphi_i}{\partial z} \right|_{z=0} = 0 \quad \text{for all } i \quad (\text{A2-47})$

The set 1 boundary conditions on  $\psi$  correspond to a vibrational temperature initially zero, with the vibrational temperature at the lower boundary remaining zero, presumably due to quenching. The set 2 boundary conditions for  $\psi$  correspond to the initial vibrational temperature of 355°K (the kinetic temperature at the lower boundary) and the vibrational temperature at the lower boundary remaining at

355°K. In both cases the upper boundary condition on  $\psi$  corresponds to a zero flux of quanta through the top of the atmosphere.

The boundary conditions on the  $\varphi_i$ 's correspond to zero deviations from a Boltzmann distribution initially, with zero deviation being maintained at the lower boundary (presumably due to the rapid vibration-vibration energy exchange among  $N_2$  at this altitude).

Calculation shows that the source term for vibrational quanta due to electron collisions in equation (A2-30) is only mildly non-linear (less than 30%) for the electron and vibrational temperatures of interest here. It can also be argued, that for the relatively weak source of vibrational excitation for this problem, the departures from a Boltzmann solution will be such that the term  $\epsilon_j/n$  will be small relative to 1. Thus by dropping the  $\epsilon_j/n$  term in (A2-30), the  $\psi$  and  $\varphi_i$  equations are uncoupled, and a first approximation to  $\psi$  may be obtained by solving the equation

$$\begin{aligned} \frac{\partial \psi}{\partial t} - \frac{1}{n} \frac{\partial D n}{\partial z} \frac{\partial \psi}{\partial z} - D \frac{\partial^2 \psi}{\partial z^2} = \sum_{j=0} \sum_{i=0} \left[ \frac{1}{\psi + 1} \left( \frac{\psi}{\psi + 1} \right)^j \right] (i - j) A_{ij} \\ + C_{1,0} \nu' n [0] [\psi + 1 - e^{\theta/T} \psi] \end{aligned} \quad (2-23)$$

When  $\psi$  has been obtained, the vibrational temperature may be calculated by

$$T_v(z, t) = \frac{\theta}{\ln \left[ \frac{\psi(z, t) + 1}{\psi(z, t)} \right]} \quad (2-24)$$

and the coefficients of equations (A2-46) are known functions of altitude and time.

A first approximation to the  $\varphi_i$ 's can then be obtained by solving equation (A2-46).

If necessary, a second approximation to  $\psi$  may be obtained from equation (A2-30) by using the first approximation of the  $\varphi_i$ 's to determine  $\epsilon_j/n$  in the source term of equation (A2-30) and resolving equation (A2-30). A second approximation to the  $\varphi_i$ 's can then be obtained by using the second approximation for  $\psi$  in equations (A2-46). Higher approximations may in principle be found by repeating this process.

## 2.7 Finite difference equations and solutions.

In Appendix III it is shown that the finite difference equations for both equations (A2-30) and (A2-46) take the general forms

$$-A_{\ell} \psi_{\ell+1}^{m+1} + B_{\ell} \psi_{\ell}^{m+1} - A_{\ell} \psi_{\ell}^{m+1} = D_{\ell}^m \quad (\text{A3-7})$$

and

$$-{}^{\ell}A_i {}^{\ell+1}\varphi_i^{m+1} + {}^{\ell}B_i {}^{\ell}\varphi_i^{m+1} - {}^{\ell}A_i {}^{\ell-1}\varphi_i^{m+1} = {}^{\ell}C_i^m \quad (\text{A3-17})$$

where  $\ell$  refers to an altitude grid point, with  $\ell = 1$  the bottom boundary and  $\ell = L$  the top boundary,  $m$  refers to a time grid point and  $i$  refers to the energy level being solved for. The boundary conditions become for  $\psi$

	set 1	set 2	
(A3-8)	$m = 1$	$\psi_{\ell}^1 = 0$	$\psi_{\ell}^1 = 7.329241 \times 10^{-5}$
	$\ell = 1$	$\psi_1^m = 0$	$\psi_1^m = \psi_{\ell}^1$
	$\ell = L$	$\psi_L^m - \psi_{L-1}^m = 0$	$\psi_L^m - \psi_{L-1}^m = 0$

(A3-9)

and for the  $\phi_i$  's

$$\begin{aligned}
 m = 1 \quad \ell \phi_i^1 &= 0 & \text{for all } i \\
 \ell = 1 \quad {}^1\phi_i^m &= 0 & \text{for all } i \\
 \ell = L \quad {}^L\phi_i^m - {}^{L-1}\phi_i^m &= 0 & \text{for all } i
 \end{aligned} \tag{A3-18}$$

The two equations (A3-7) and (A3-17) are of the same form. We follow Richtmyer, (36), pages 103-104, for the solutions of (A3-7) and (A3-17). Only the solution of (A3-7) is presented here, because the extension to each of the equations in (A3-17) is clear.

It is seen that the right hand side of (A3-7) is a known quantity. Equation (A3-7) is a one parameter family, because any value of  $\psi_2^{m+1}$  determines a solution. Let

$$\psi_\ell^{m+1} = E_\ell \psi_{\ell+1}^{m+1} + F_\ell \tag{2-25}$$

which is also a one parameter family. We seek to find  $E_\ell$  and  $F_\ell$  such that the two families of solutions (2-25) and (A3-7) are the same. If (2-25) is to be true for any member of the family, the boundary conditions (A3-8) and (A3-9) require

$$E_1 = 0 \tag{2-26}$$

$$F_1 = \begin{cases} 0 & \text{set 1} \\ 7.329241 \times 10^{-5} & \text{set 2} \end{cases} \tag{2-27}$$

$$\tag{2-28}$$

Substituting (2-25) into (A3-7) and placing the result in the form of (2-25) we have

$$\psi_{\ell}^{m+1} = \frac{A_{\ell}}{B_{\ell} - A_{\ell} E_{\ell-1}} \psi_{\ell+1}^{m+1} + \frac{D_{\ell}^m + A_{\ell} F_{\ell-1}}{B_{\ell} - A_{\ell} E_{\ell-1}} \quad (2-29)$$

Comparing equation (2-29) with (2-25) we have

$$E_{\ell} = \frac{A_{\ell}}{B_{\ell} - A_{\ell} E_{\ell-1}} \quad (2-30)$$

$$F_{\ell} = \frac{D_{\ell}^m + A_{\ell} F_{\ell-1}}{B_{\ell} - A_{\ell} E_{\ell-1}} \quad (2-31)$$

Using (2-26) and (2-27) or (2-28) we can calculate the  $E_{\ell}$ 's and  $F_{\ell}$ 's from  $\ell = 1$  to  $\ell = L$ , that is, from the lower boundary to the upper boundary, by using (2-30) and (2-31), respectively.

When  $\ell = L - 1$ , equation (2-25) gives

$$\psi_{L-1}^{m+1} = E_{L-1} \psi_L^{m+1} + F_{L-1} \quad (2-32)$$

Using the upper boundary condition of (A3-8) or (A3-9) in (2-32) we have

$$\psi_{L-1}^{m+1} = \frac{F_{L-1}}{1 - E_{L-1}} \quad (2-33)$$

We now repeat the process, for  $\ell = L - 2, L - 3, \dots, 1$ , to solve for the  $\psi_{\ell}^{m+1}$ 's, that is, we solve for the  $\psi_{\ell}^{m+1}$ 's from the upper boundary to the lower boundary.

This total process is repeated for each time step from  $m = 1$  to the maximum time step of interest.

Only slight modification of this method is needed to solve for the six, coupled  $\phi_i$ 's of equation (A3-17).

The technique embodied in equations (A3-7) (A3-17) and equations (2-25) through (2-33) was programmed for the IBM 360-75 for both sets of finite difference equations (A3-7) and (A3-17). The program to solve for  $\psi$  was called BOLTSOL and the program to solve for the  $\phi_i$ 's was called BOLTDEV. Both programs are listed in Appendix IV. Details of the numerical solutions are discussed in Chapter III.

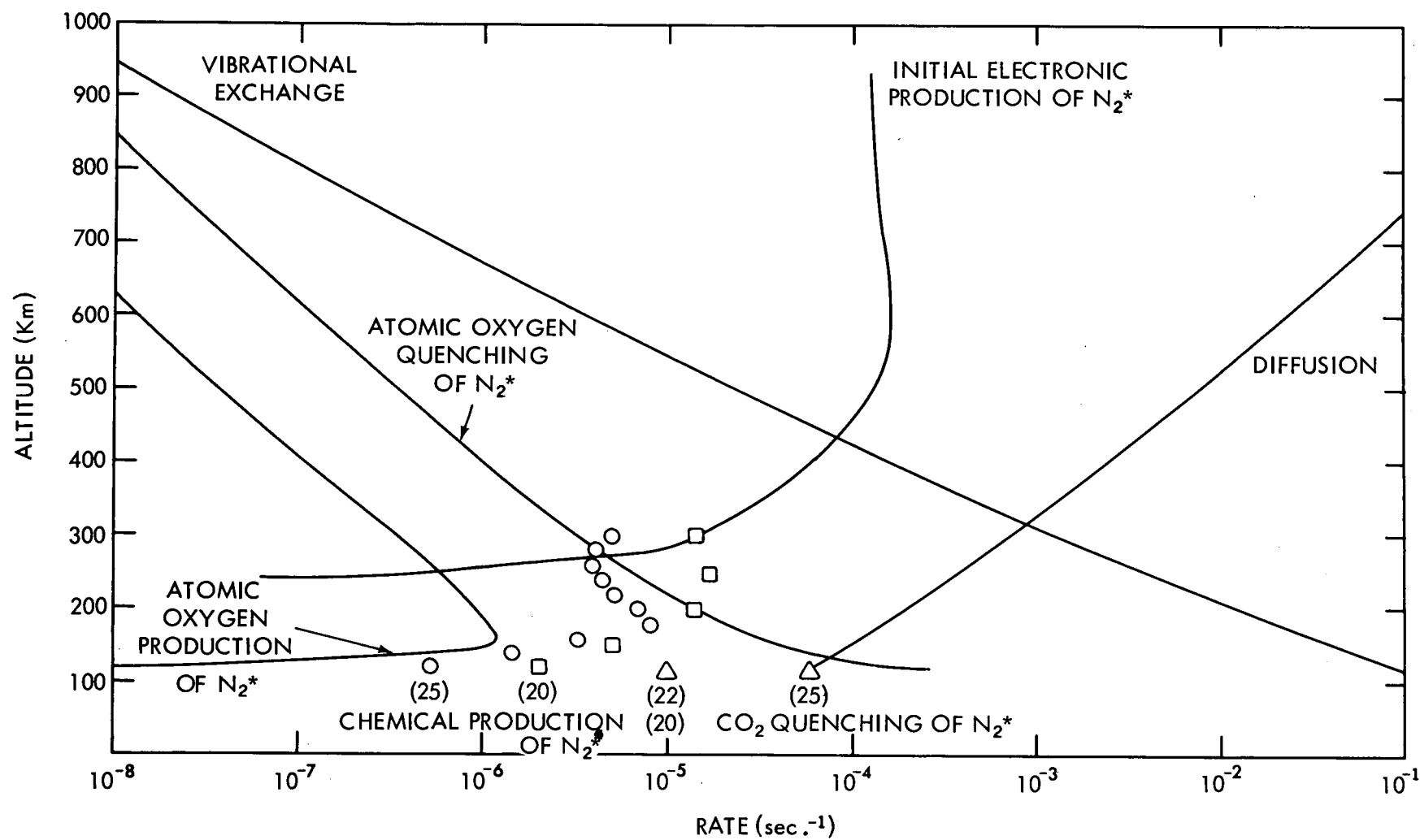


Figure 2-1. Rates of production and loss of vibrational energy and diffusion



### CHAPTER III. APPLICATION TO SAR-arc

The finite difference equations (A3-7) and (A3-17) were solved in single precision over the altitude interval of 120 km to 920 km for conditions corresponding to those of a 17.7 KR SAR-arc, as shown in Figure 1-2 and 1-3. The upper altitude limit was lowered to 840 km. with negligible effect (less than 5° in the vibrational temperature and less than 2% in the  $\phi_i$ 's) on the solutions. The altitude step was taken as 40 km. and variation of the time step by a factor of 10, from 100 sec. to 10 sec. had no significant effect on the results. The solutions were generated over a time interval of 100000 seconds and approached (or reached) a steady state during that time.

Figure 3-1 shows the number of density of vibrational quanta versus altitude for a time into the solution of 95200 seconds. The number density of quanta was calculated from the solutions of equation (A3-7) corresponding to equation (2-23) (that is ignoring the  $\epsilon_j/n$  term in the source term). Also shown in Figure 3-1 is the quantity  $\sum_{i=0}^{\infty} i \epsilon_i$  calculated from the solutions of equations (A3-17). Theoretically equations (A2-4) and (A2-5) should be satisfied, however, because of the finite difference and other approximations,  $\sum_{i=0} i \epsilon_i$  will not be zero. A measure of its significance is a comparison with the number of quanta calculated from the solutions of (A3-7). From Figure 3-1 it is seen that  $\sum_{i=0} i \epsilon_i$  represents a negligible (<1%) portion of the energy in the Boltzmann solution for altitudes below 300 km. Between 300 and 600 km altitude,  $\sum_{i=0} i \epsilon_i$  increases relative to the quantal number density, so that at altitudes of 600 km. and above  $\sum_{i=0} i \epsilon_i$  represents only about 3% of the energy of the Boltzmann solution. These conclusions are valid at all other time steps.

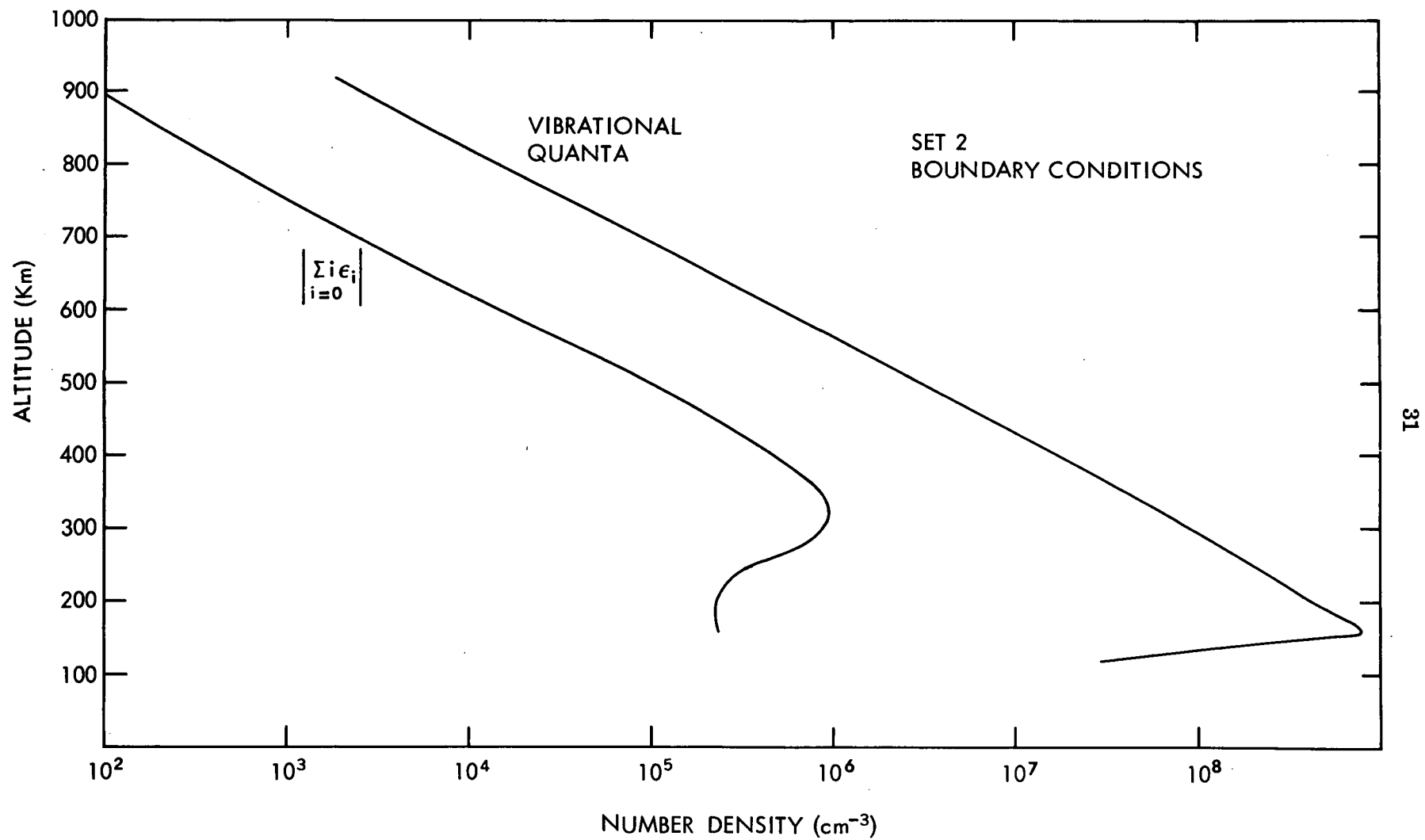


Figure 3-1. Comparison of  $\sum_{i=0} i \epsilon_i$  and the number density of vibrational quanta

Figure 3-2 is a plot of  $|\sum_{i=0} \epsilon_i / \epsilon_i|$  versus altitude for each of the six energy levels corresponding to a time into the solution of 94700 seconds. This figure is also representative of the results at other times. It is seen in Figure 3-2 that below 400 km altitude  $\sum_{i=0} \epsilon_i$  is comparable to or greater than the number densities of each of the deviations for all 6 energy levels. Above 400 km  $\sum_{i=0} \epsilon_i$  is only several tens of percent of the deviations for levels 2 through 5 and a few percent of the deviations for levels 0 and 1. It should be pointed out that at 160 km. the ratio of the magnitudes of the deviations of level zero to level five (that is  $\epsilon_0 / \epsilon_5$ ) is  $10^7$  initially, and for the time corresponding to Figure 3-2, is near  $10^6$ . This explains why the ratios at 160 km. increase with level number. At 840 km. altitude, for the time corresponding to Figure 3-2, the ratio of  $\epsilon_0 / \epsilon_5$  is near  $10^2$ . It is significant that the ratio  $|\sum_{i=0} \epsilon_i / \epsilon_i|$  has its largest values at the lowest altitudes where the deviations  $\epsilon_i$  are numerically the largest. At low altitudes  $\sum_{i=0} \epsilon_i$  is about  $10^{-4}$  of the molecular nitrogen number density and at high altitudes it is about  $10^{-3}$  of the molecular nitrogen number density. Figure 3-2 indicates that caution should be exercised in using the calculated deviations,  $\epsilon_i$ , only for altitudes below 370 km. However, as later sections show, the influence of the deviations below 370 km. altitude is not large, but the  $\epsilon_i$  do become physically important at higher altitudes where the precision of determination is considerably improved.

### 3.1 Solution for the Boltzmann part.

The vibrational temperatures calculated from the solution of the  $\psi$  equation are shown versus altitude and time in Figures 3-3 and 3-4, respectively. The solutions are for the set 2 (initial and lower boundary vibrational temperature of 355°K) boundary conditions.

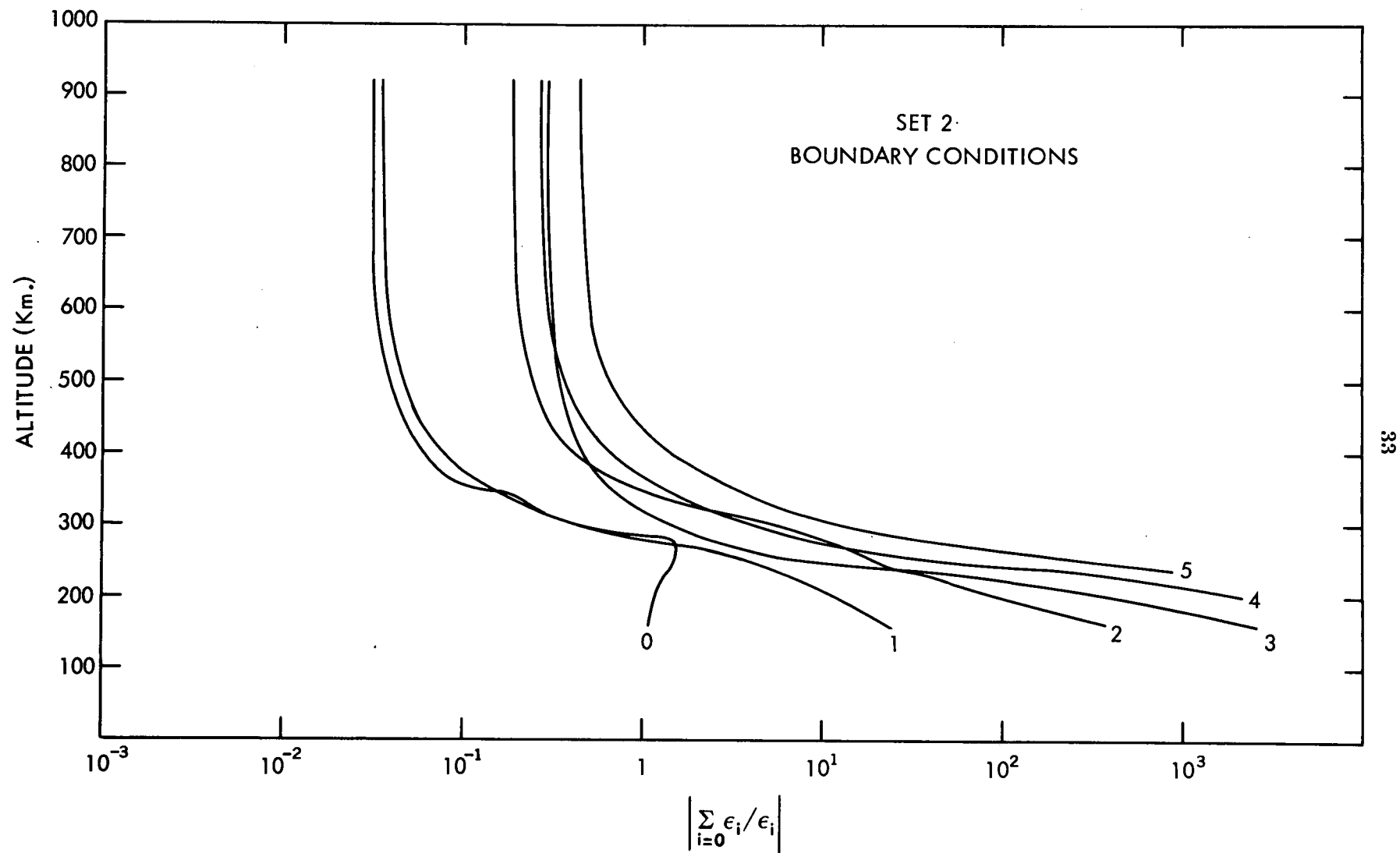


Figure 3-2.  $\sum_{i=0} \epsilon_i / \epsilon_i$  for energy levels 0 through 5

Figure 3-3 shows the vibrational temperature profiles, calculated at five time steps, versus altitude. It is seen from this figure that at altitudes above 600 km the vibrational temperature is nearly isothermal at each time step, a result of the rapidity of the diffusion process at these altitudes. The downward movement of the energy is apparent in the figure. Vertical vibrational temperature gradients of as much as 25°K/km. are observed in the steady state.

Figure 3-4 is a plot of vibrational temperature versus time at ten altitudes of interest. It is seen from the figure that a steady state is reached in about one day. However, in 10 hours, or less depending on altitude, the vibrational temperature has achieved 90% or more of the steady state value. Notice that the vibrational temperature at the higher altitudes has a very steep gradient with time, initially. This rapid heating rate is important to the solutions of the deviation equations discussed in the next section. It should be noticed that the temperature at 240 km altitude has reached 1350°K, a value large enough to significantly effect the reaction constant of reaction (1-1), as discussed in section 3.3.

### 3.2 Solutions for the deviation parts.

It was found that convergence of the deviation solutions could not be achieved, even with 1 second time steps, if the solution was started at the "turn on" of the SAR-arc. It was determined that the difficulty was caused by terms involving derivatives of  $\psi$  and was apparently due to the initially very large changes in  $\psi$  primarily, those with time. Convergence of the solutions of the  $\phi_i$  equations was obtained if the solutions were started at 5200 seconds "into" the arc, and this was the approach adopted. The physical conditions corresponding to the initial stages of a SAR-arc are unknown. However, it is expected that the characteristic times

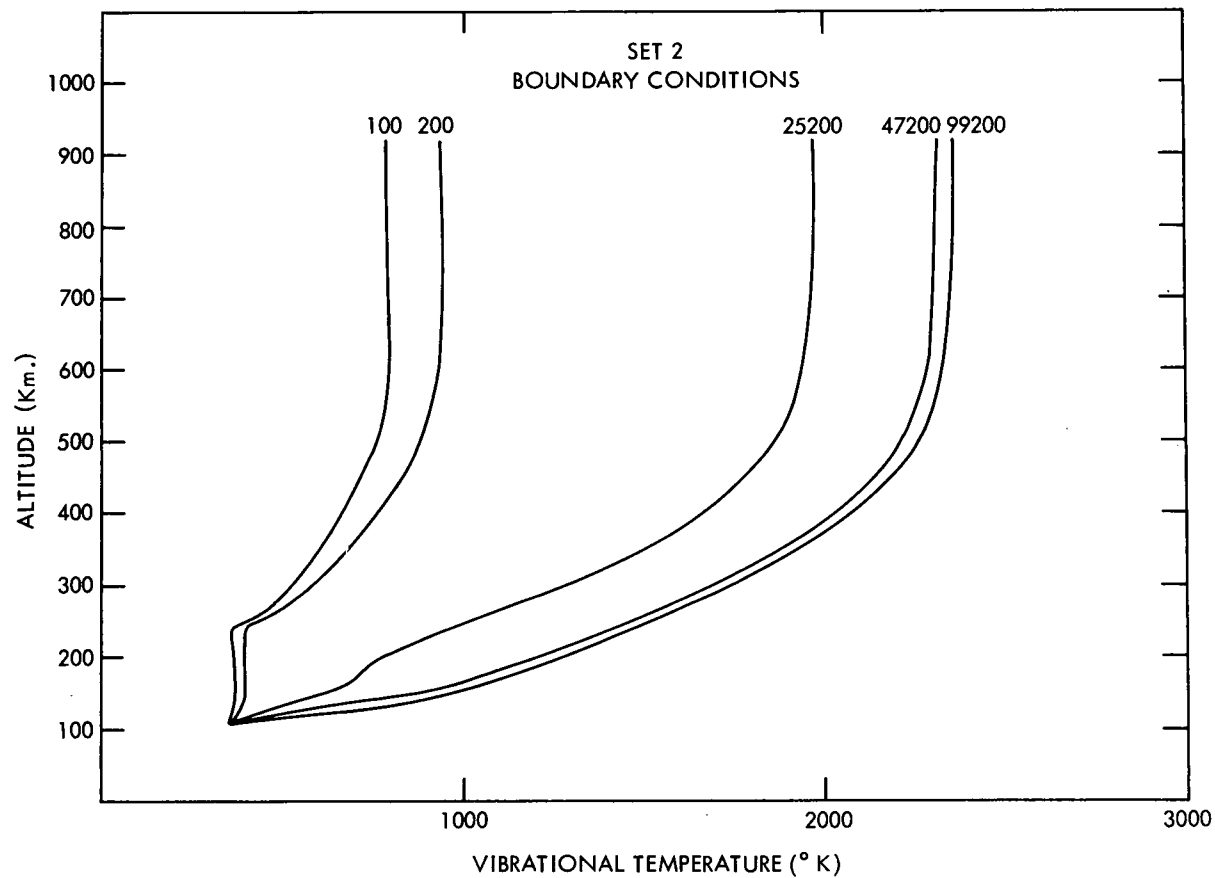


Figure 3-3. Vibrational temperatures calculated from the  $\psi$  equation solutions versus altitude for five time steps

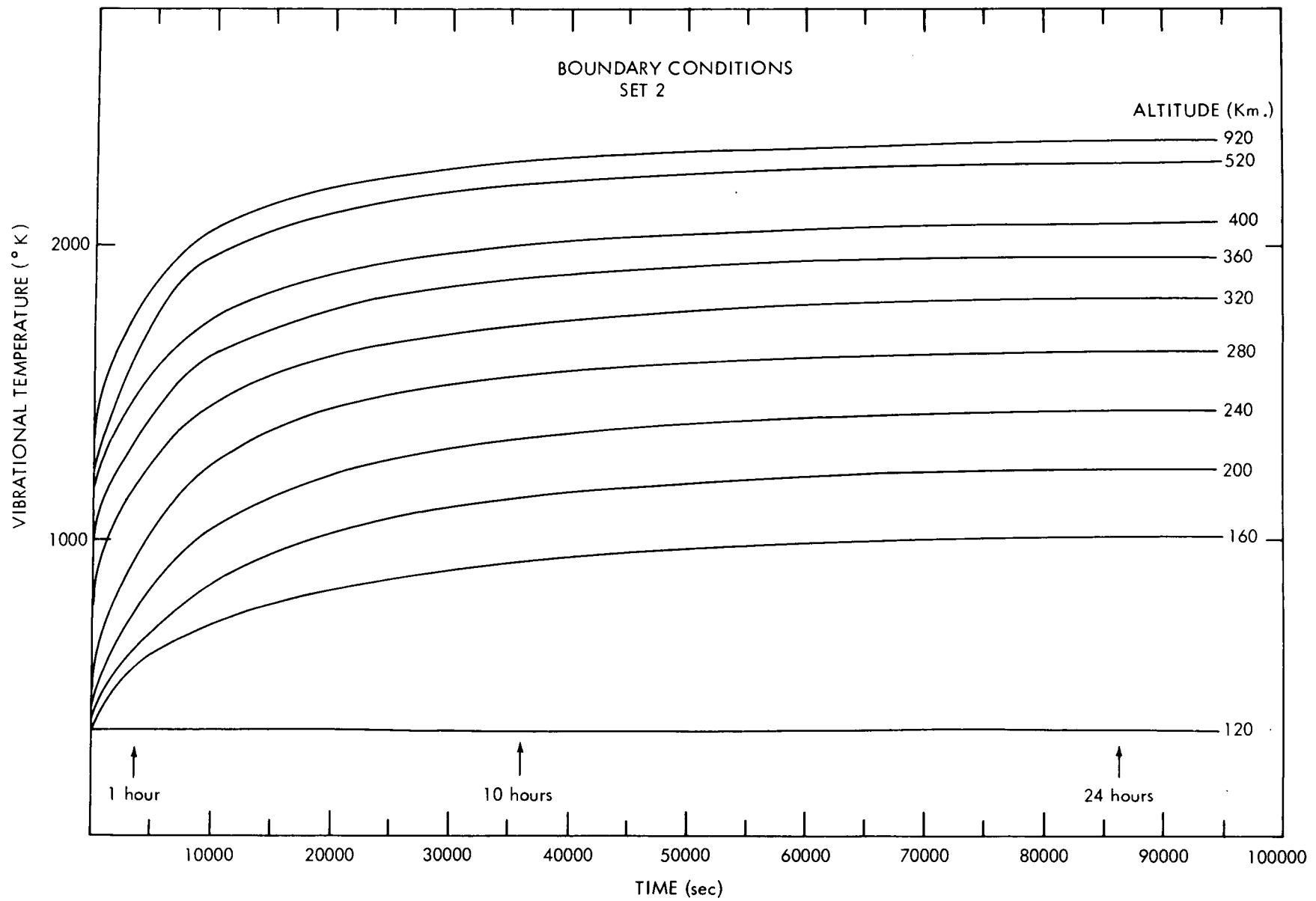


Figure 3-4. Vibrational temperatures calculated from the  $\psi$  equation versus time for several altitudes

of the important processes are measured in terms of one or more hours. Thus, the imposition of SAR-arc conditions in a step-wise manner is not realistic; so that little physical content has been lost by the adopted calculational approach.

Figures 3-5 through 3-10 show the  $\phi_i$ 's versus altitude for three time steps. These figures show that above 500 km the ratio of the deviation from the Boltzmann solution to the Boltzmann population, at the energy level of interest, is nearly constant with altitude. This result is again due to the rapidity of the diffusion process at these altitudes. It is also apparent from these figures that at altitudes of 300 km and above the  $\phi_i$ 's rapidly reach a maximum and then decrease to their "steady state" values. In these figures, where  $\phi_i$  changes sign with altitude the absolute value has been plotted. It is seen that the "steady state" deviation populations above 300 km altitude, are less than the Boltzmann population of the corresponding energy levels 0, 1, 2 and 3 and are greater than the Boltzmann population for levels 4 and 5. This will be important in the calculation of an effective reaction coefficient for reaction (1-1) (see section 3.3).

Figures 3-11 through 3-16 show the  $\phi_i$ 's versus times for several altitudes. From these figures it is seen that above 300 km altitude a nearly constant, significant, deviation is maintained from a Boltzmann distributed population for the upper energy levels.

### 3.3 Reaction rate constant for reaction (1-1) and ionospheric loss time constant.

The effective reaction rate constant for the ion-atom interchange reaction (1-1) was calculated from



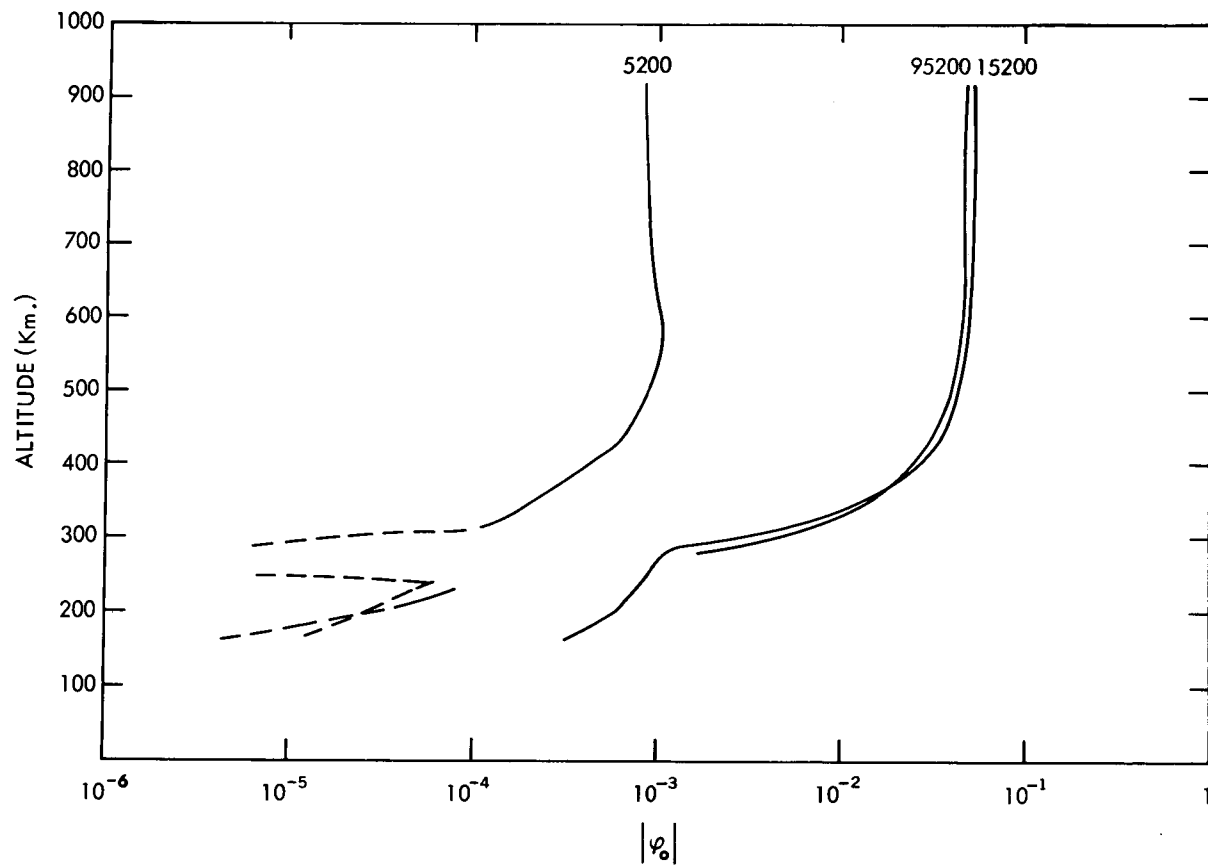


Figure 3-5.  $|\phi_0|$  versus altitude for 3 time steps

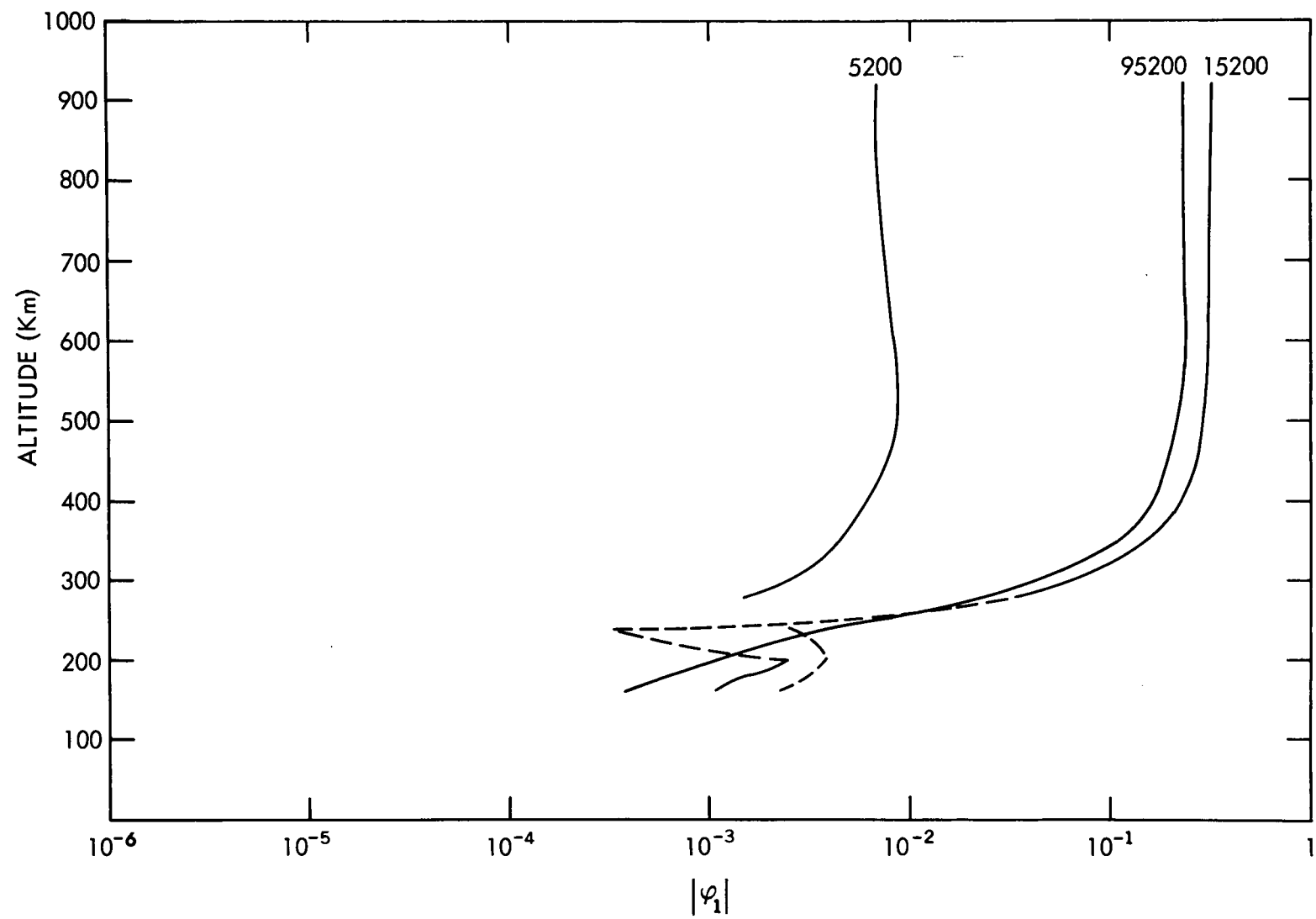


Figure 3-6.  $|\phi_1|$  versus altitude for 3 time steps

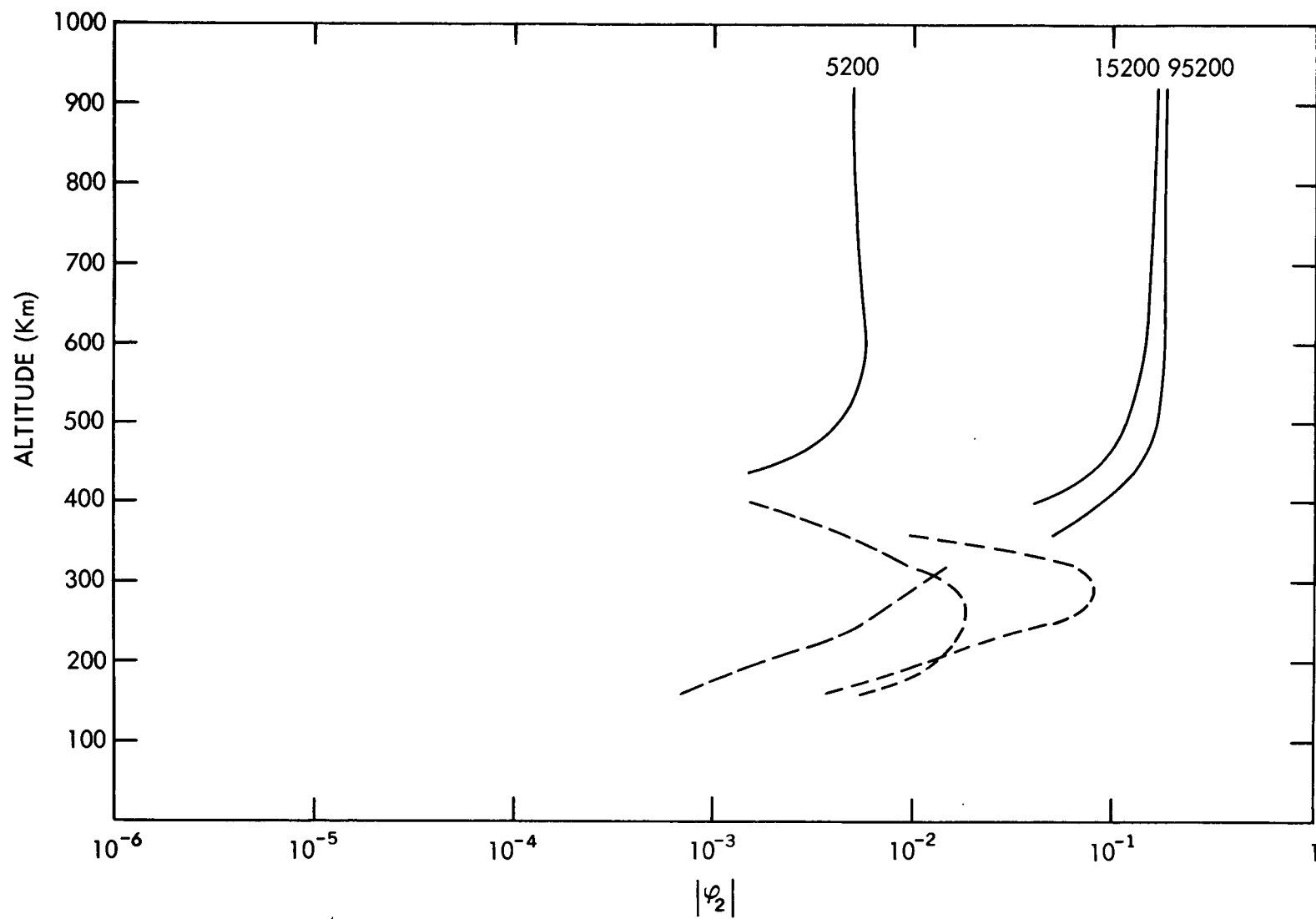


Figure 3-7.  $|\phi_2|$  versus altitude for 3 time steps

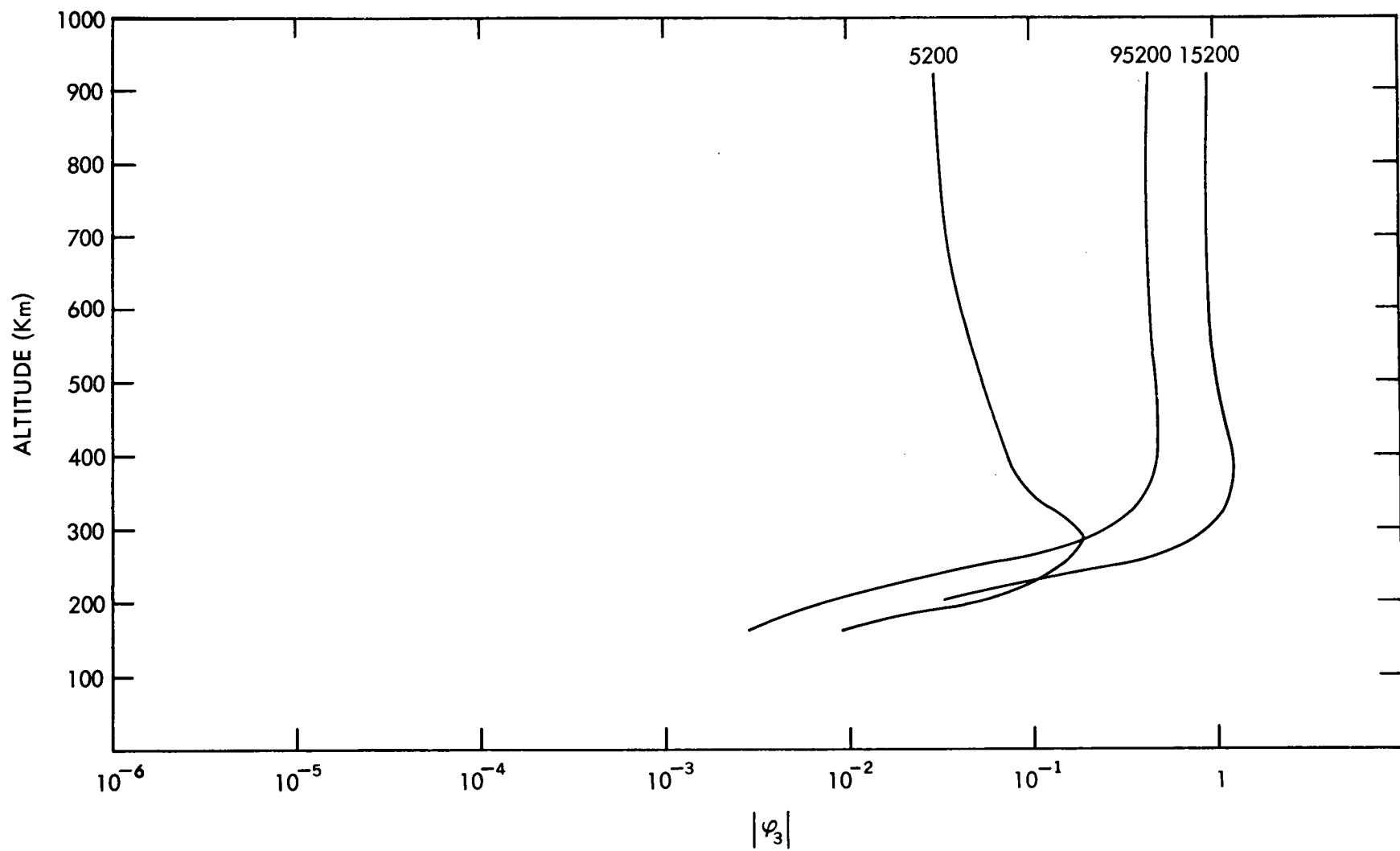


Figure 3-8.  $|\phi_3|$  versus altitude for 3 time steps

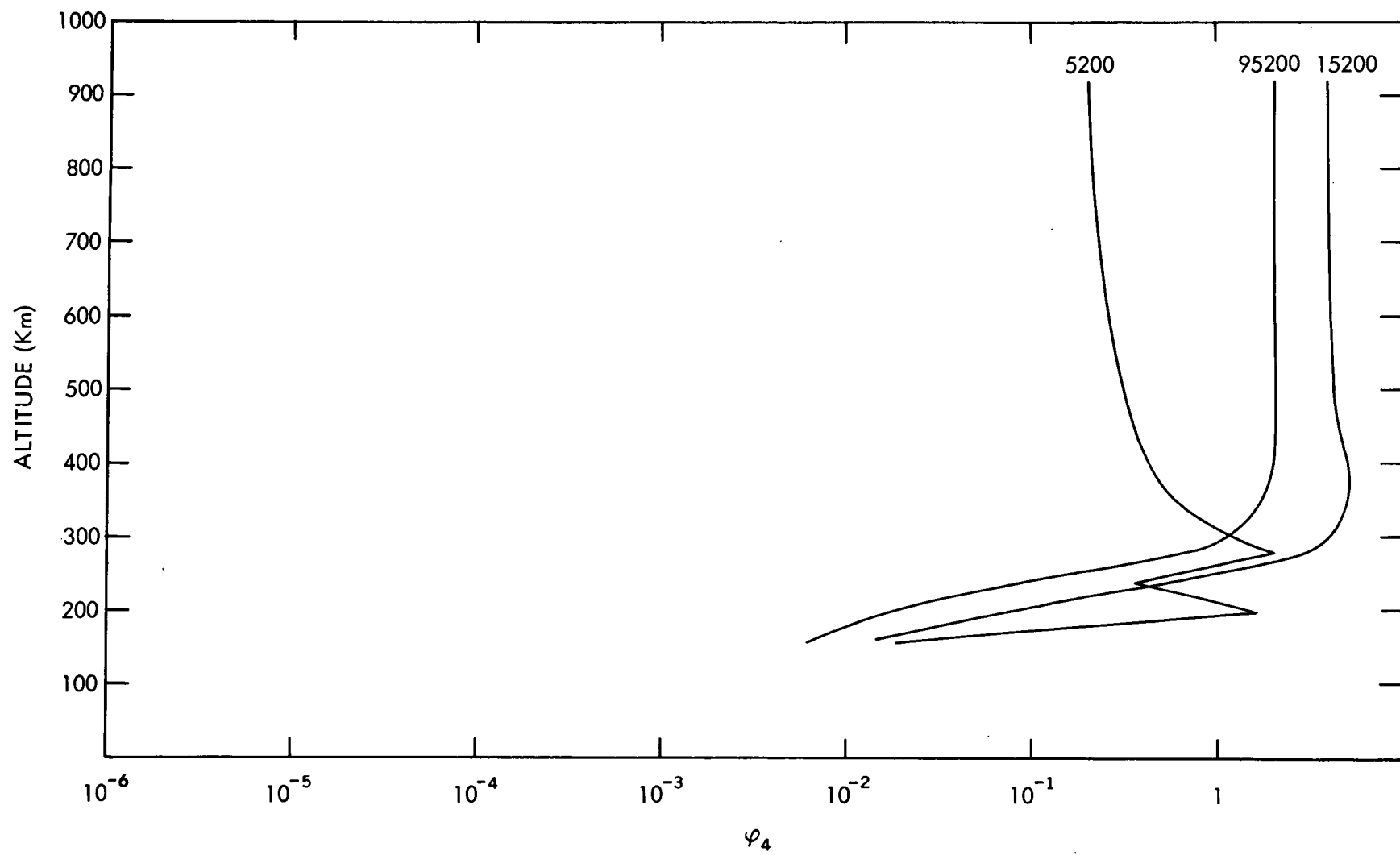


Figure 3-9.  $\phi_4$  versus altitude for 3 time steps

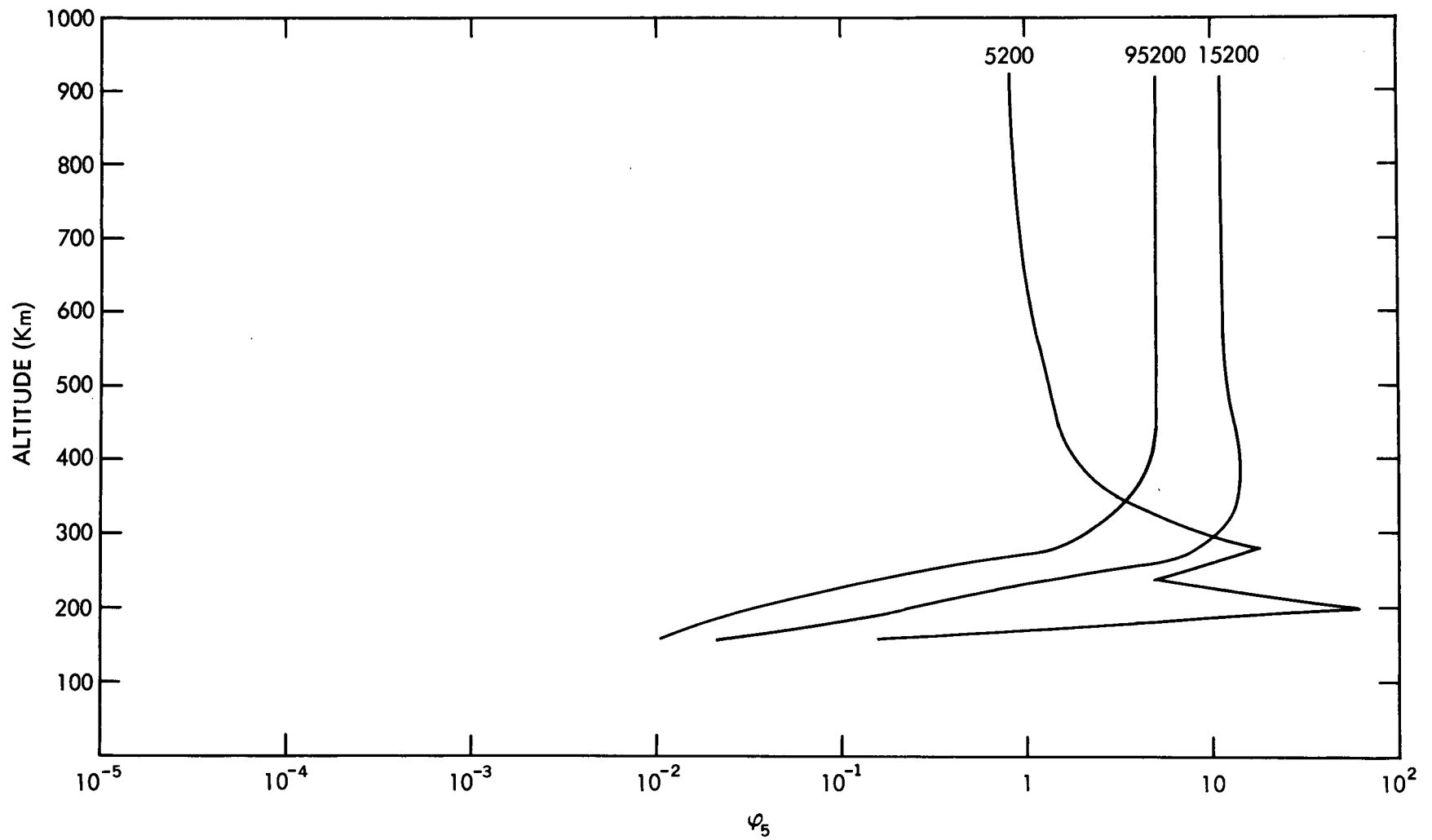


Figure 3-10.  $\phi_5$  versus altitude for 3 time steps

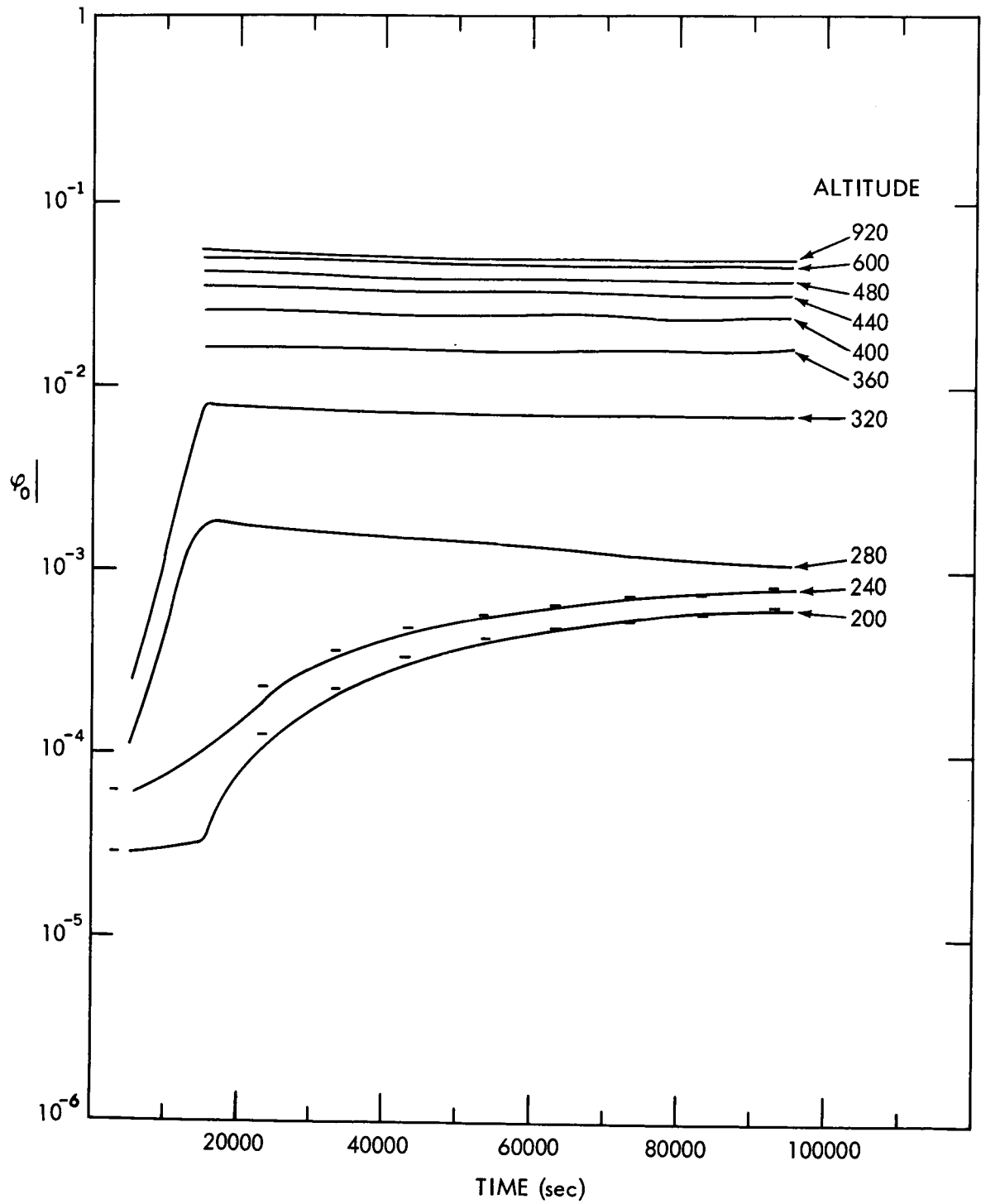


Figure 3-11.  $|\phi_0|$  versus time for several altitudes

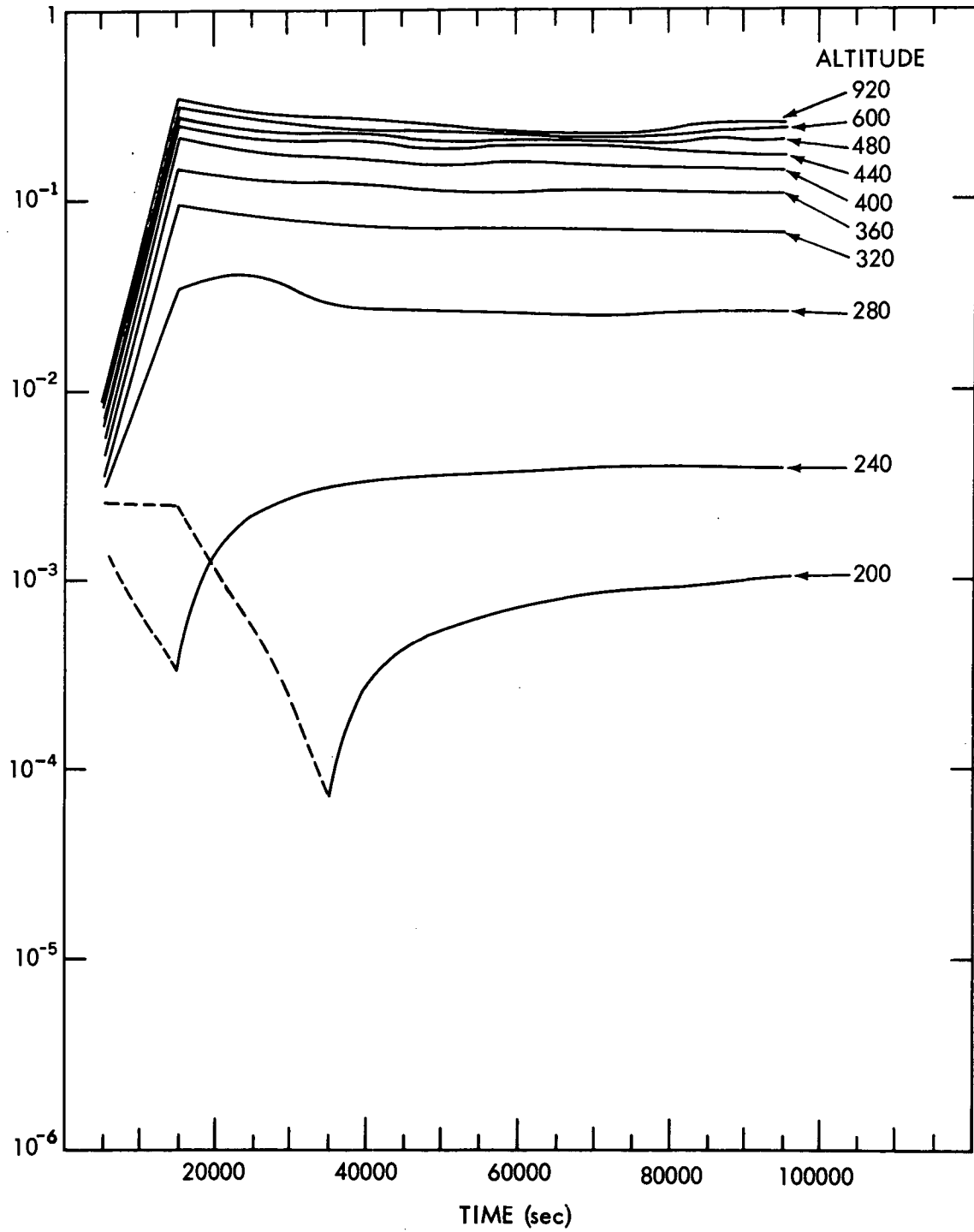


Figure 3-12.  $|\phi_1|$  versus time for several altitudes



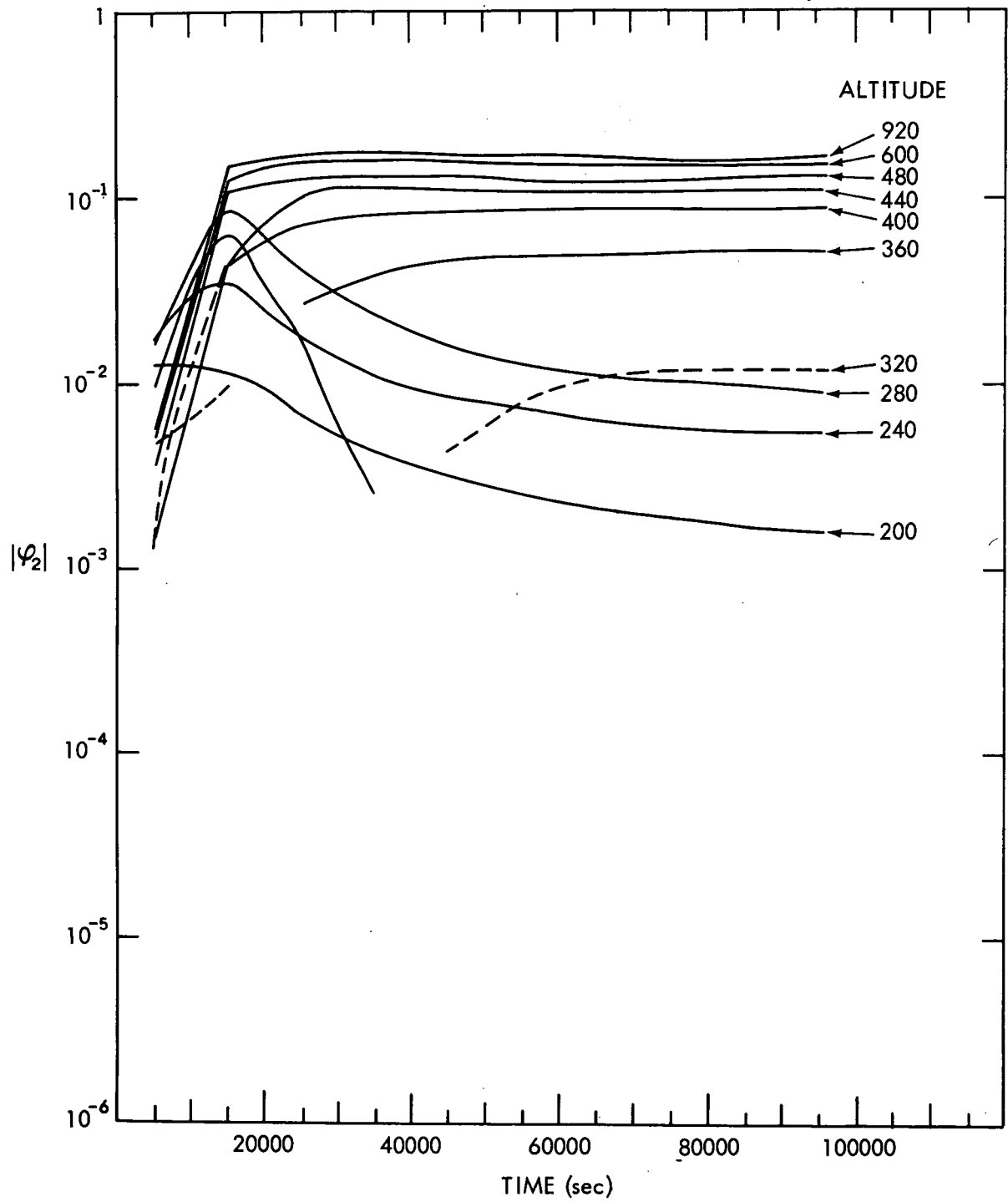


Figure 3-13.  $|\phi_2|$  versus time for several altitudes

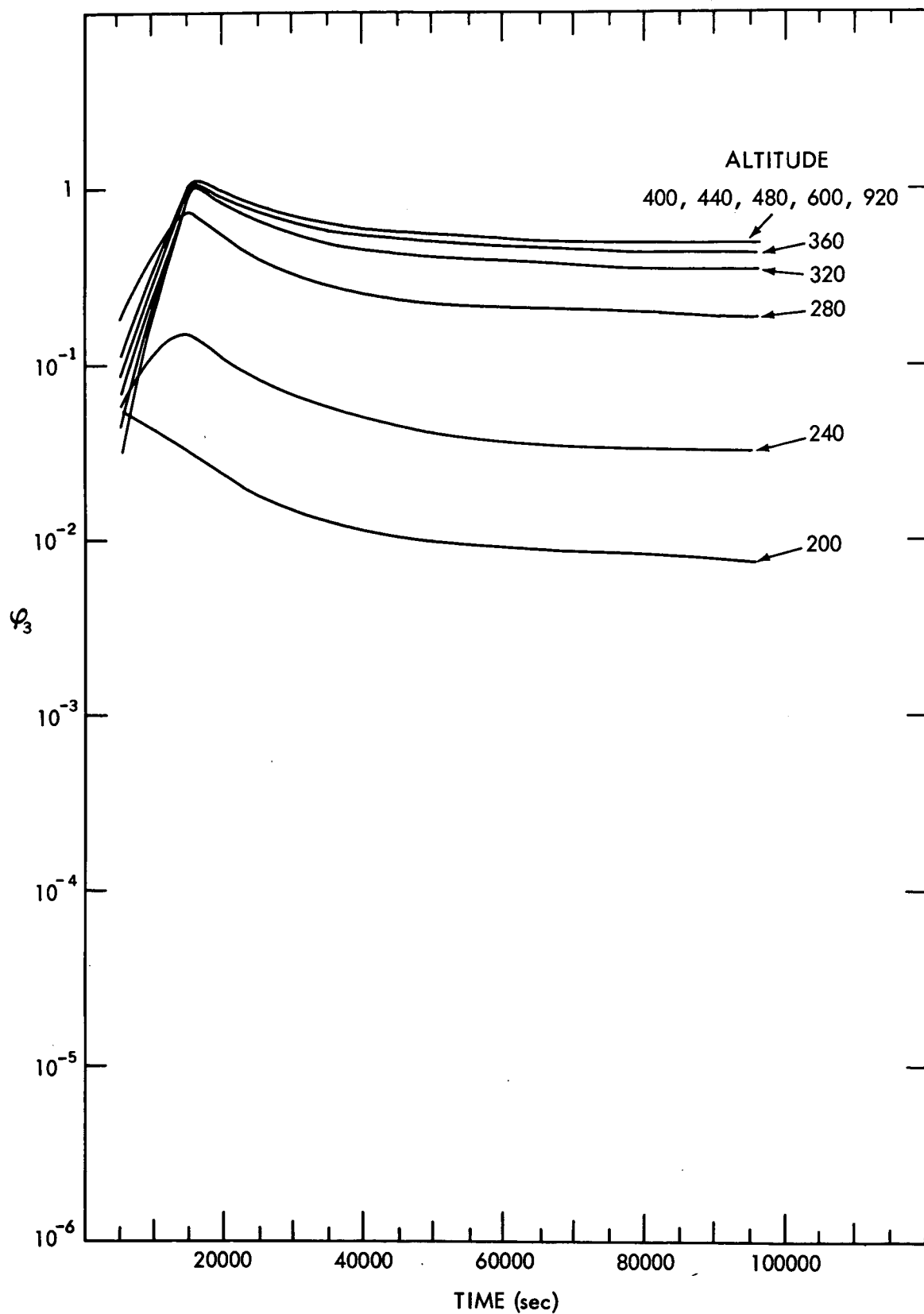


Figure 3-14.  $|\phi_3|$  versus time for several altitudes

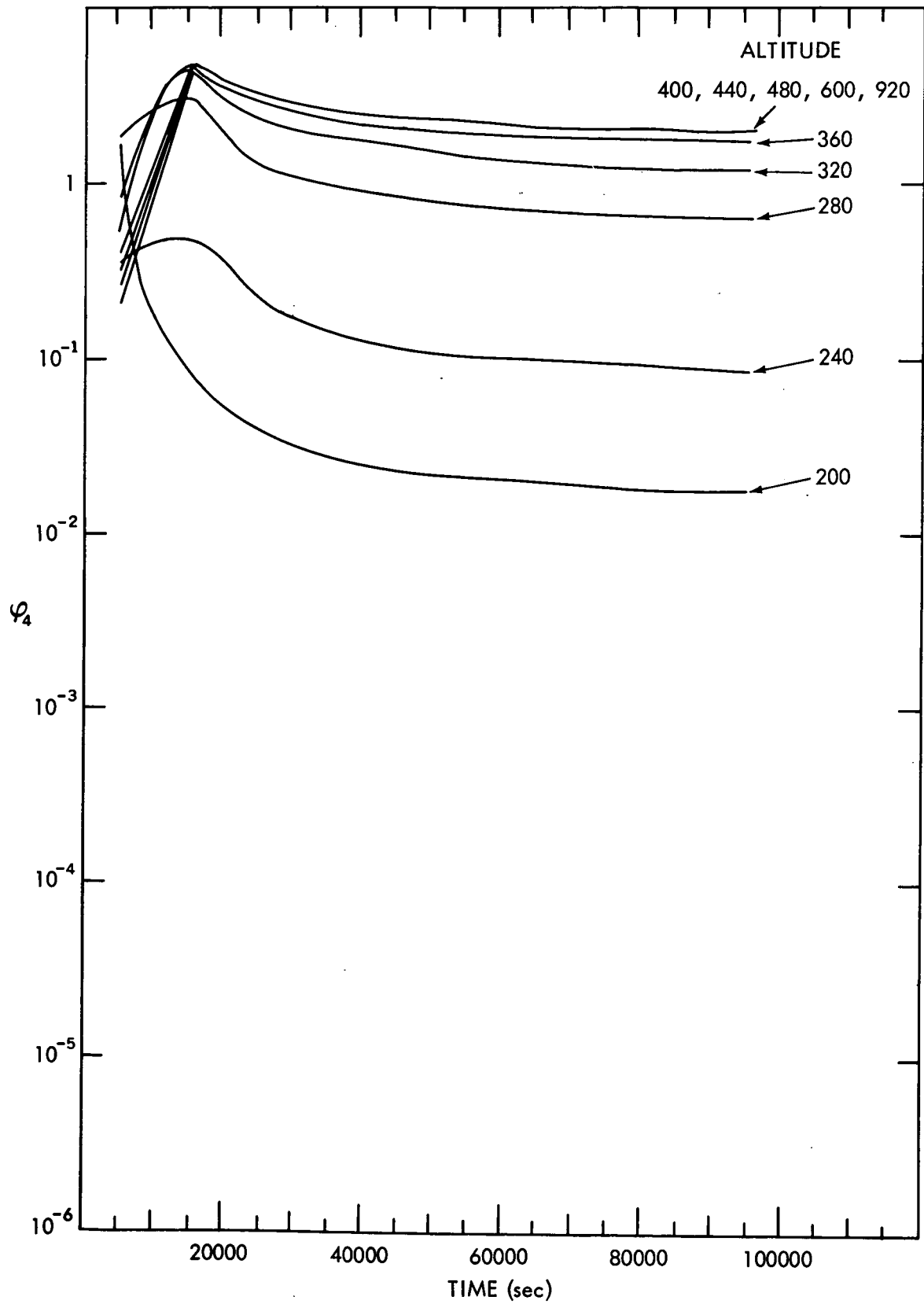


Figure 3-15.  $\phi_4$  versus time for several altitudes

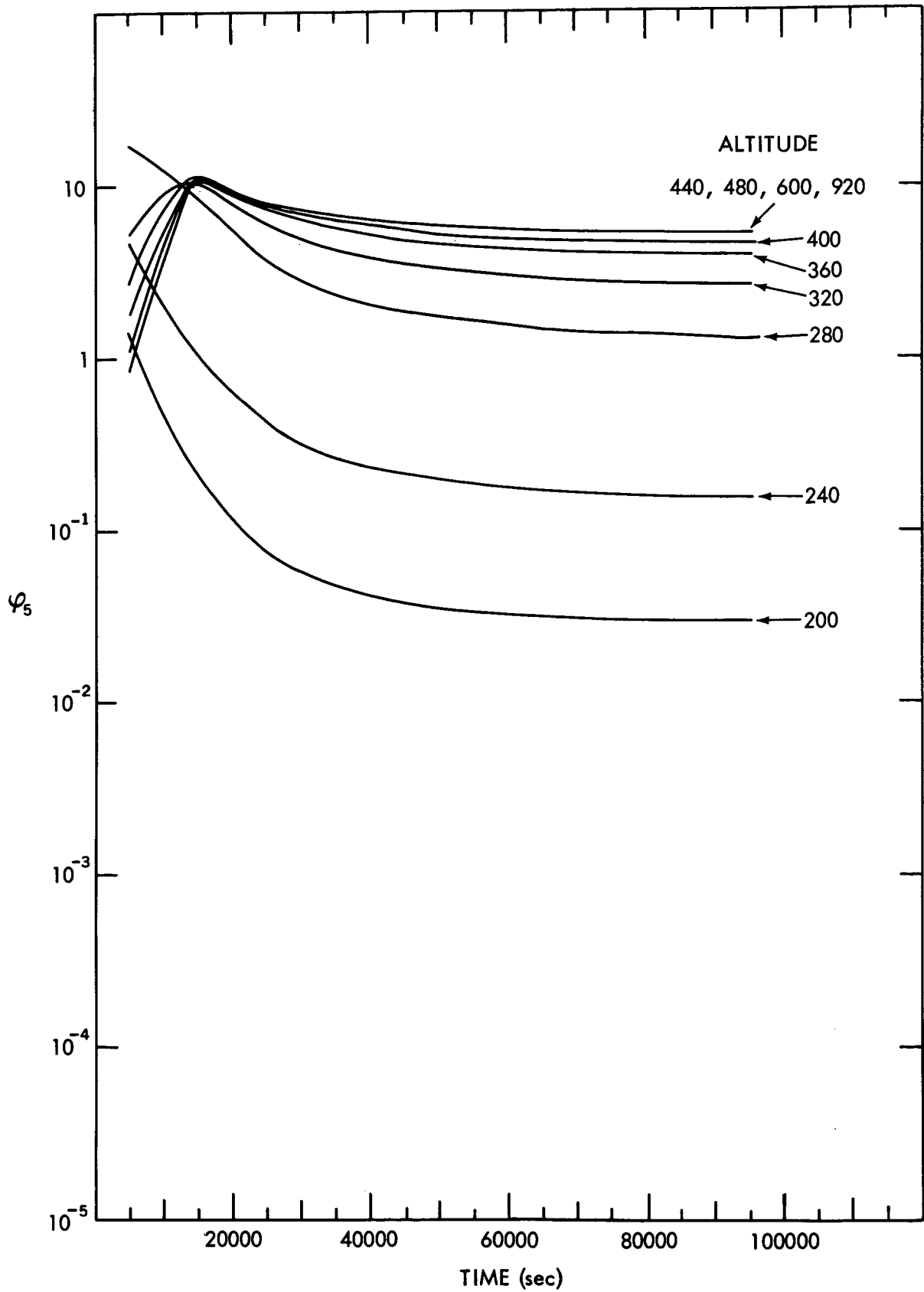


Figure 3-16.  $\phi_5$  versus time for several altitudes

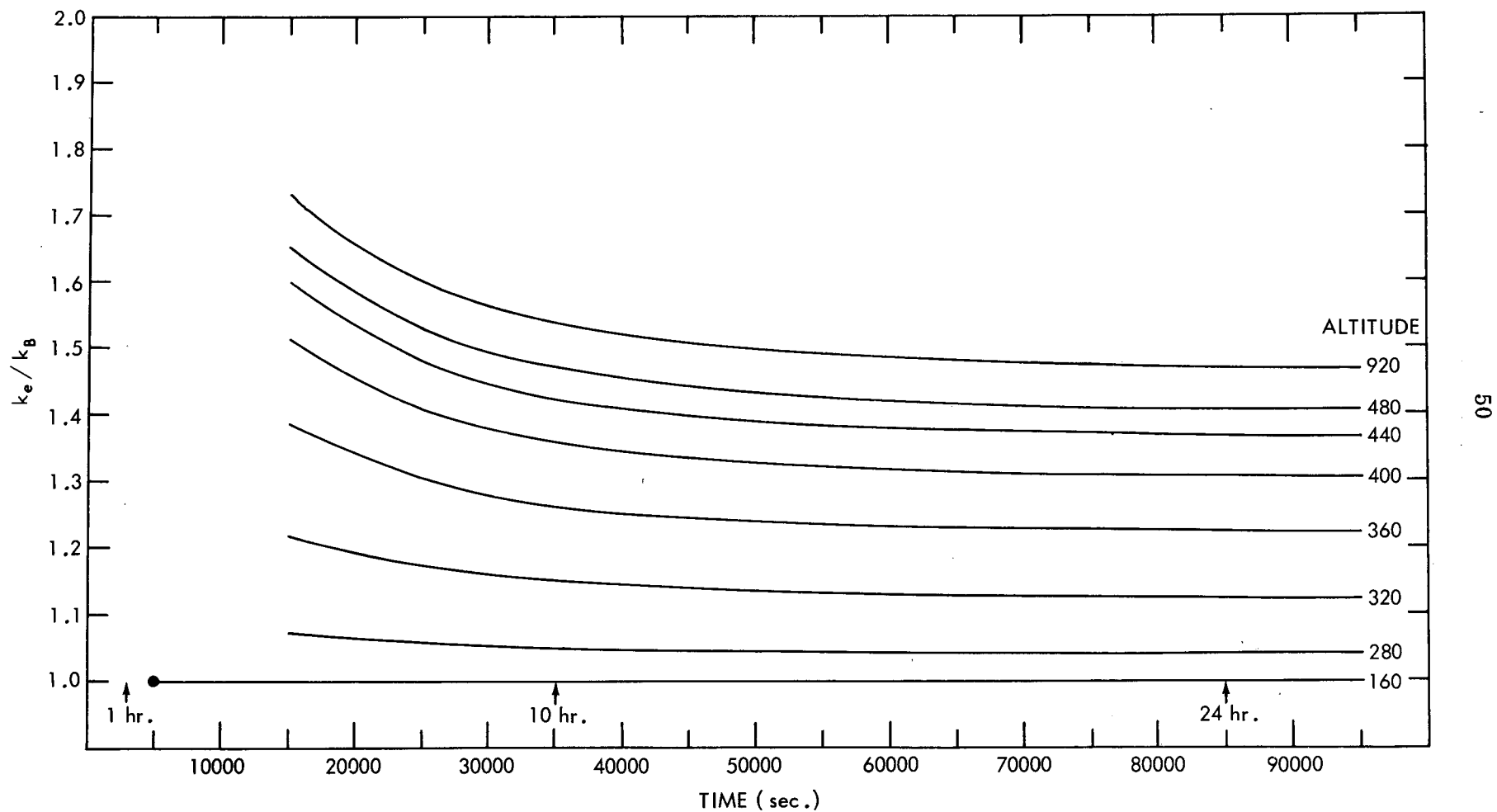


Figure 3-17. Ratio of the effective to the energetically equivalent reaction constant,  $k_e/k_B$ , versus time for several altitudes

$$\begin{aligned}
 k_e &= \sum_{i=0} k(i) \frac{n_i}{n} \\
 &= \sum_{i=0} k(i) \frac{(n'_i + \epsilon_i)}{n}
 \end{aligned}
 \tag{3-1}$$

where  $k_e$  is the effective rate constant and  $k(i)$  is the rate constant for level  $i$ , taken from reference (13) and listed in Table 3. The reaction rate for the Boltzmann part of the solution,  $k_B$ , was calculated from equation (3-1) with the  $\epsilon_i$  terms set to zero. The computer program for these calculations, REACTRAT, is listed in Appendix III. A comparison of  $k_e$  and  $k_B$  is a measure of the importance of the deviation from a Boltzmann distribution to the  $F_2$  region ionospheric ionization loss.

Figure 3-17 shows the ratio  $k_e/k_B$  versus time for several altitudes of interest. It is apparent in the figure, that for altitudes above 320 km the ratio is significantly larger than 1 throughout the time interval of the solutions, and particularly during the first 10 hours, the approximate duration of SAR-arcs.

Figure 3-18 shows the ratio  $k_e/k_B$  versus altitude for five time steps. It is seen in the figure that for a given time step the ratio is relatively constant with altitude for altitudes above 500 km. There is a large variation of the ratio with altitude between 280 km and 500 km, the region of the atmosphere where diffusion becomes the dominant process. This figure shows that the deviations from a Boltzmann solution are noticeable for altitudes as low as 300 km.

Figures 3-19 and 3-20 show the effective rate constant, calculated from equation 3-1 using the  $\psi$  and  $\phi_i$  equation solutions, versus time and altitude, respectively. These figures show that the rate constant can be factors of 2 to 8 times larger than

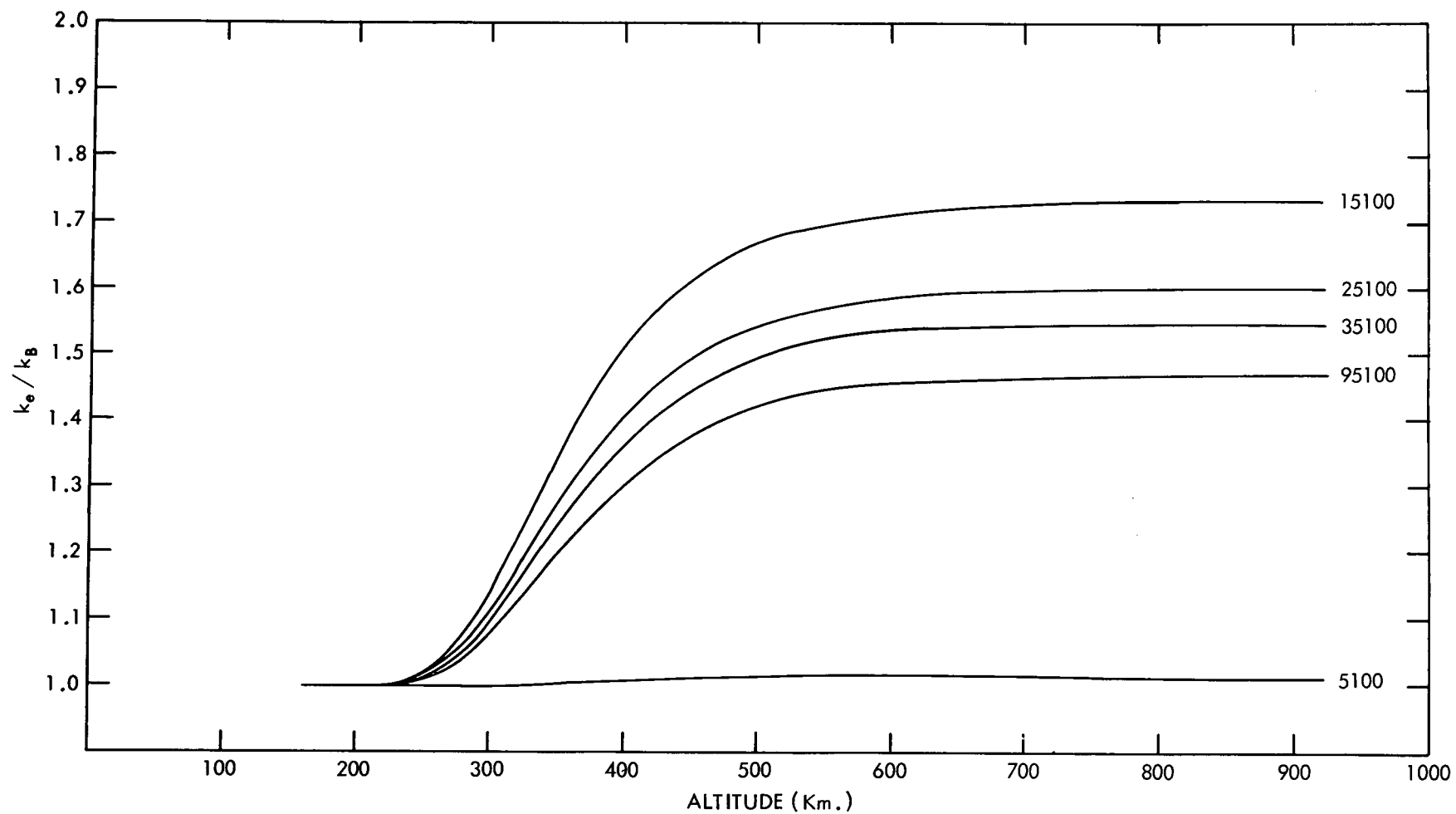


Figure 3-18. Ratio of the effective to the energetically equivalent reaction constant,  $k_e/k_B$ , versus altitude for five time steps

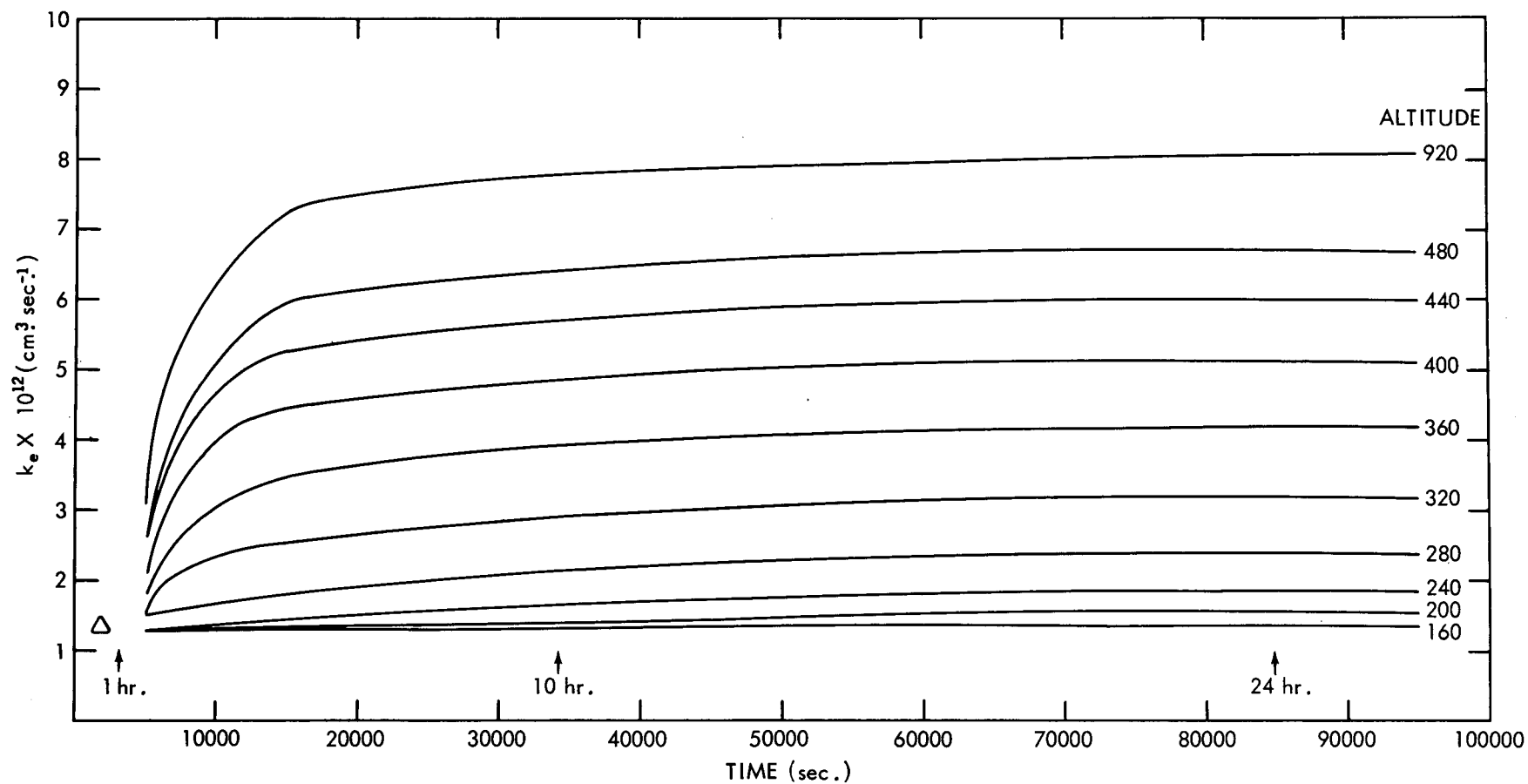


Figure 3-19. Effective reaction rate constant versus time for several altitudes



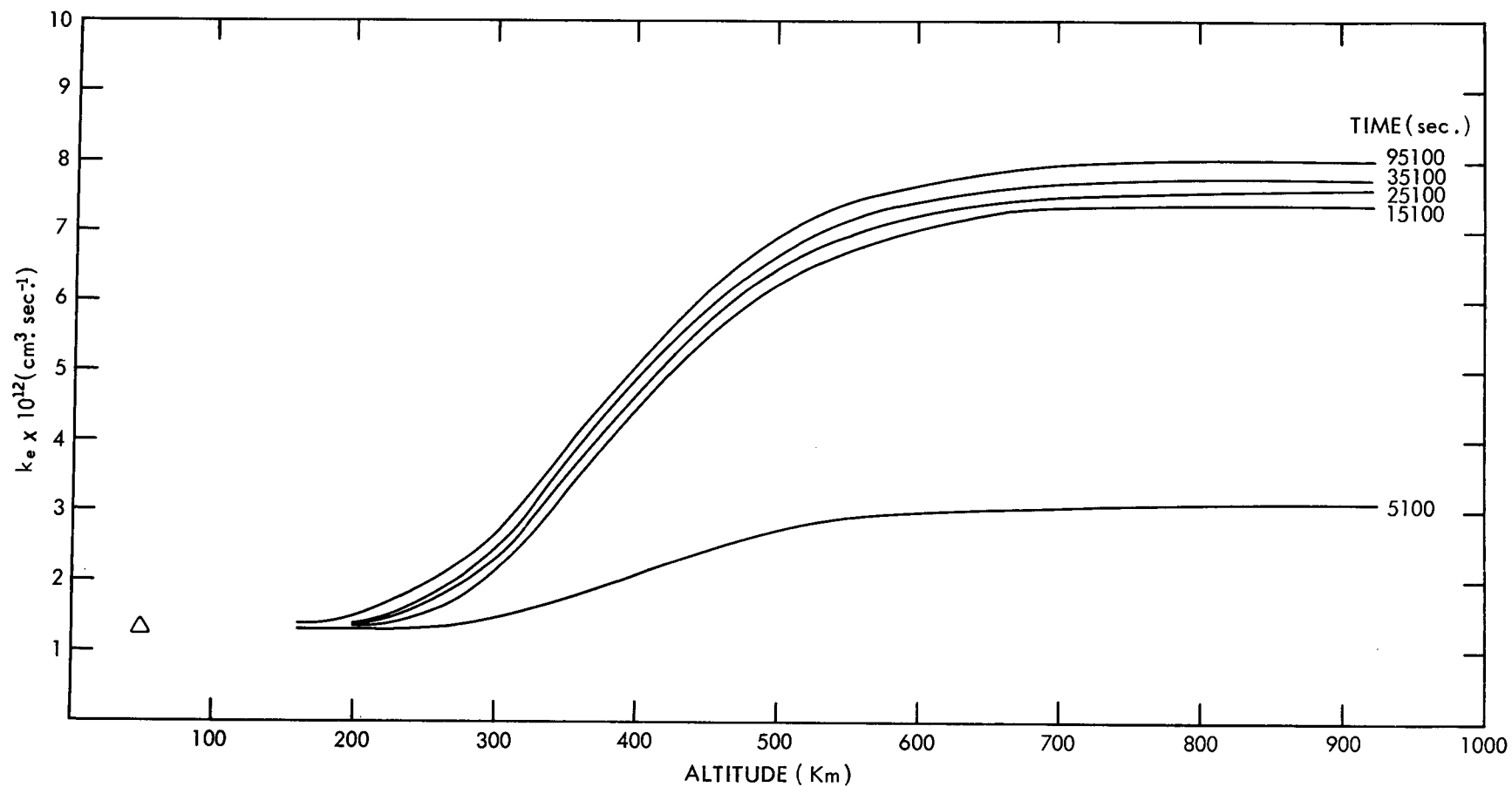


Figure 3-20. Effective reaction rate constant versus altitude for five time steps

the value for vibrational temperatures near 300°K (shown as a triangle in the two figures).

The  $k_e$  values, shown in Figures 3-19 and 3-20, have been used to calculate the loss rate for the ionospheric electrons and the ionospheric "loss time constant" in the following way. Assuming reaction (1-2) is infinitely fast, then the electron loss rate will be the same as the  $O^+$  ion loss rate. Further assuming the electron density and the  $O^+$  ion density are the same, we have

$$\frac{d n_e}{d t} = - k_e n n_e \quad (3-2)$$

where  $n_e$  is the electron density. The loss rate for the electrons is defined from (3-2) to be

$$\frac{1}{\tau} = k_e n \quad (3-3)$$

where  $\tau$  is the ionospheric loss time constant.

Figure 3-21 and 3-22 show the loss time constant calculated from (3-3) versus altitude and time respectively. In Figure 3-21 the loss rate for four time steps and the "normal" (vibrational temperature of 300°K) ionospheric time constant are shown. Noticeable decreases in the ionospheric loss time constant from the "normal" value is observed at altitudes as low as 280 km.

Figure 3-22 shows the loss time constant versus time for several altitudes where the time constant is one day or less. It is seen from the figure that in the first 10 hours, the time constant at 360 km. altitude, where the "normal" value is approximately 90 minutes, decreases to a value of 30 minutes. This figure shows

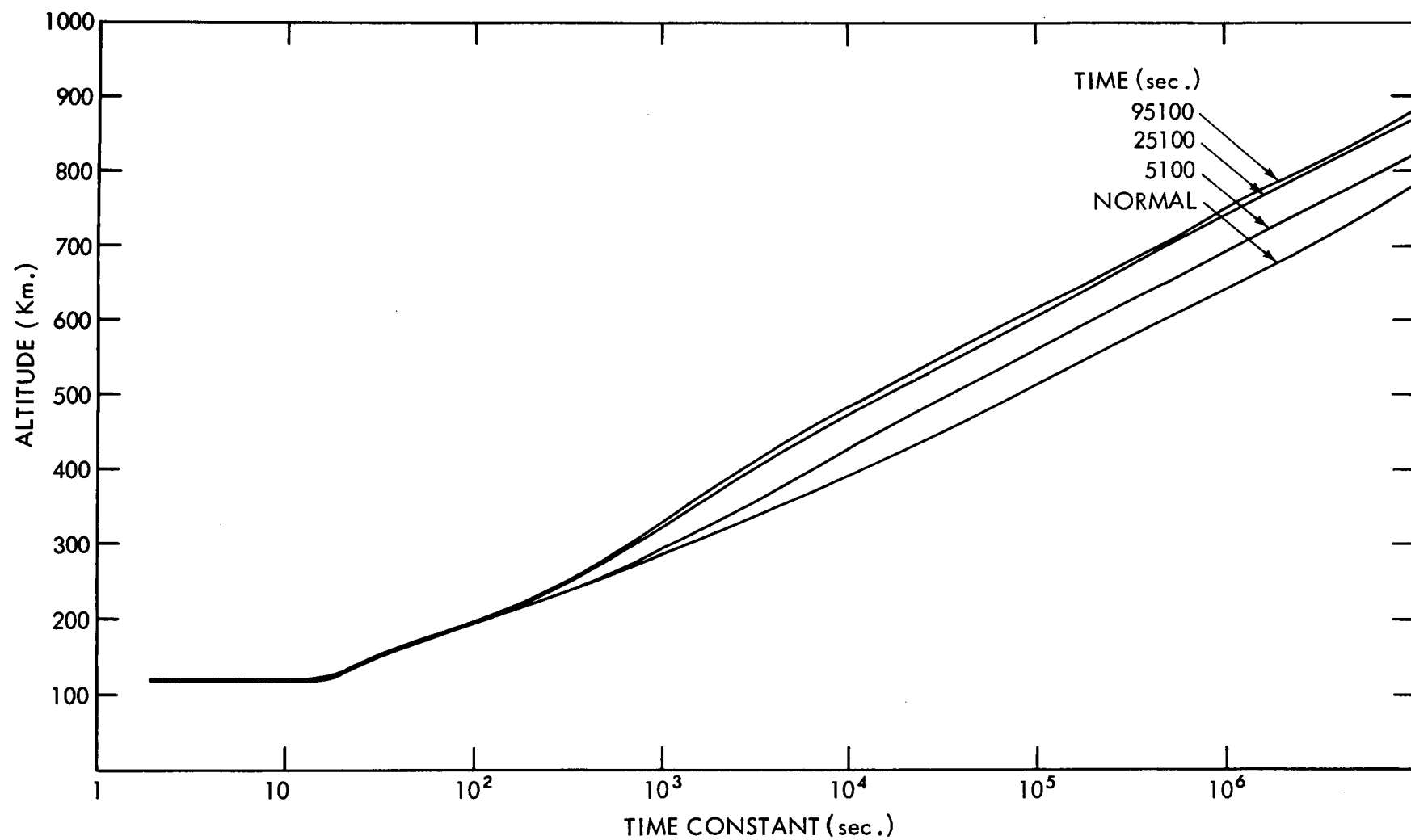


Figure 3-21. Ionospheric loss time constant versus altitude for four time steps

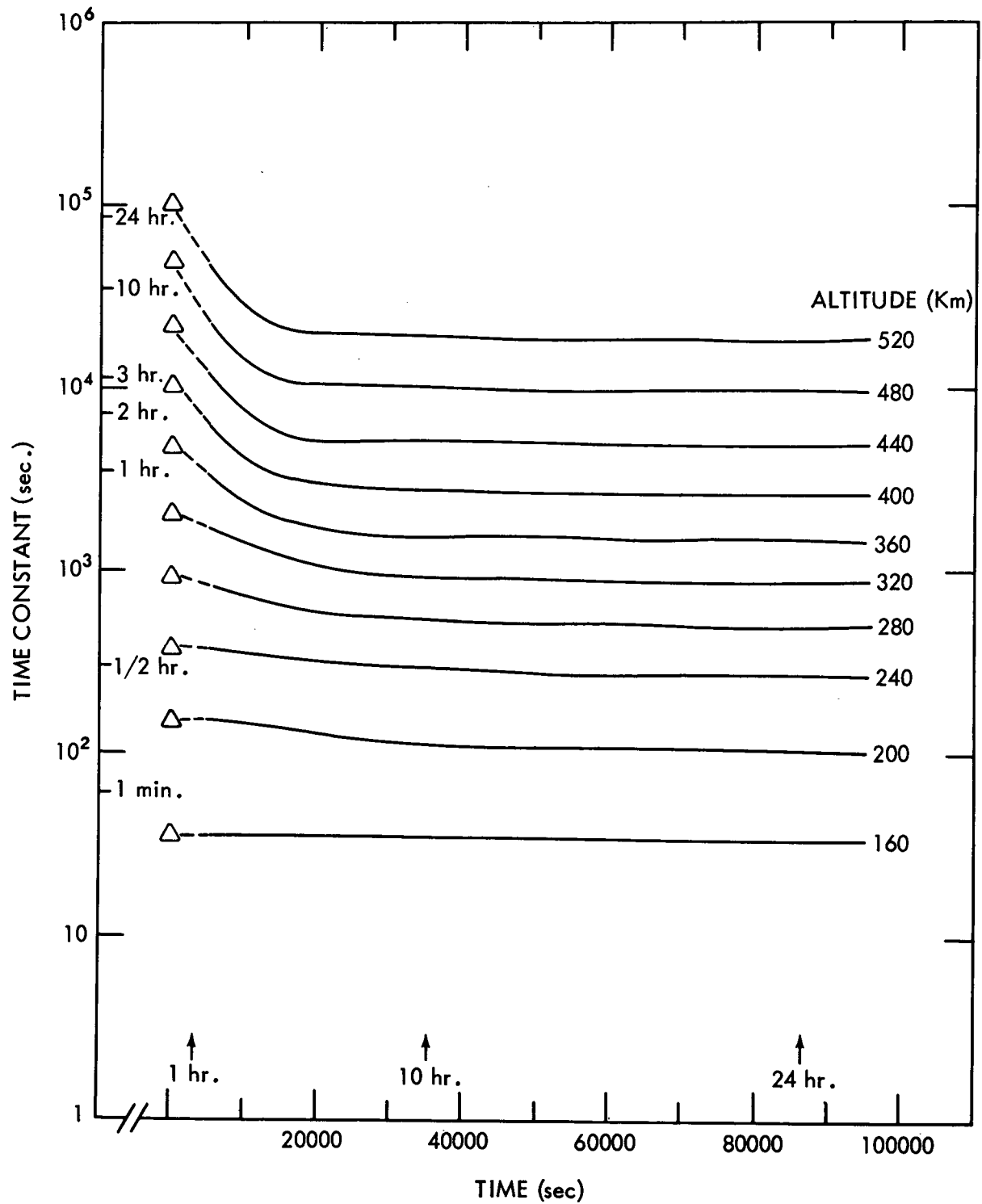


Figure 3-22. Ionospheric loss time constant versus time for altitudes where the time constant is 24 hours or less

that the ionospheric loss time constant is decreased by factors larger than three in altitude regions between 360 km and 440 km where the ionospheric loss time constant is measured in hours.

### 3.4 The effects of: neglect of $\epsilon_j/n$ ; boundary conditions; and atomic oxygen loss process.

To determine the effect of the approximation of neglecting the  $\epsilon_j/n$  term in the right hand side of the  $\psi$  equation, (A2-30), the solutions of the  $\phi_i$  equations were used to calculate the  $\epsilon_j/n$  terms. Equation (A2-30) was then solved using those  $\epsilon_j/n$  terms. The second approximation to  $\psi$  was then used to recalculate the  $\phi_i$  's.

The second approximation to  $\psi$  yielded a vibrational temperature which was different from that obtained from the first approximation by 67°K, or less, at higher altitudes. At lower altitudes the difference was only a few degrees. The  $\sum_{i=0}^1 \epsilon_i$  terms from the new solutions were also reduced by as much as a factor of 3. Thus, as expected on the basis of the  $\sum_{i=0}^1 \epsilon_i$  results from the first solution, the second approximation to  $\psi$  produces only a few percent correction to the results of the first approximation. The  $\epsilon_i$  's calculated from the second approximation differed from those of the first approximation by 30%, or less, with most of the difference occurring at altitudes below 360 km. The  $\sum_{i=0}^1 \epsilon_i$  term changed by a few tens of percent only. It is concluded, that the second approximation produces a negligible correction to the  $\psi$  equation. Because most of the influence of the  $\epsilon_i$  's is at altitudes above 300 km. (see section 3.3), the second approximation to the  $\epsilon_i$  's is different from the first by only several percent in its impact on the ionospheric electron loss rates, and is therefore also negligible.

The  $\psi$  and  $\phi_i$  equations were resolved using set 1 boundary conditions. It was found that the vibrational temperature calculated from the  $\psi$  equation solution differed from that obtained using set 2 boundary conditions by only a few degrees. The  $\epsilon_i$  results differed by less than 3%. These results indicate that the solutions are not sensitive to the details of the loss mechanisms at the lower boundary.

An interesting result was obtained by comparing the behavior of the solutions with and without inclusion of the atomic oxygen production and loss processes for vibrational excitation, for set 1 boundary conditions (that is  $T_v(120, t) = T_v(z, 0) = 0^\circ\text{K}$ ). The solution including the oxygen process yielded vibrational temperatures that were larger at all altitudes than those obtained from solutions not including the atomic oxygen processes. The largest differences between the two solutions initially occurred at altitudes below 320 km and was greater than  $150^\circ\text{K}$ . This location for the differences is expected because this is the altitude region where the oxygen effects are relatively the most important. This result can be explained by the fact that the boundary condition of  $0^\circ\text{K}$  vibrational temperature causes the initial vibrational temperatures to be less than the gas temperature, thus the atomic oxygen is a source of vibrational excitation through translational-vibrational energy exchange. Eventually the electronic source of vibrational energy dominates the solution. In the "steady state" the vibrational temperature corresponding to the solution with no atomic oxygen processes has a vibrational temperature only  $8^\circ\text{K}$  greater at 160 km altitude and  $6^\circ\text{K}$  greater at 920 km altitude than that corresponding to the solution containing the atomic oxygen processes.

A comparison of the  $\phi_i$  equation solutions for these two cases is complex. At altitudes below 280 km, the  $\epsilon_i$  initially changed by factors as large as 30 and 40

with the largest values of  $\epsilon_i$  corresponding to the solutions containing the oxygen processes. Above 320 km altitude the two solutions for the  $\epsilon_i$  's differ by approximately 25% or less. The  $\epsilon_i$  's of the upper two energy levels show the smallest differences between the two solutions. The two sets of solutions for the  $\epsilon_i$  's approach the same values in the steady state. The influence of the differences in the two sets of solutions on the ionospheric loss rates is small because the large differences occur below 320 km. altitude where the deviations from the Boltzmann part of the solutions play a small part in the determination of the reaction rate constant.

## CHAPTER IV. SUMMARY AND CONCLUSIONS

The objective of this work was to determine if the observed decrease in ionospheric electron density occurring in SAR-arcs could be explained by an increase in the reaction constant for the rate determining ion-atom interchange reaction (1-1). The increase in the reaction constant is due to vibrational excitation of molecular nitrogen by subexcitation, inelastic collisions between ambient, thermal, electrons and nitrogen molecules. The finding of this work is that the vibrational excitation of molecular nitrogen is indeed important to the ionosphere under SAR-arc conditions and can cause the loss time constant for the  $F_2$  region to change to lower values by factors of 1.6 to 5 with an attendant decrease in the electron density.

Previous work, (20), (22) on the related problem of the diurnal variation of the molecular nitrogen vibrational temperature assumed the vibrational distribution to be Boltzmann and considered diffusion processes. Earlier work (23) in the vertical distribution of vibrationally excited molecular nitrogen in aurora ignored diffusion and solved the continuity equations for the excited energy levels of molecular nitrogen. This work solves the continuity equations for the first six energy levels of molecular nitrogen including the diffusion process. Thus, it combines into one solution, the previous approaches.

The continuity equations to be solved are six, coupled, mildly non-linear, partial differential equations containing the dominant source and loss terms for vibrational excitation of molecular nitrogen. The solutions were divided into an energetically equivalent part that is Boltzmann distributed and a part representing deviations from the Boltzmann solution. The resulting equations were solved



numerically, using finite difference equations, to provide the populations of the energy levels as functions of time and altitude.

It was found, under conditions where the ionospheric electron temperature reaches values near 5000°K at 500 km altitude, that the vibrational temperature of molecular nitrogen reached a steady state value near 2300°K. at that altitude. The deviations from the Boltzmann distribution depends strongly on altitude for altitudes below 400 km. This is the region of the atmosphere where the diffusion process becomes dominant with increasing altitude over the vibrational-vibrational energy exchange process. It was found that for the highest three energy levels, above 300 km. altitude, the deviations from a Boltzmann distribution increased the populations of these levels by factors of 2 to 10. These results were insensitive to plausible variations of the boundary conditions.

The deviations from a Boltzmann distribution caused the effective reaction rate for reaction (1-1) to be increased by as much as a factor of 1.7 over the value obtained from the energetically equivalent Boltzmann solution. This indicates the possible importance of these deviations in problems involving chemical reactions at altitudes as low as 500 km. The effective reaction rate, calculated using the total population densities, was as much as a factor of 8 greater than the reaction rate for a vibrational temperature of 300°K. Significant enhancements of the reaction rate were found to occur at altitudes as low as 300 km.

Because of these increased reaction rates, the times required to significantly decrease the electron density in the ionosphere were reduced from their normal value by factors of 1.6 to 5, depending on altitude. Over most of the altitude range

where the loss time is short compared to SAR-arc durations, the loss time was reduced by factors exceeding 1.8.

These results lead to the conclusions that the vibrational excitation of molecular nitrogen, under conditions corresponding to SAR-arcs, causes a large increase in the loss rate of ionospheric electrons in the  $F_2$  region. The enhanced loss rate is of such magnitude, that it alone will account for the observed electron density depressions in SAR-arcs.

## REFERENCES

1. Barbier, D., "L'Activite aurorale aux basses latitudes," *Ann. Geophys.*, 14, 334, 1958.
2. Roach, F. E. and Roach, J. R., "Stable 6300 Å auroral arcs in mid-latitudes," *Planet. Space Sci.*, 11, 523, 1963.
3. Nagy, A. F., Roble, R. G., Hays, P. B., "Stable mid-latitude red arcs: observations and theory," *Space Science Rev.*, 11, 709, 1970.
4. Cole, K. D., "Stable auroral red arcs; sinks for energy of  $D_{st}$  main phase," *J. Geophys. Res.*, 70, 1689, 1965.
5. Roble, R. G., Hays, P. B., and Nagy, A. F., "Comparison of calculated and observed features of a stable midlatitude red arc," *J. Geophys. Res.*, 75, 4261, 1970.
6. Roble, R. G., Norton, R. B., Findlay, J. A., and Marovich, E., "Calculated and observed features of stable auroral red arcs during three geomagnetic storms," *J. Geophys. Res.*, 76, 7648, 1971.
7. Chandra, S., Maier, E. J., Troy, Jr., B. E. and Narasinga Rao, B. C., "Sub-auroral red arcs and associated ionospheric phenomena," *J. Geophys. Res.*, 76, 920, 1971.
8. Nagy, A. F., Hanson, W. B., Hoch, R. J., Aggson, T. L., "Satellite and ground-based observations of a red arc," *J. Geophys. Res.*, 77, 3613, 1972.
9. Norton, R. B. and Findlay, J. A., "Electron Density and temperature in the vicinity of the 29 September 1967 middle latitude red arc," *Planet. Space Sci.*, 17, 1867, 1969.

10. Roble, R. G., "A theoretical and experimental study of the stable mid-latitude red arc (SAR-ARC)," Ph.D. Thesis, University of Michigan, 1969.
11. Rishbeth, H. and Garriott, O. K., Introduction to Ionospheric Physics, 106, Academic Press, New York, 1969.
12. Schmeltekopf, A. L., Fehsenfeld, F. C., Gilman, G. I. and Ferguson, E. E., "Reaction of atomic oxygen ions with vibrationally excited nitrogen molecules," *Planet. Space Sci.*, 15, 401, 1967.
13. Schmeltekopf, A. L., Ferguson, E. E. and Fehsenfeld, F. C., "Afterglow studies of the reactions  $\text{He}^+$ ,  $\text{He}(2^3\text{S})$ , and  $\text{O}^+$  with vibrationally excited  $\text{N}_2$ ," *J. Chem. Phys.* 48, 2966, 1968.
14. Jacchia, L. G., "The temperature above the thermopause," *Space Res.*, 5, 1152, 1965.
15. Dalgarno, A., "Vibrationally excited molecules in atmospheric reactions," *Planet. Space Sci.*, 10, 19, 1963.
16. Dalgarno, A., McElroy, M. B., and Moffett, R. J., "Electron temperatures in the ionosphere," *Planet. Space Sci.*, 11, 463, 1963.
17. Hunten, D. M., "Some photometric observations of auroral spectra," *J. Atmos. Terr. Phys.*, 7, 141, 1955.
18. Thomas, L. and Norton, R. B., "Possible importance of internal excitation in ion-molecule reactions in the F region," *J. Geophys. Res.*, 71, 227, 1966.
19. Walker, J.C.G., "Electron and nitrogen vibrational temperature in the E-region of the ionosphere," *Planet. Space Sci.*, 16, 321, 1968.
20. Walker, J.C.G., Stolarsky, R. S. and Nagy, A. F., "The vibrational temperature of molecular nitrogen in the thermosphere," *Ann. Geophys.*, 25, 831, 1969.

21. McNeal, R. J., Whitson, Jr., M. E. and Cook, G. R., "Quenching of vibrationally excited  $N_2$  by atomic oxygen," The Aerospace Corporation SPL 3303, L. A. Cal., July 1972.
22. Breig, E. L., Brennan, M. E. and McNeal, R. J., "Effect of atomic oxygen upon the  $N_2$  vibrational temperature in the lower thermosphere," the Aerospace Corporation SPL Report 3301, L. A. Cal, July 1972.
23. Schunk, R. W. and Hays, P. B., "Theoretical  $N_2$  Vibrational Distribution in an Aurora," Planet. Space Sci., 19, 1457, 1971.
24. Walker, J.C.G., "Oxygen and Nitrogen Vibration in the Thermosphere," paper presented at Summer Advanced Study Institute, Physics and Chemistry of Upper Atmosphere, Univ. of Orléans, Orléans, France, 9 August 1972.
25. Kummler, R. H. and Bortner, M. H., "Vibrational temperatures in the E and F regions," Space Research XII, 711, Akademie-Verlag, Berlin, West Germany, 1972.
26. Bauer, E., Kummler, R. and Bortner, M. H., "Internal energy balance and energy transfer in the lower thermosphere," App. Optics, 10, 1861, 1971.
27. Herzfeld, K. F. and Litovitz, T. A., Absorption and dispersion of ultrasonic waves, Academic Press, New York, 1959.
28. Chen, J.C.Y., "Theory of subexcitation electron scattering by molecules. I. formalism and the compound negative ion states," J. Chem. Phys., 40, 3507, 1964.
29. Chen, J.C.Y., "Theory of subexcitation electron scattering by molecules. II. excitation and de-excitation of molecular vibration," J. Chem. Phys., 40, 3513, 1964.

30. Chen, J.C.Y., "Erratum: theory of subexcitation electron scattering by molecules. II. excitation and de-excitation of molecular vibration," J. Chem. Phys., 41, 1964.
31. Treanor, C. E., Rich, J. W. and Rehm, R. G., "Vibrational relaxation of anharmonic oscillators with exchange-dominated collisions," J. Chem. Phys., 48, 1798, 1968.
32. Fisher, E. R. and Kummler, R. H., "Relaxation by vibration-vibration exchange processes. part 1, pure gas case," J. Chem. Phys., 49, 1075, 1968.
33. Sharp, F. E. and Rapp, D., "Evaluation of approximations used in the calculation of excitation by collision. I. vibrational excitation of molecules," J. Chem. Phys., 43, 1233, 1965.
34. Hirschfelder, J. O., Curtiss, C. F. Bird, R. B., Molecular theory of gases and liquids, John Wiley and Sons, New York, 1954.
35. Chapman, S. and Cowling, T. G., "The mathematical theory of non-uniform gases", Cambridge Univ. Press, London, 2nd edition, 1960.
36. Richtmyer, R. D., Difference methods for initial-value problems, Interscience publishers, Inc., New York, 1957.
37. Feshback, H., "Unified theory of nuclear reactions," Ann. Phys., 5, 357, 1958.
38. Davydov, A. S., Quantum Mechanics, trans. by D. ter Haar, Pergamon press, New York, 1965.

TABLE 1

Cross Sections used from Reference (30) in Equation (A1-19)

Cross-Section	Comment
$\sigma_{10}$	Numerical data available
$\sigma_{20}$	Numerical data available
$\sigma_{03}$	Numerical data available
$\sigma_{04}$	Numerical data available
$\sigma_{50}$	All that is available
$\sigma_{12}$	All that is available
$\sigma_{13}$	All that is available
$\sigma_{14}$	All that is available
$\sigma_{51}$	All that is available
$\sigma_{23}$	All that is available
$\sigma_{24}$	All that is available
$\sigma_{52}$	All that is available
$\sigma_{34}$	All that is available
$\sigma_{53}$	All that is available
$\sigma_{54}$	All that is available

TABLE 2

Parameters for Reaction Rate Constants for Production and

Loss of Vibrational Excitation by Electron Collisions

I.D.	P1	P2	P3	P4	Max Error %
10	-1.837483E01	-2.218530E04	1.684328E07	-4.558864E09	-19@2500°
20	-1.887149E01	-1.851033E04	-1.317388E06	2.310335E09	-37@1500°
50	-2.004471E01	-1.797215E04	-6.671288E06	2.076589E09	-14@2000°
51	-2.025835E01	-1.628830E04	-2.509007E06	7.790528E08	- 5@1500°
12	-1.874858E01	-1.222789E04	1.102594E07	-2.993175E09	14@5000°
52	-1.974898E01	-1.314905E04	-2.739562E06	9.167196E08	- 9@1500°
03	-1.950456E01	-5.705000E03	-6.362043E06	1.917276E09	-13@1500°
13	-1.972427E01	-4.652598E03	-6.585213E06	1.931419E09	-12@1500°
23	-1.939743E01	-8.030383E03	5.607227E06	-1.257535E09	-16@2000°
53	-1.980759E01	-8.800227E03	-2.526216E06	9.740170E08	-12@1500°
04	-1.964117E01	-3.913067E03	-5.735326E06	1.842685E09	-13@1500°
14	-2.019481E01	-3.588698E03	-4.862049E06	1.688892E09	- 9@1500°
24	-1.999716E01	-4.421176E03	-3.194914E06	1.243446E09	-10@1500°
35	-1.943835E01	-4.869426E03	2.078704E06	-1.935087E08	-15@1500°
54	-1.983298E01	-4.700520E03	-4.217622E05	4.723745E08	-14@1500°



TABLE 3

Reaction Rates for Vibrational Levels

Level	$k_v$ [cm. <sup>3</sup> sec. <sup>-1</sup> ]
0	$1.3 \times 10^{-12}$
1	$1.3 \times 10^{-12}$
2	$5.0 \times 10^{-11}$
3	$1.20 \times 10^{-10}$
4	$2.6 \times 10^{-10}$
5	$3.6 \times 10^{-10}$
6	$4.4 \times 10^{-10}$
7	$4.6 \times 10^{-10}$
8	$4.6 \times 10^{-10}$
9	$4.6 \times 10^{-10}$
10	$4.6 \times 10^{-10}$
11	$4.6 \times 10^{-10}$

## ELECTRONIC PRODUCTION AND LOSS OF VIBRATIONAL EXCITATION

Production and loss rates for the first six vibrational levels of molecular nitrogen were calculated using theoretically calculated (28), (29), (30) cross-sections for inelastic, sub-excitation, electron scattering for these levels. The cross-sections were averaged over the Maxwell-Boltzmann energy distribution representing the electron gas to produce the production and loss rates. This section contains an amplified outline of the content of the theoretical cross-section calculations in Chen's, (28), (29) papers as well as discussion of the calculation of reaction rates.

Chen (28), (29) applies the unified theory of Feshbach (37), for nuclear reactions involving the formation of a compound state, to inelastic scattering of electrons by molecules. Hereafter Chen (28) will be called paper I and equations contained therein referenced as I X.XX. Chen (29) will be referenced as paper II and equations contained therein will be referenced as II X.XX.

A1.1 Paper I:

Paper I starts with the consideration of an N-electron system consisting of an incident electron and a diatomic target molecule with N-1 electrons. The system is separated into relative and center of mass coordinates and the center of mass part is removed from the Schrodinger equation. The relative coordinates for the electrons,  $\vec{X}$ ,  $\vec{r}_1$ ,  $\vec{r}_2$  . . . ,  $\vec{r}_{N-1}$  , are referenced to the center of mass of the nuclei. X refers to the incident electron.  $\vec{R}$  is the vector separation of the two heavy nuclei a and b with masses  $M_a$  and  $M_b$  respectively. The Schrodinger

equation is (in atomic units)

$$[K_0(\vec{X}) + V_0(\vec{X}, \vec{r}, \vec{R}) + H_{ab}(\vec{r}, \vec{R})] \Omega = E\Omega \quad (\text{I-2.1})$$

where

$$V_0(\vec{X}, \vec{r}, \vec{R}) = \sum_{i=1}^{N-1} \frac{1}{|\vec{X} - \vec{r}_i|} - \frac{Z_a}{X_a} - \frac{Z_b}{X_b} \quad (\text{I-2.2})$$

and  $\vec{r}$  is the collective notation of  $\vec{r}_1, \vec{r}_2, \dots, \vec{r}_{N-1}$  for the molecular electrons;  $K_0$  is the kinetic energy operator of the incident electron;  $V_0$  is the Coulombic potential energy of the incident electron;  $H_{ab}$  is the Hamiltonian for the target molecule;  $\Omega$  is the total wavefunction for the system having the total energy  $E$ ;  $X_a$  and  $X_b$  are the position vectors of the incident electron with respect to the two nuclei having  $Z_a$  and  $Z_b$  as their charges.

It is assumed that the unperturbed molecule is described by the set of Schrodinger equations

$$H_{e1}(\vec{r}, \vec{R}) \Phi_n(\vec{r}, \vec{R}) = \epsilon_n(R) \Phi_n(\vec{r}, \vec{R}) \quad (\text{I-2.3})$$

$$[-(2\mu)^{-1} \nabla_R^2 + \epsilon_n(R)] \chi_{n\gamma}(\vec{R}) = \epsilon_{n\gamma} \chi_{n\gamma}(\vec{R}) \quad (\text{I-2.4})$$

where

$$H_{e1}(\vec{r}, \vec{R}) = \frac{1 + M_a + M_b}{2(M_a + M_b)} \sum_{i=1}^{N-1} \nabla_i^2 + U_{e1}(\vec{r}, \vec{R}) \quad (\text{I-2.5})$$

and

$$\mu = \frac{M_a M_b}{M_a + M_b}; \quad \nabla_i^2$$

is the Laplacian operator on coordinate  $i$  and  $U_{e1}$  is the potential energy of the molecular electrons.

$$H_{ab}(\vec{r}, \vec{R}) = - (2\mu)^{-1} \nabla_{\vec{R}}^2 + H_{e1}(\vec{r}, \vec{R}) \quad (\text{I-2.6})$$

The cross terms for electrons and electron-nuclei contained in the Born-Oppenheimer separation are neglected because they do not enter, in the zeroth order approximation, in the expression for the excitation of nuclear motion, (34), pages 925-928. The electronic wavefunctions,  $\Phi_n$ , and nuclear wavefunctions  $\chi_{n\gamma}$  having eigenvalues  $\epsilon_n(R)$  and  $\epsilon_{n\gamma}$ , respectively, form a complete, orthogonal set in their corresponding spaces.

The total wavefunction is expanded in terms of  $\Phi_n$  and  $\chi_{n\gamma}$  to give

$$\Omega(\vec{X}, \vec{r}, \vec{R}) = \sum_{n,\gamma} \Phi_n(\vec{r}, \vec{R}) \chi_{n\gamma}(\vec{R}) \psi_{n\gamma}(\vec{X}) \quad (\text{I-2.7})$$

where exchange effects are neglected. The expansion coefficients  $\psi_{n\gamma}(\vec{X})$  are assumed not to depend on the inter-nuclear separation as a parameter. It is assumed that the inter-nuclear separation is fixed at its equilibrium value  $R_e^{(0)}$  for  $\psi_{n\gamma}(\vec{X})$ . The effect of this assumption is estimated to be of order  $\mu^{-1}$ .

Substituting equation (I-2.7) into the Schrodinger equation (I-2.1), multiplying on the left by  $\Phi_n^*$ ,  $\chi_{n'\gamma'}^*$ , integrating over  $\vec{r}$  and  $\vec{R}$  and using (I-2.3) through (I-2.6) we have the coupled sets of equations

$$[K_0(\vec{X}) + \epsilon_{n\gamma} - E] \psi_{n\gamma}(\vec{X}) = - \sum_{n',\gamma'} V_{nn'}^{\gamma\gamma'}(\vec{X}) \psi_{n'\gamma'}(\vec{X}) \quad (\text{I-2.8})$$

with

$$V_{nn'}^{\gamma\gamma'}(\vec{X}) = \langle \chi_{n\gamma} | V_{nn'}(\vec{X}, \vec{R}) - (2\mu)^{-1} C_{nn'}(R, \nabla_{\vec{R}}) | \chi_{n'\gamma'} \rangle \quad (\text{I-2.9})$$

$$V_{nn'}(\vec{X}, \vec{R}) = \langle \Phi_n | V_0(\vec{X}, \vec{R}, \vec{r}) | \Phi_{n'} \rangle \quad (\text{I-2.10})$$

$$C_{nn'} = 2 \langle \Phi_n | \nabla_R | \Phi_{n'} \rangle \cdot \nabla_R + \langle \Phi_n | \nabla_R^2 | \Phi_{n'} \rangle \quad (\text{I-2.11})$$

Because we are interested in subexcitation electron impact, the  $\psi_{0\gamma}$ 's are of particular interest. Thus writing (I-2.8) as

$$[K_0(\vec{X}) + \epsilon_{0\gamma} - E] \psi_{0\gamma}(\vec{X}) = - \sum_{\gamma'} V_{00}^{\gamma\gamma'} \psi_{0\gamma'}(\vec{X}) - \sum_{\substack{n', \gamma' \\ n' \neq 0}} \psi_{n'\sigma}(\vec{X}) \quad (\text{A1-1})$$

and

$$[K_0(\vec{X}) + \epsilon_{n\gamma} - E] \psi_{n\gamma}(\vec{X}) = - \sum_{\gamma'} V_{n0}^{\gamma\gamma'} \psi_{0\gamma'}(\vec{X}) - \sum_{\substack{n', \gamma' \\ n' \neq 0}} V_{nn'}^{\gamma\gamma'} \psi_{n'\gamma'}(\vec{X}) \quad (\text{A1-2})$$

for  $n \neq 0$ .

Rewriting (1) and (2) we have

$$[K_0(\vec{X}) + \epsilon_{0\gamma}] \psi_{0\gamma}(\vec{X}) + \sum_{\gamma'} V_{00}^{\gamma\gamma'} \psi_{0\gamma'}(\vec{X}) - E \psi_{0\gamma}(\vec{X}) = - \sum_{\substack{n', \gamma' \\ n' \neq 0}} V_{0n'}^{\gamma\gamma'} \psi_{n'\gamma'}(\vec{X}) \quad (\text{A1-3})$$

$$[K_0(\vec{X}) + \epsilon_{n\gamma}] \psi_{n\gamma}(\vec{X}) + \sum_{\substack{n', \gamma' \\ n' \neq 0}} V_{nn'}^{\gamma\gamma'} \psi_{n'\gamma'}(\vec{X}) - E \psi_{n\gamma}(\vec{X}) = - \sum_{\gamma'} V_{n0}^{\gamma\gamma'} \psi_{0\gamma'}(\vec{X}) \quad (\text{A1-4})$$

Defining

$$T_n = \begin{bmatrix} K_0 + \epsilon_{n0} & & \\ & K_0 + \epsilon_{n1} & 0 \\ & & K_0 + \epsilon_{n2} \\ 0 & & & \end{bmatrix} \quad (\text{I-2.14})$$

$$\psi_n = \begin{bmatrix} \psi_{n0} \\ \psi_{n1} \\ \psi_{n2} \\ . \\ . \\ . \end{bmatrix} \quad (\text{I-2.12})$$

$$\Psi = \begin{bmatrix} \psi_1 \\ \psi_2 \\ . \\ . \\ . \end{bmatrix} \quad (\text{I-2.15})$$

$$U_{nn'} = \begin{bmatrix} V_{nn'}^{00} & V_{nn'}^{01} & V_{nn'}^{02} & . & . \\ V_{nn'}^{10} & V_{nn'}^{11} & V_{nn'}^{12} & . & . \\ V_{nn'}^{20} & V_{nn'}^{21} & V_{nn'}^{22} & . & . \\ . & . & . & . & . \\ . & . & . & . & . \end{bmatrix} \quad (\text{I-2.13})$$

$$U_0 = (U_{01}, U_{02}, U_{03}, \dots) \quad (\text{I-2.16})$$

$$U'_0 = \begin{bmatrix} U_{10} \\ U_{20} \\ U_{30} \\ . \\ . \end{bmatrix} \quad (\text{I-2.17})$$

(3) and (4) become

$$T_0 \psi_0 + U_{00} \psi_0 - E \psi_0 = - \sum_{\substack{n' \\ n' \neq 0}} U_{0n'} \psi_n' = - U_0 \psi \quad (\text{I-2.19})$$

and

$$T_n \psi_n + \sum_{\substack{n' \\ n' \neq 0}} U_{nn'} \psi_n' - E \psi_n = - U_{n0} \psi_0$$

or

$$(H - E) \Psi = - U'_0 \psi_0 \quad (\text{I-2.20})$$

where

$$H = \begin{bmatrix} T_1 + U_{11} & U_{12} & U_{13} & \cdot & \cdot \\ U_{21} & T_2 + U_{22} & U_{23} & \cdot & \cdot \\ U_{31} & U_{32} & T_3 + U_{33} & \cdot & \cdot \\ \cdot & \cdot & \cdot & \cdot & \cdot \\ \cdot & \cdot & \cdot & \cdot & \cdot \end{bmatrix} \quad (\text{I-2.18})$$

and

$$E_{nn'} = E \delta_{nn'}$$

Following Fishbach's formalism, (37), the formal solution of (I-2.20) is

$$\Psi = (E - H + i\eta)^{-1} U'_0 \psi_0 \quad (\text{I-2.21})$$

where  $\eta = \eta \delta_{ij}$  and  $\eta \rightarrow 0^+$  to ensure outgoing waves in the exit channels, (I-2.21)

gives  $\psi$  in terms of  $\psi_0$ . Using (I-2.21) in (I-2.19), we obtain

$$(T_0 + \Lambda - E) \psi_0 = 0 \quad (\text{I-2.22})$$

where

$$\Lambda = U_{00} + U_0 (E - H + i\eta)^{-1} U'_0 \quad (\text{I-2.23})$$

and is the effective scattering potential for subexcitation scattering of electrons by molecules.

The formal solution (I-2.21) contains the Green's function operator  $\lim_{n \rightarrow 0^+} (E_1 - H + i\eta)^{-1}$  which implies the need for a set of eigenfunctions of the effective Hamiltonian  $H$ . Thus we write

$$H\Psi_m = W_m \Psi_m \quad (\text{I-3.2})$$

where a set of eigenfunctions  $\{\Psi_m\}$  approximates the set of compound negative ion eigenfunctions with energy spectrum  $\{W_m\}$ .

The physical significance of these states is illustrated in the weak coupling limit where  $H$  is diagonal. In this case (I-3.2) gives the equations

$$(T_n + U_{nn}) \psi_n^{(m)} = W_n^{(m)} \psi_n^{(m)} \quad n \neq 0 \quad (\text{I-3.3})$$

which is expanded further to become

$$[K_0 + V_{nn}^{\gamma\gamma} + \epsilon_{n0} - W_{n\gamma}^{(m)}] \psi_{n\gamma}^{(m)} = - \sum_{\gamma' \neq \gamma} V_{nn}^{\gamma\gamma'} \psi_{n\gamma'}^{(m)} \quad (\text{I-3.4})$$

The compound negative ion states  $\psi_n^{(m)}$  describe, in this instance, a set of states of the incident electron in resonance with the field of the excited target molecule.

Expanding the Green's function operator contained in (I-2.21) in terms of the eigenfunctions  $\Psi_m$  we have



$$G^{(+)}(E) = \sum_m \frac{|\Psi_m\rangle \langle \Psi_m|}{E - W_m} + \int d\rho \int dW \frac{|\Psi(\rho, W)\rangle \langle \Psi(\rho, W)|}{E - W + i\eta} \quad (I-4.1)$$

where the sum over  $m$  is for the discrete states and the integral over  $\rho$  contains the continuous eigenspectrum for energy  $E$ . Expression (I-4.1) implies a resonance part of the operator and a non-resonance part. Therefore we write

$$G^{(+)}(E) = Q(E) + G_0^{(+)}(E) \quad (I-4.2)$$

with

$$Q(E) = \sum_m \frac{|\Psi_m\rangle \langle \Psi_m|}{E - W_m} \quad (I-4.3)$$

$Q(E)$  is the resonance part of the operator and the prime means that only those negative ion states having energies comparable to that of the system are included in the summation. The effective potential (I-2.23) is now written, using (I-4.2) in (I-2.23) as

$$\Lambda = u' + u \quad (I-4.4)$$

where

$$u' = U_0 Q(E) U'_0 \quad (I-4.5)$$

$$u = U_{00} + U_0 G_0^{(+)}(E) U'_0 \quad (I-4.6)$$

Let  $\pi_0^{(-)}$  be the solution for an outgoing wave of the equation

$$(T_0 - E) \pi_0^{(-)} = 0$$

Using (I-4.4) in (I.22) we have

$$(T_0 + U - E) \psi_0 = -u' \psi_0 \quad (\text{A1-5})$$

where the resonance part of the effective scattering potential is treated as the scattering potential.

From scattering theory, (38), Chapter 12, the solution for the outgoing wave is

$$\psi_0 = \psi_0^{(+)} + (E - T_0 - u + i\eta)^{-1} u' \psi_0 \quad (\text{I-4.12})$$

where

$$(T_0 + u - E) \psi_0^{(+)} = 0 \quad (\text{I-4.10})$$

and  $\psi_0^{(+)}$  is an incoming wave and contains the effects of the direct scattering potential  $u$ .

The transition matrix describing transitions from the incident channel  $\gamma'$  to channel  $\gamma$  for  $n = 0$  is

$$\mathfrak{S}_0(\gamma, \gamma') = \langle \pi_0^{(-)}(\gamma) | u + u' | \psi_0(\gamma') \rangle \quad (\text{I-4.13})$$

Consider the outgoing wave solutions to

$$(T_0 + u - E) \psi_0^{(-)} = 0 \quad (\text{A1-6})$$

which may be written as

$$\psi_0^{(-)} = \pi_0^{(-)} + (E - T_0 - i\eta)^{-1} u \psi_0^{(-)} \quad (\text{I-4.14})$$

Multiplying by  $(E - T_0 - i\eta)$  and adding and subtracting  $u\pi_0^{(-)}$  to the right hand side we have

$$(E - T_0 - i\eta) \psi_0^{(-)} = (E - T_0 - i\eta) \pi_0^{(-)} + u\psi_0^{(-)} + u\pi_0^{(-)} - u\pi_0^{(-)} \quad (\text{A1-7})$$

$$\therefore \psi_0^{(-)} = \pi_0^{(-)} + (E - T_0 - u - i\eta)^{-1} u \pi_0^{(-)} \quad (\text{I-4.15})$$

$$\therefore \pi_0^{(-)} = \psi_0^{(-)} - (E - T_0 - u - i\eta) u \pi_0^{(-)} \quad (\text{A1-8})$$

Substituting (A-1-8) in (I-4.13) we have

$$\mathfrak{I}_0(\gamma, \gamma') = \langle \pi_0^{(-)} | u | \psi_0 \rangle - \langle (E - T_0 - u - i\eta)^{-1} u \pi_0^{(-)} | u' | \psi_0 \rangle \quad (\text{I-4.16})$$

$$+ \langle \psi_0^{(-)} | u' | \psi_0 \rangle$$

$$= \langle \pi_0^{(-)} | u | \psi_0 - (E - T_0 - u + i\eta)^{-1} u' \psi_0 \rangle$$

$$+ \langle \psi_0^{(-)} | u' | \psi_0 \rangle \quad (\text{A1-9})$$

$$= \langle \pi_0^{(-)} | u | \psi_0^{(+)} \rangle + \langle \psi_0^{(-)} | u' | \psi_0 \rangle \quad (\text{I-4.17})$$

using (I-4.12). Consider  $\langle \psi_0^{(-)} | u' | \psi_0 \rangle$  and repeatedly substitute (I-4.12) for  $\psi_0$  to obtain

$$\begin{aligned} \langle \psi_0^{(-)} | u' | \psi_0 \rangle &= \langle \psi_0^{(-)} | u' | \psi_0^{(+)} \rangle + \langle \psi_0^{(-)} | u' (E - T_0 - u + i\eta)^{-1} u' | \psi_0 \rangle \\ &= \langle \psi_0^{(-)} | u' | \psi_0^{(+)} \rangle + \langle \psi_0^{(-)} | u' (E - T_0 - u + i\eta)^{-1} u' | \psi_0^{(+)} \rangle \\ &\quad + \langle \psi_0^{(-)} | u' (E - T_0 - u + i\eta)^{-1} u (E - T_0 - u + i\eta)^{-1} u' | \psi_0^{(+)} \rangle \\ &\quad + \dots \\ &= \langle \psi_0^{(-)} | u' + u' (E - T_0 - u + i\eta)^{-1} u' + u' (E - T_0 - u + i\eta)^{-1} u' \\ &\quad \cdot (E - T_0 - u + i\eta)^{-1} u' + \dots | \psi_0^{(+)} \rangle \end{aligned} \quad (\text{A1-10})$$

For an isolated resonance, the summation over  $m$  in (I-4.3) reduces to one term and (I-4.5) becomes

$$u' = \frac{U_0 |\Psi_m\rangle \langle \Psi_m| U'_0}{E - W_m} \quad (\text{A1-11})$$

Thus (11) becomes

$$\begin{aligned} \langle \psi_0^{(-)} | u' | \psi_0 \rangle &= \frac{\langle \psi_0^{(-)} | U_0 | \Psi_m \rangle \langle \Psi_m | U'_0 | \psi_0^{(+)} \rangle}{E - W_m} \\ &\quad \left\{ 1 + \frac{\langle \Psi_m | U'_0 (E - T_0 - u + i\eta)^{-1} U_0 | \Psi_m \rangle}{E - W_m} + \dots \right\} \end{aligned}$$

Let

$$R_m = \langle \Psi_m | U'_0 (E - T_0 - u + i\eta)^{-1} U_0 | \Psi_m \rangle \quad (\text{I-4.23})$$

Therefore

$$\begin{aligned} \langle \psi_0^{(-)} | u' | \psi_0 \rangle &= \frac{\langle \psi_0^{(-)} | U_0 | \Psi_m \rangle \langle \Psi_m | U'_0 | \psi_0^{(+)} \rangle}{E - W_m} \\ &\quad \left\{ 1 + \frac{R_m}{E - W_m} + \frac{R_m^2}{E - W_m} + \dots \right\} \\ &= \frac{\langle \psi_0^{(-)} | U_0 | \Psi_m \rangle \langle \Psi_m | U'_0 | \psi_0^{(+)} \rangle}{E - W_m - R_m} \quad (\text{I-4.24}) \end{aligned}$$

## A1.2 Paper II.

In his application to molecular nitrogen, (29), Chen makes the following assumptions:

- (1) an isolated resonance occurs.
- (2) the direct transition amplitude is negligible.

- (3) a single excited electronic state,  $n$ , of the target molecule is responsible for the resonance.
- (4) the nuclear states of the target molecule are not strongly coupled and the Born-Oppenheimer coupling matrix elements are negligible.
- (5) the total contribution to the transition amplitudes due to resonance effects of the set of compound negative-ion states may be accounted for as a linear sum of the individual contribution of each compound state.

From assumptions (1) and (2) equation (I-4.24) gives the transition matrix element. Thus

$$\mathfrak{D}_0(\gamma, \gamma') = \frac{\langle \psi_0^{(-)}(\gamma) | U_0 | \Psi_m \rangle \langle \Psi_m | U'_0 | \psi_0^{(+)}(\gamma') \rangle}{E - W_m - R_m} \quad (\text{II-2.2})$$

From assumption (3) only  $V_{on}$ ,  $V_{no}$ ,  $V_{nn}$  and  $V_{oo}$  in equation (I-2.10) are non-zero. Thus  $H$  in equation (I-2.18) becomes a single element matrix. Assumption (4) gives from equations (I-2.11) and (I-2.9) respectively

$$C_{nn'} = 0 \quad \text{and} \quad V_{nn}^{\gamma\gamma'} = 0$$

Thus  $U_{nn}$  in equation (I-2.13) is diagonal. Therefore we have

$$H\Psi_m = W_m \Psi_m$$

giving

$$H_n \psi_n^{(m)} = W_n^{(m)} \psi_n^{(m)}$$

or

$$(T_n + U_{nn}) \psi_n^{(m)} = W_n^{(m)} \psi_n^{(m)} \quad (\text{A1-12})$$

where

$$\psi_n^{(m)}(\lambda) = \begin{bmatrix} 0 \\ 0 \\ \vdots \\ \psi_{n\lambda}^{(m)} \\ 0 \\ \vdots \\ \cdot \end{bmatrix}$$

Expanding (A1-12) further and rearranging terms

$$\begin{aligned} [K_0 + V_{nn}^{\lambda\lambda}] \psi_{n\lambda}^{(m)} &= (W_{n\lambda}^{(m)} - \epsilon_{n0}) \psi_{n\lambda}^{(m)} \\ &\equiv \{\epsilon_{n\lambda}^{(m)} - \epsilon_n(R_e^{(m)})\} \psi_{n\lambda}^{(m)} \end{aligned} \quad (\text{II-2.4})$$

Now consider

$$\begin{aligned} (U_0 | \psi_m \rangle)_\gamma &= \left( \sum_r U_{0r} \psi_r^{(m)} \right)_\gamma \\ &= (U_{0n} \psi_n^{(m)})_\gamma \\ &= V_{0n}^{\gamma\lambda} \psi_{n\lambda}^{(m)} \end{aligned} \quad (\text{A1-13})$$

Similarly

$$(U_0^\dagger | \psi_m \rangle)_\gamma = V_{on}^{\gamma'\lambda\dagger} \psi_{n\lambda}^{(m)} \quad (\text{A1-14})$$

The  $\gamma' \rightarrow \gamma$  transition due to the  $\lambda$  th vibrational level in the negative ion state is

$$\mathfrak{F}_0^\lambda(\gamma, \gamma') = \frac{\langle \psi_{0\gamma}^{(-)} | V_{0n}^{\gamma\lambda} | \psi_{n\lambda}^{(m)} \rangle \langle \psi_{n\lambda}^{(m)} | V_{n0}^{\lambda\gamma'} | \psi_{0\gamma'}^{(+)} \rangle}{E - W_{n\lambda}^{(m)} + R_{n\lambda}^{(m)}}$$

Using assumption (5), the total transition matrix element is

$$\begin{aligned} \mathfrak{S}_0(\gamma, \gamma') &= \sum_{\lambda} \mathfrak{S}_0^{\lambda}(\gamma, \gamma') \\ &= \sum_{\lambda} \frac{\langle \psi_{0\gamma}^{(-)} | V_{0n}^{\gamma\lambda} | \psi_{n\lambda}^{(m)} \rangle \langle \psi_{n\lambda}^{(m)} | V_{n0}^{\lambda\gamma'} | \psi_{0\gamma'}^{(+)} \rangle}{E - W_{n\lambda}^{(m)} + R_{n\lambda}^{(m)}} \end{aligned} \quad (\text{II-2.3})$$

And

$$R_{n\lambda}^{(m)} = \langle \psi_{n\lambda}^{(m)} | \sum_{\gamma} V_{n0}^{\lambda\gamma} (E - H_0 + i\eta)^{-1} V_{0n}^{\gamma\lambda} | \psi_{n\lambda}^{(m)} \rangle \quad (\text{II-2.5})$$

Expanding

$$(E - H_0 + i\eta)^{-1} = \int dE_{\gamma} \frac{|\psi_{0\gamma}^{(+)}\rangle \langle \psi_{0\gamma}^{(-)}|}{E - E_{\gamma} + i\eta} \xi_{\gamma}$$

where  $\xi_{\gamma}$  is the density of states in the exit channel  $\gamma$ , and using

$$\frac{1}{E - E_{\gamma} + i\eta} = \frac{E - E_{\gamma}}{(E - E_{\gamma})^2 + \eta^2} - \frac{i\eta}{(E - E_{\gamma})^2 + \eta^2}$$

we have

$$R_{n\lambda}^{(m)} = \Delta_{n\lambda}^{(m)} - i \frac{1}{2} \Gamma_{n\lambda}^{(m)} \quad (\text{II-2.5})$$

where

$$\Delta_{n\lambda}^{(m)} = \langle \psi_{n\lambda}^{(m)} | \sum_{\gamma} P \int V_{n0}^{\lambda\gamma} \frac{E - E_{\gamma}}{(E - E_{\gamma})^2 + \eta^2} |\psi_{0\gamma}^{(+)}\rangle \langle \psi_{0\gamma}^{(-)}| V_{0n}^{\gamma\lambda} \xi_{\gamma} dE_{\gamma} | \psi_{n\lambda}^{(m)} \rangle \quad (\text{II-2.8})$$

and

$$\Gamma_{n\lambda}^{(m)} = 2 \Im (R_{n\lambda}^{(m)})$$

$$= 2 \langle \psi_{n\lambda}^{(m)} | \sum_{\gamma} \int V_{n0}^{\lambda\gamma} \frac{\eta |\psi_{0\gamma}^{(+)} \rangle \langle \psi_{0\gamma}^{(-)}|}{(E - E_{\gamma})^2 + \eta^2} V_{0n}^{\gamma\lambda} \xi_{\gamma} dE_{\gamma} | \psi_{n\lambda}^{(m)} \rangle \quad (A1-15)$$

$$= 2 \langle \psi_{n\lambda}^{(m)} | \sum_{\gamma} \int V_{n0}^{\lambda\gamma} |\psi_{0\gamma}^{(+)} \rangle \langle \psi_{0\gamma}^{(+)}| \langle \psi_{0\gamma}^{(-)} | \pi \delta(E - E_{\gamma}) V_{0n}^{\gamma\lambda} \xi_{\gamma} dE_{\gamma} | \psi_{n\lambda}^{(m)} \rangle \quad (A1-16)$$

Using

$$\begin{aligned} \xi_{\gamma} &= \frac{d\Omega_f}{(2\pi)^3} \frac{k_{\gamma} d(k_{\gamma}^2)}{dE_{\gamma}} \\ &= \frac{d\Omega_f}{(2\pi)^3} \frac{1}{2} \frac{k_{\gamma} d(k_{\gamma}^2)}{dE_{\gamma}} \end{aligned}$$

and

$$E_{\gamma} = \frac{1}{2} k_{\gamma}^2$$

then

$$\xi_{\gamma} = \frac{d\Omega_f}{(2\pi)^3} k_{\gamma} \quad (A1-17)$$

Using (A1-17) to (A1-16) we have

$$\Gamma_{n\lambda}^{(m)} = \frac{1}{(2\pi)^2} \sum_{\gamma} \int |\langle \psi_{0\gamma}^{(-)} | V_{0n}^{\gamma\lambda} | \psi_{n\lambda}^{(m)} \rangle|^2 k_{\gamma} d\Omega_f \quad (II-2.9)$$

Using the definitions of  $V_{0n}^{\gamma\lambda}$  and  $V_{n0}^{\lambda\gamma'}$  from equation (I-2.10) and interchanging the order of integration in (II-2.3) we obtain

$$\Im_0(\gamma, \gamma') = \sum_{\lambda} \frac{\langle \chi_{0\gamma} | \alpha_{\gamma\lambda} | \chi_{n\lambda} \rangle \langle \chi_{n\lambda} | \alpha_{\lambda\gamma'}^* | \chi_{0\gamma'} \rangle}{E - E_{n\lambda}^{(m)} + i 1/2 \Gamma_{n\lambda}^{(m)}} \quad (II-2.11)$$



and

$$\Gamma_{n\lambda}^{(m)} = \sum_{\gamma} \frac{k_{\gamma}}{(2\pi)^2} \int |\langle \chi_{0\gamma} | \alpha_{\gamma\lambda} | \chi_{n\lambda} \rangle|^2 d\Omega_f \quad (\text{II-2.12})$$

where

$$\alpha_{\gamma\lambda} = \langle \psi_{0\gamma}^{(-)} | \Phi_0 | V_0 | \Phi_n \psi_{n\lambda}^{(m)} \rangle \quad (\text{II-2.13a})$$

$$\alpha_{\lambda\gamma}^* = \langle \psi_{n\lambda}^{(m)} | \Phi_n | V_0 | \Phi_0 \psi_{0\lambda'}^{(+)} \rangle \quad (\text{II-2.13b})$$

$$E_{n\lambda}^{(m)} = W_{n\lambda}^{(m)} + \Delta_{n\lambda}^{(m)} = \epsilon_{n\lambda}^{(m)} + \Delta_{n\lambda}^{(m)} + \epsilon_{n\lambda} - \epsilon_n(R_e^{(n)}) \quad (\text{II-2.14})$$

The differential partial cross section  $d\sigma_{\gamma\gamma'}$ , is expressed as a function of the incident angles of the impinging electron by

$$d\sigma_{\gamma\gamma'} = (4\pi^2)^{-1} |\mathfrak{F}_0(\gamma, \gamma')|^2 d\Omega_f$$

where

$$k_{\gamma}^2 = k_{\gamma'}^2 + 2(\epsilon_{0\gamma'} - \epsilon_{0\gamma})$$

with the initial and final wavenumbers of the electron given by  $k_{\gamma'}$  and  $k_{\gamma}$  respectively.

Because the rotational motion of the molecule is relatively slow, the molecular orientation is considered fixed throughout the vibrational excitation or de-excitation. If the molecule remains in the ground rotational state then the partial cross-section can be obtained by averaging the transition matrix elements over the incident angles and integrating the resultant over the sphere of the final angles.

The result is

$$\sigma_{\nu\nu'} = (16\pi^3)^{-1} \frac{k_{\nu}}{k_{\nu'}} \iint |\mathfrak{F}_0(\nu, \nu')|^2 d\Omega_0 d\Omega_f \quad (\text{II-2.17})$$

where the  $\gamma$ 's have been replaced by  $\nu$ 's to reflect that the  $\chi$ 's now represent vibrational wave functions only.

The further assumption that the compound negative-ion state does not depend on the vibrational state is made. This assumption allows the cross-section to be written as

$$\sigma_{\nu\nu'} = \frac{\beta_\nu \beta_{\nu'}}{16\pi^3} \frac{k_\nu}{k_{\nu'}} \left| \sum_\lambda \frac{\langle \chi_{0\nu} | \chi_{n\lambda} \rangle \langle \chi_{n\lambda} | \chi_{0\nu'} \rangle}{E - E_{n\lambda}^{(m)} + i \frac{1}{2} \Gamma_{n\lambda}^{(m)}} \right|^2 \quad (\text{II-2.18})$$

with

$$\Gamma_{n\lambda}^{(m)} = \sum_\nu \beta_\nu k_\nu (2\pi)^{-2} |\langle \chi_{0\nu} | \chi_{n\lambda} \rangle|^2 \quad (\text{II-2.19})$$

$$\beta_\nu = \int |\alpha_{\nu 0}|^2 d\Omega_f \quad (\text{II-2.20})$$

$$\beta_{\nu'} = \int |\alpha_{0\nu'}|^2 d\Omega_0 \quad (\text{II-2.21})$$

$$E_{n\lambda}^{(m)} = \epsilon_{n0}^{(m)} + \Delta_{n0}^{(m)} + \epsilon_{n\lambda} - \epsilon_n (\text{Re}^{(n)}) \quad (\text{II-2.22})$$

where the  $\alpha$ 's have been taken outside of the R integrals because they vary slowly and most of their contribution comes from a narrow range of internuclear separation  $R = \text{Re}^{(0)}$ .

Chen used Morse anharmonic wavefunctions for the  $\chi$ 's and approximated the resonance energy (II-2.22) by

$$E_{n\lambda}^{(m)} = \epsilon_{n0}^{(m)} + \Delta_{n0}^{(m)} + \left( \lambda + \frac{1}{2} \right) \omega_e^{(n)} - \left( \lambda + \frac{1}{2} \right)^2 \omega_e^{(n)} x_e^{(n)} \quad (\text{II-3.3})$$

where  $\omega_e^{(n)}/2$  is the zero point energy of the corresponding harmonic oscillator and the last term is an anharmonic correction. The  $\beta$ 's are found from the set of linear equations (II-2.19). The cross sections are then determined from (II-2.18).

The excited field for resonance was identified as the  $x^1 \sum_g^-$  of  $N_2$ . Once the excited state is identified the energy scale and averaged peak widths are shifted and altered by varying two parameters  $\epsilon_{n0}^{(m)} + \Delta_{n0}^{(m)}$  and  $\Gamma_{n0}^{(m)}$  until adjustment to the experimental data is achieved. The values giving the best fit are

$$\epsilon_{n0}^{(m)} + \Delta_{n0}^{(m)} = 1.89 \text{ e v}$$

$$\Gamma_{n0}^{(m)} = 0.152 \text{ e v}$$

These values are then used in the calculation of the cross-sections for excitation and de-excitation for other levels. (See reference (30) for the corrected figures for reference (29).)

### A1.3 Calculation of reaction rates:

The reaction rate  $I_{ij}$ , is obtained from the cross section,  $\sigma_{ij}$ , by

$$I_{ij} = \iiint_{-\infty}^{\infty} v_e \sigma_{ij}(v_e) f(v_e) d^3 v_3 \quad (A1-18)$$

where

$v_e$  is the electron velocity

$f(v_e)$  is the distribution function for the electrons (assumed Maxwell-Boltzmann).

Equation (A1-18) when expressed in terms of electron energy,  $E$  in  $\text{Ev}$ , becomes

$$I_{ij} = (1.26574 \times 10^{-6}) \pi \left( \frac{2}{\pi k T_e} \right)^{3/2} \frac{1}{\sqrt{m_e}} \int_0^{\infty} E \sigma_{ij}(E) e^{-E/kT_e} dE \quad (A1-19)$$

where  $m_e$  is the electron mass in grams.

$T_e$  is the electron temperature in °K

$k$  is Boltzmann's constant.

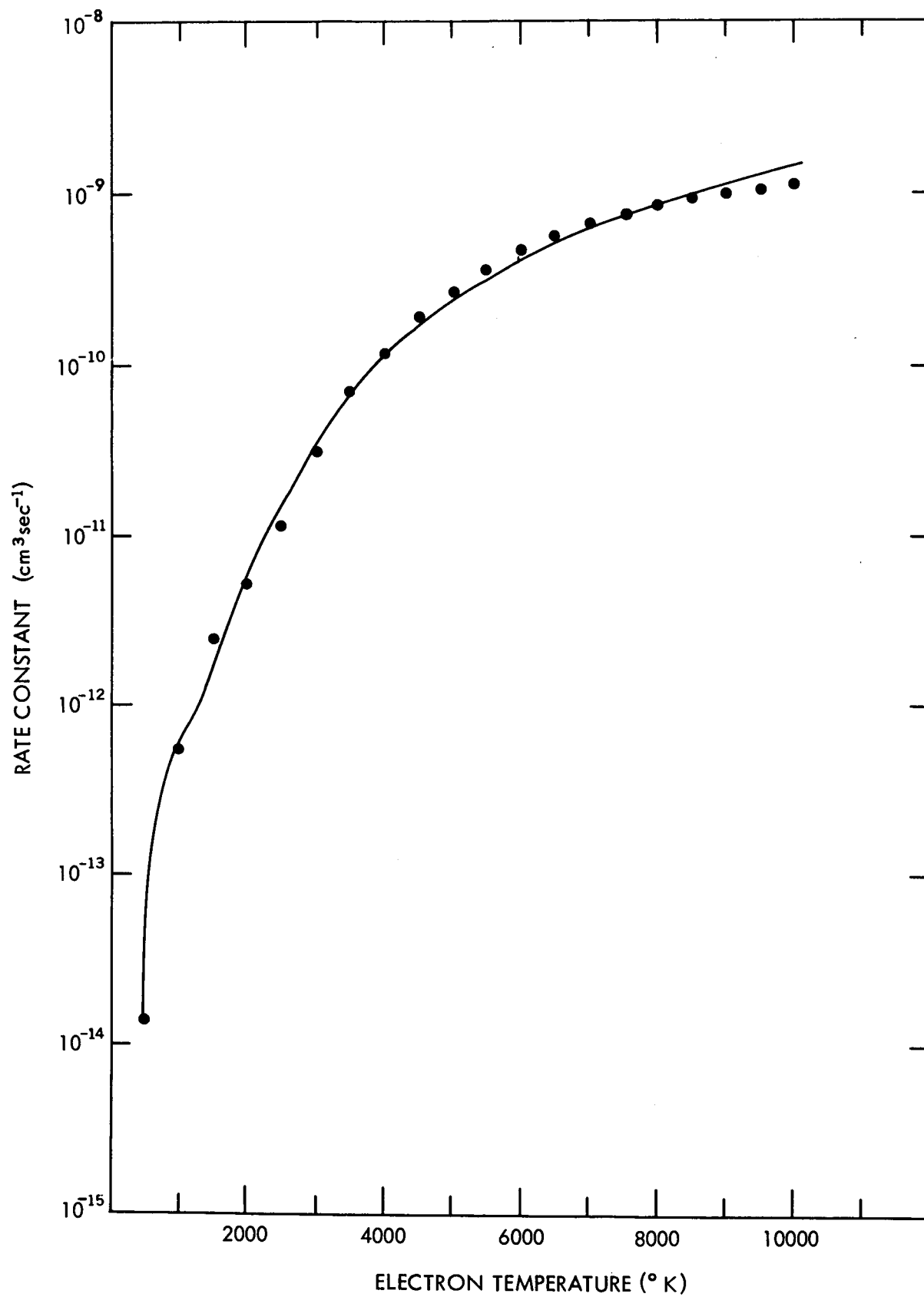
Chen presents, in graphical form, the cross sections which allow calculation of (A1-19) for all transitions among the first five excited levels of  $N_2$ . Because we are concerned with moderate electron temperatures, the low energy regions of the cross sections are of particular interest. By using (A1-19) and detailed balancing arguments we may relate the cross sections for excitation and de-excitation in the following way

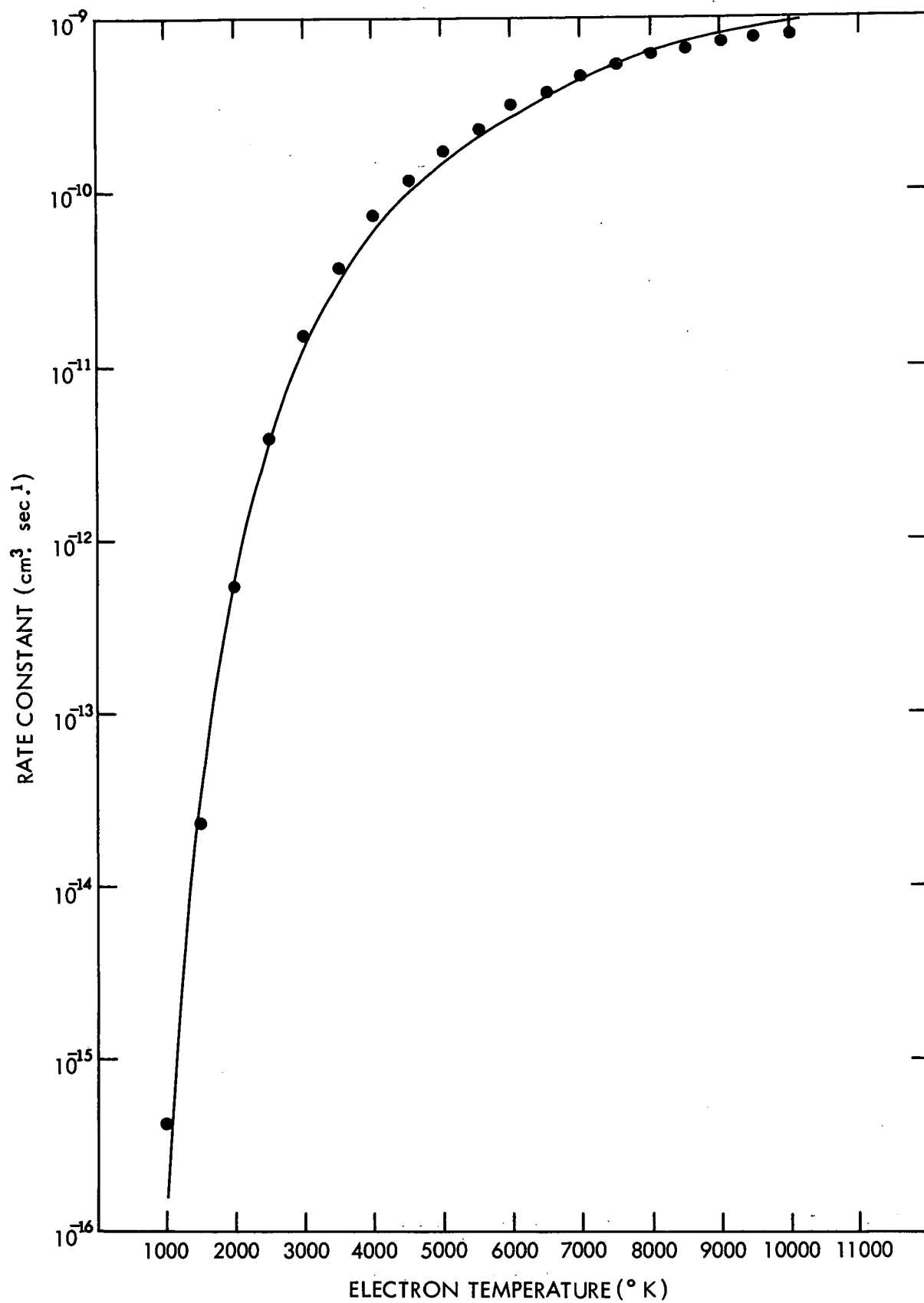
$$\sigma_{ji}(E - \epsilon_{ij}) = \frac{E}{E - \epsilon_{ij}} \sigma_{ij}(E) \quad (A1-20)$$

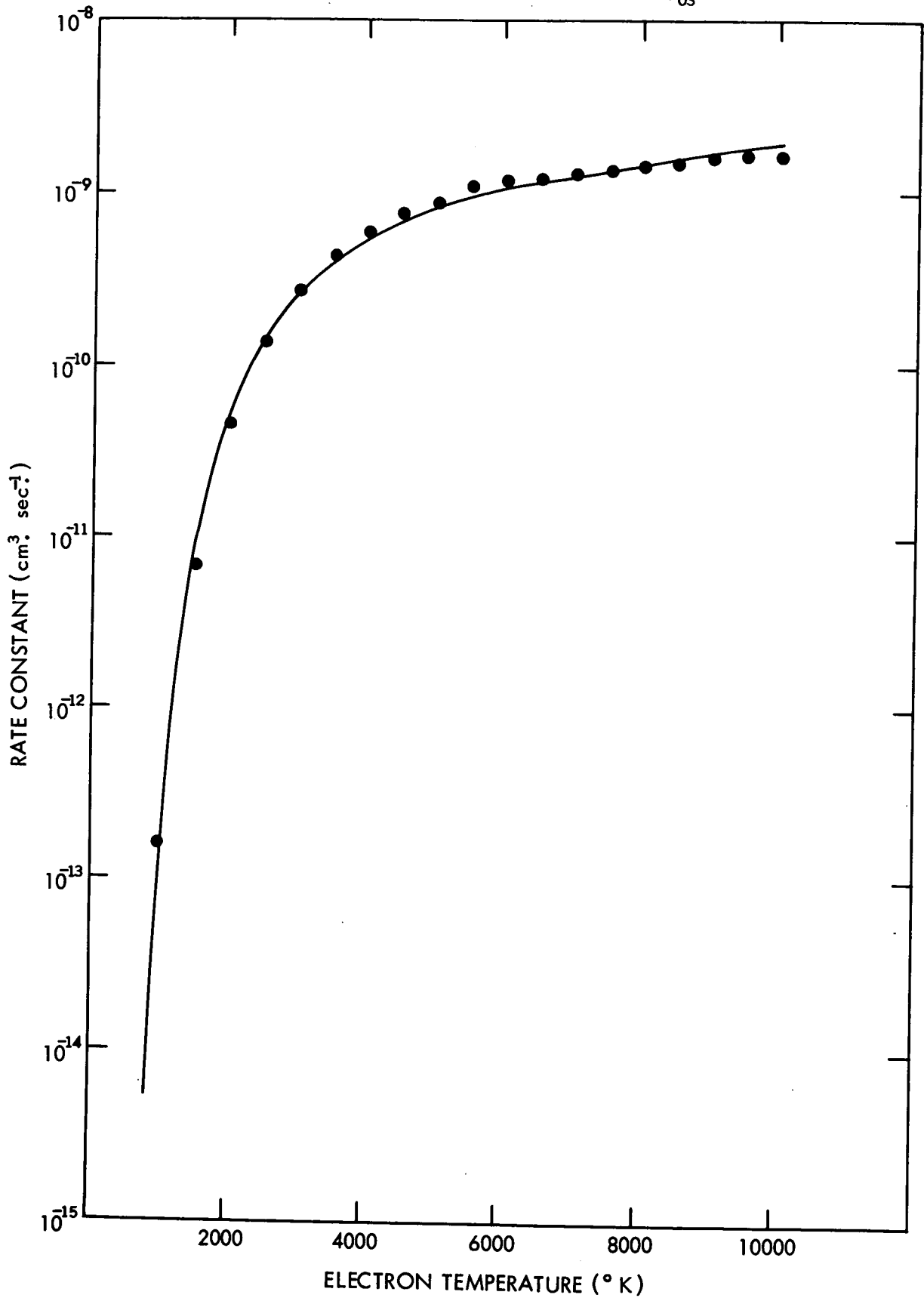
where  $\epsilon_{ij}$  is the threshold for the  $j \rightarrow i$  transition. Thus, near threshold we should use de-excitation cross sections in (A1-19) because the low energy tails are more readily observed. The principal of detailed balance allows calculation of the excitation reaction rate from

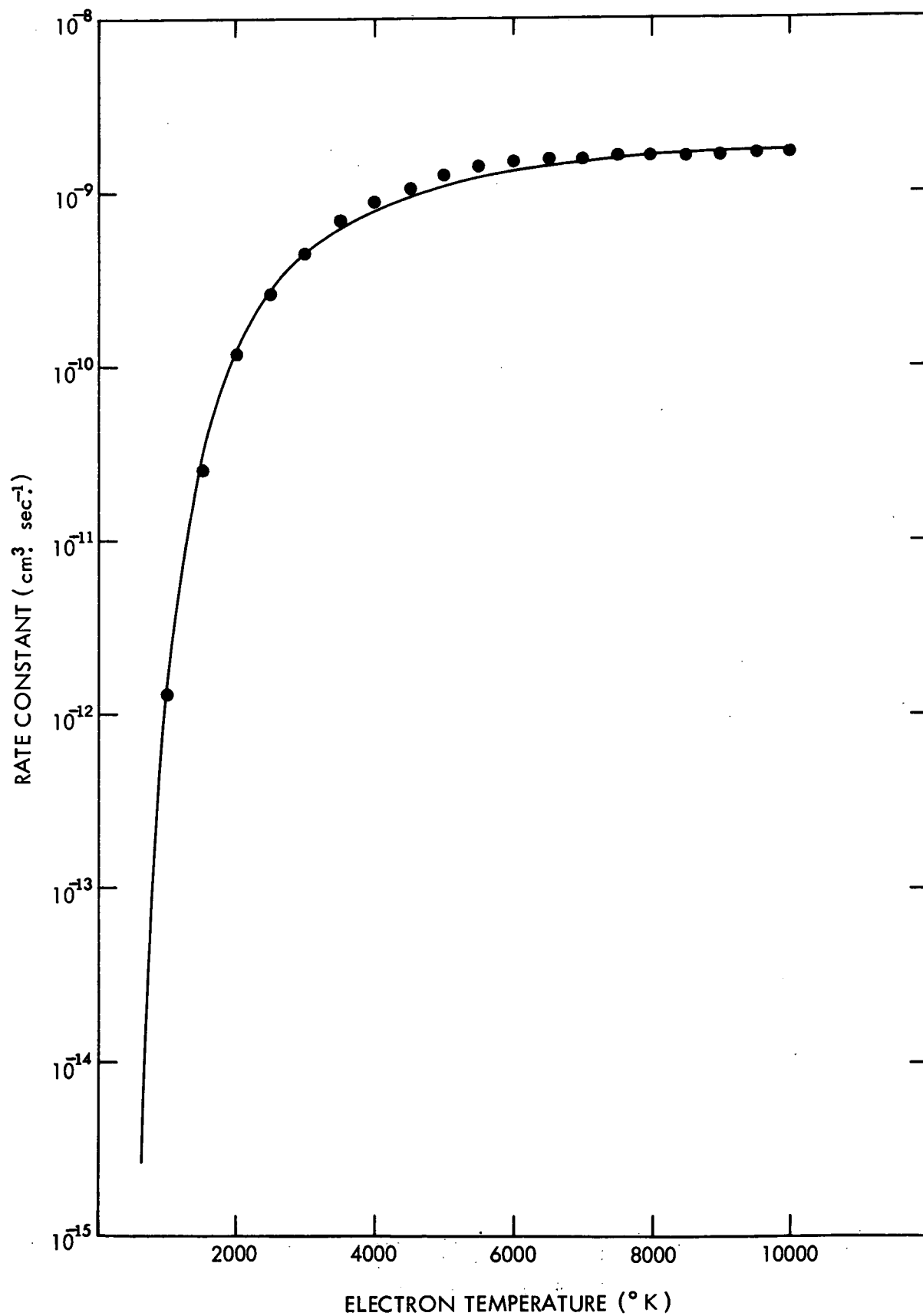
$$I_{ji} = I_{ij} e^{-(E_j - E_i)/kT_e} \quad (A1-21)$$

The cross-section graphs in Chen's paper (30) were digitized and numerical integration of (A1-19) was performed for electron temperatures between 500°K and 10000°K. The identification of the cross sections used are given in Table (1). The calculated reaction rates are plotted in Figures A1-1 through A1-15 as points.

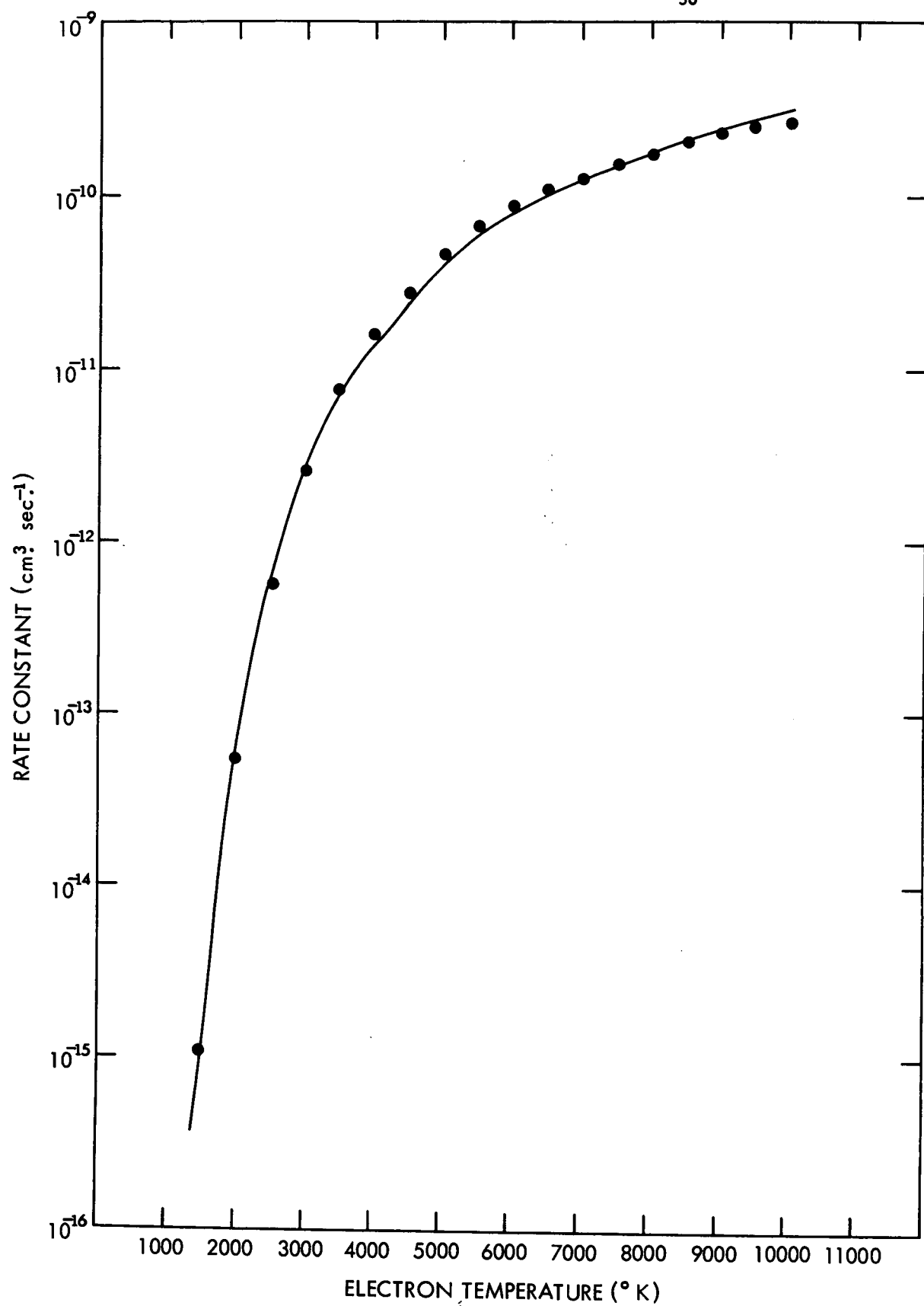
REACTION RATE CONSTANT FOR  $\sigma_{10}$ Figure A1-1. Reaction rate constant calculated from  $\sigma_{10}$

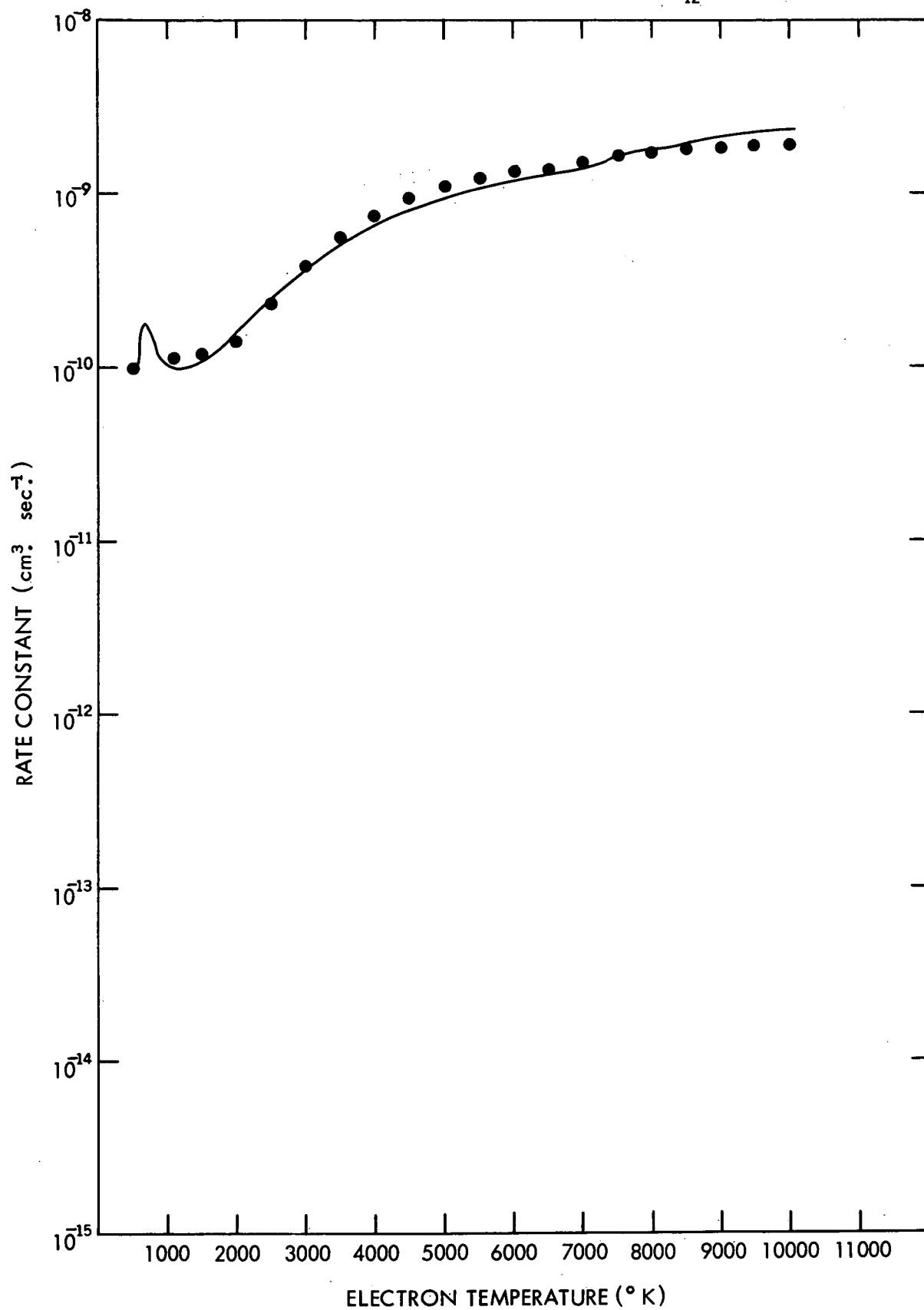
REACTION RATE CONSTANT FOR  $\sigma_{20}$ Figure A1-2. Reaction rate constant calculated from  $\sigma_{20}$

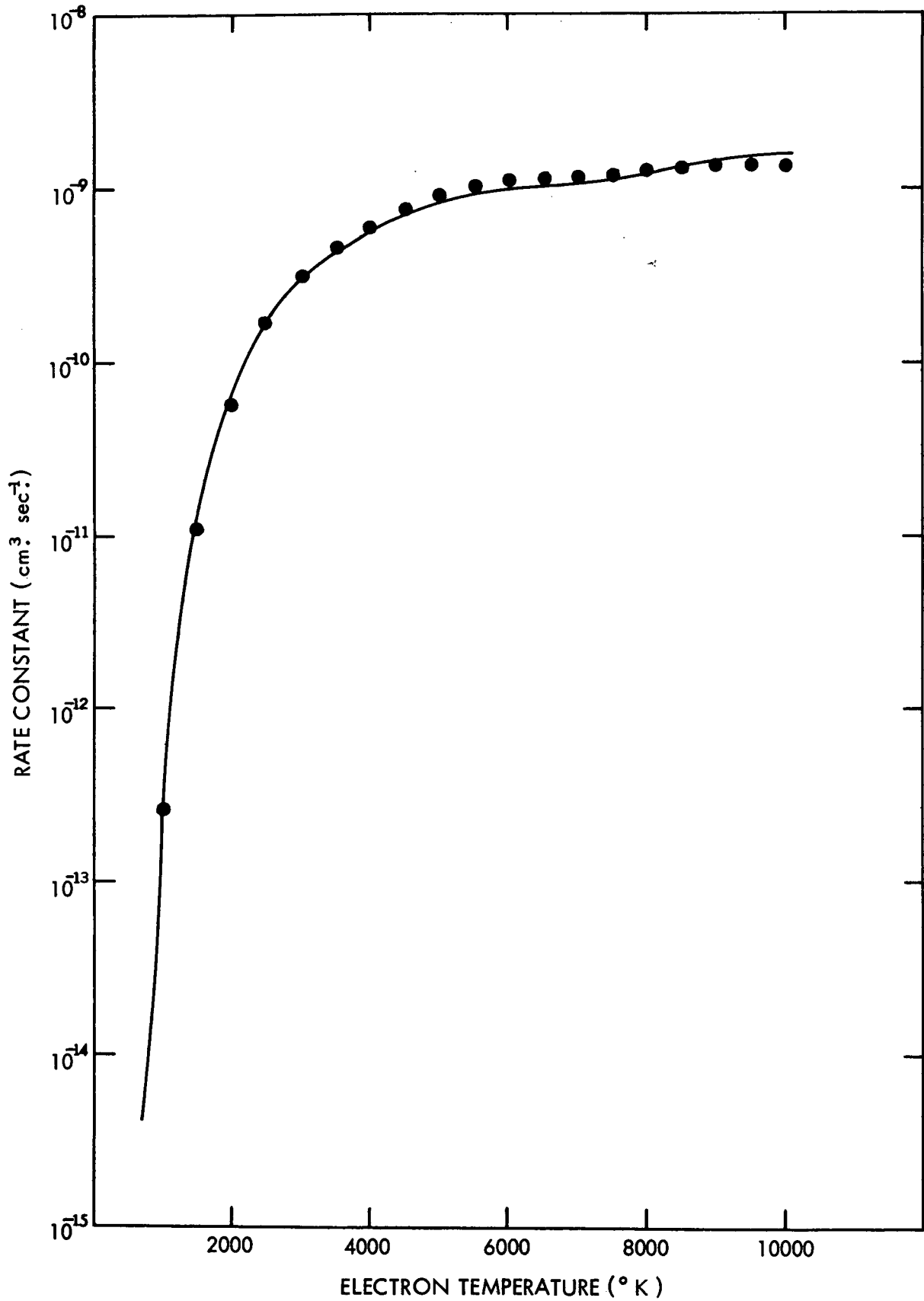
REACTION RATE CONSTANT FOR  $\sigma_{03}$ Figure A1-3. Reaction rate constant calculated from  $\sigma_{03}$

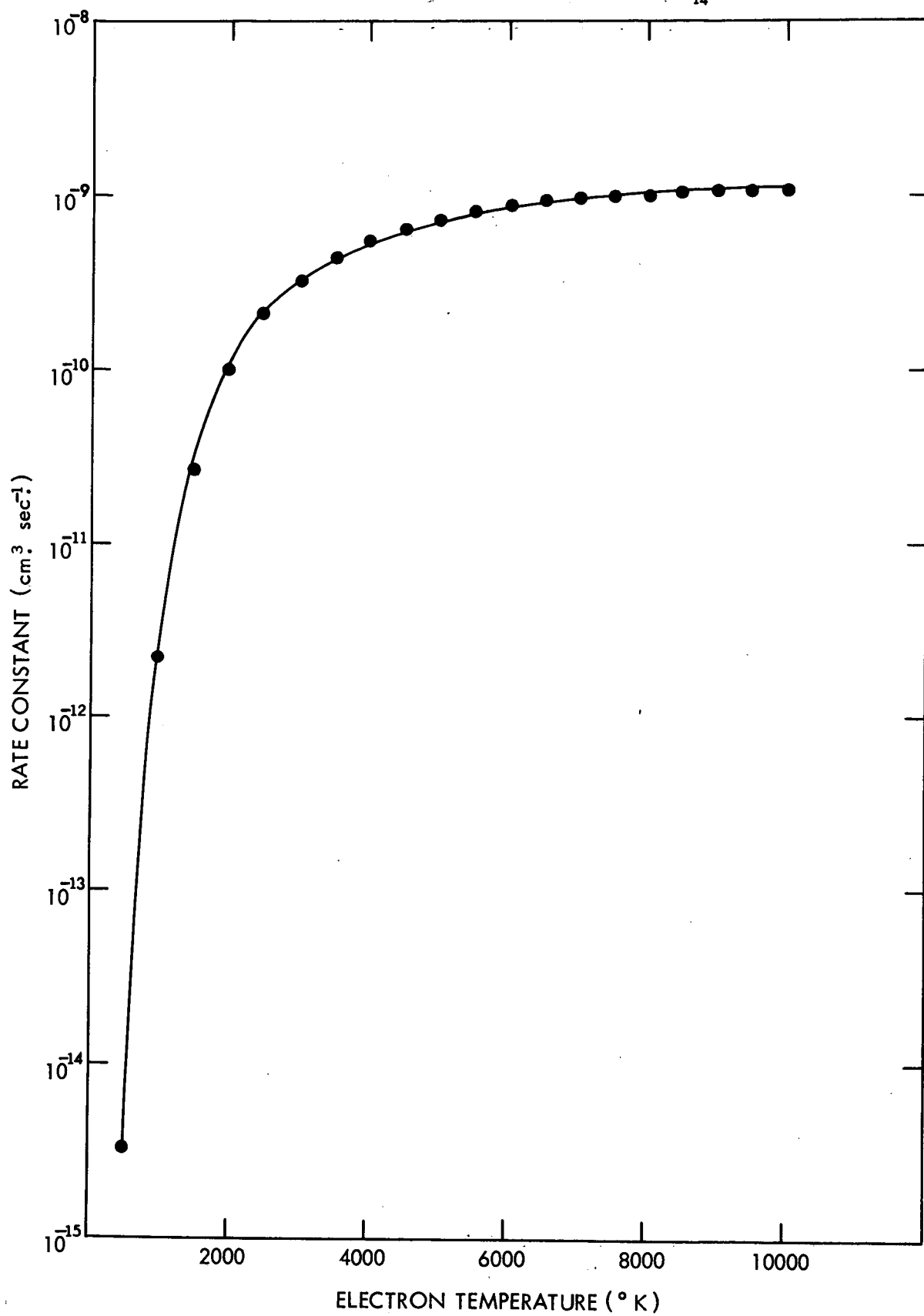
REACTION RATE CONSTANT FOR  $\sigma_{04}$ Figure A1-4. Reaction rate constant calculated from  $\sigma_{04}$

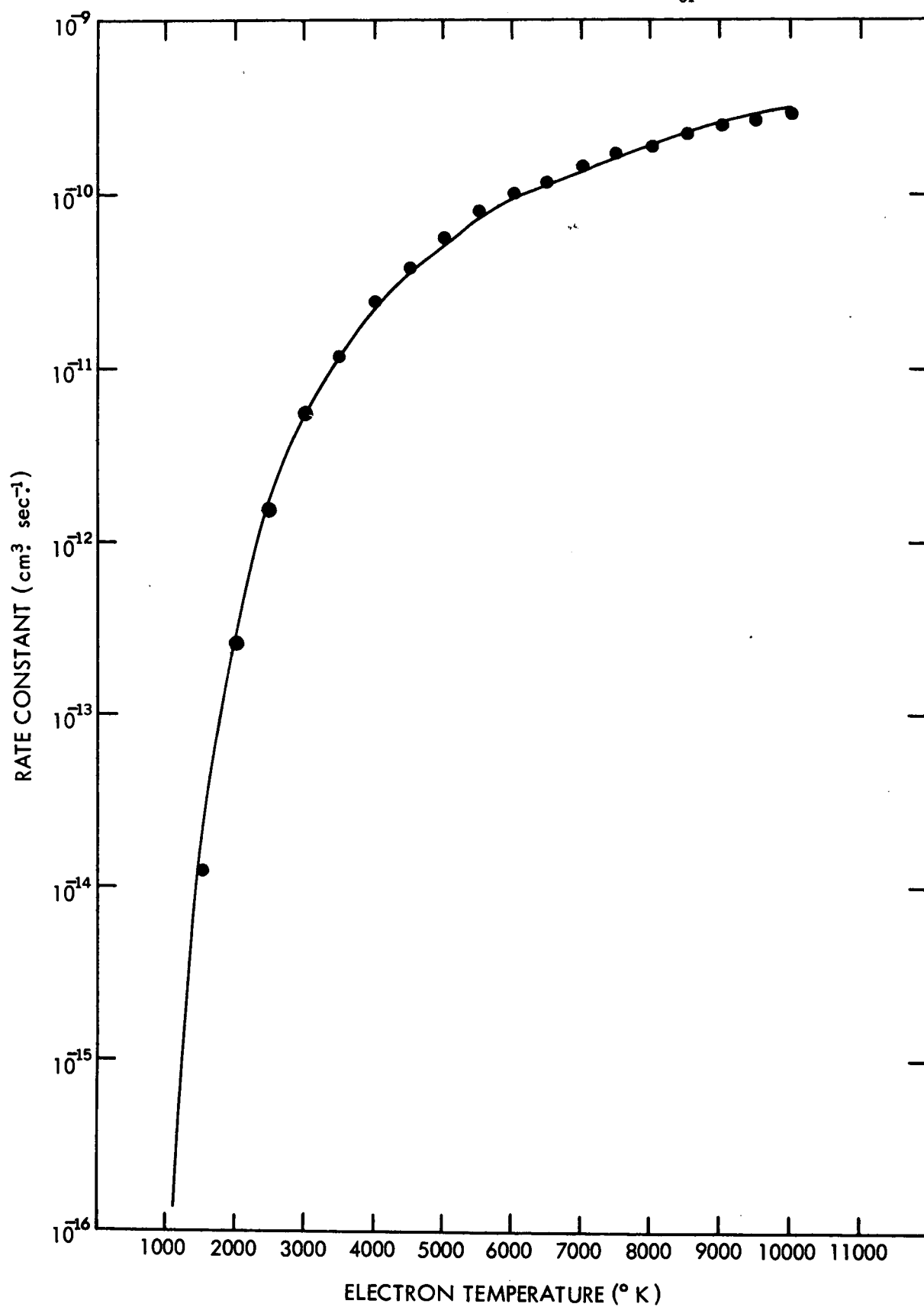


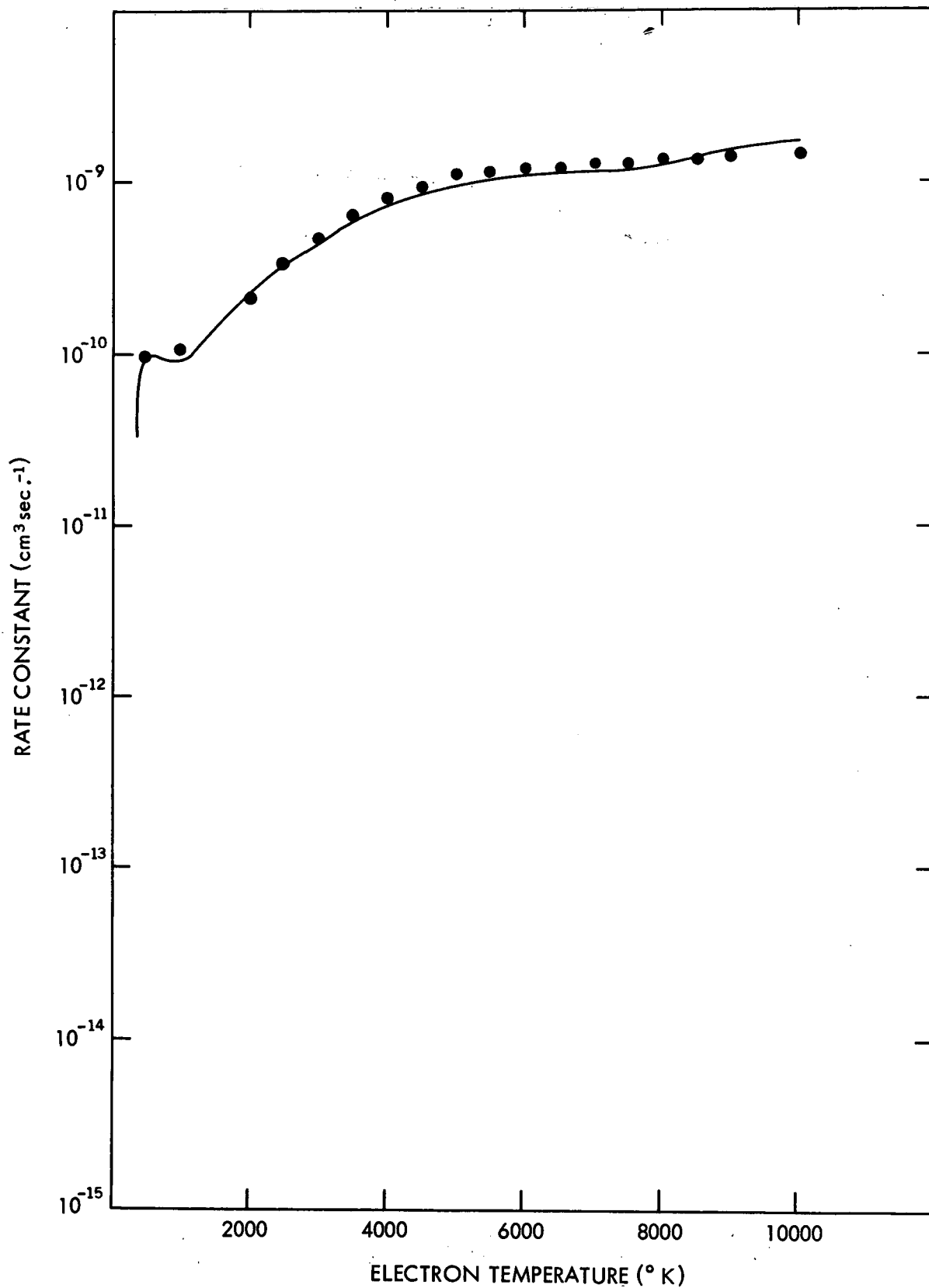
REACTION RATE CONSTANT FOR  $\sigma_{50}$ Figure A1-5. Reaction rate constant calculated from  $\sigma_{50}$

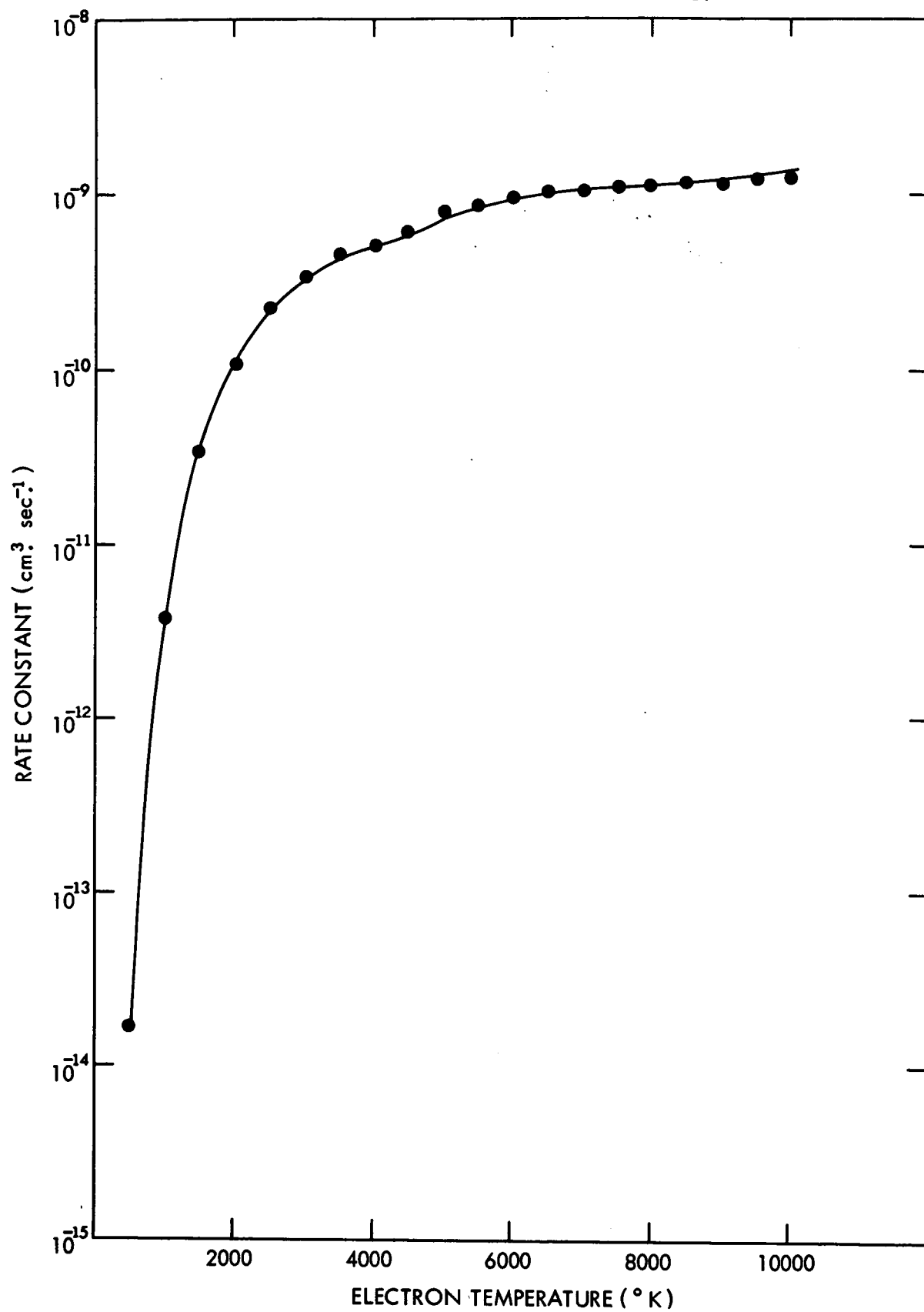
REACTION RATE CONSTANT FOR  $\sigma_{12}$ Figure A1-6. Reaction rate constant calculated from  $\sigma_{12}$

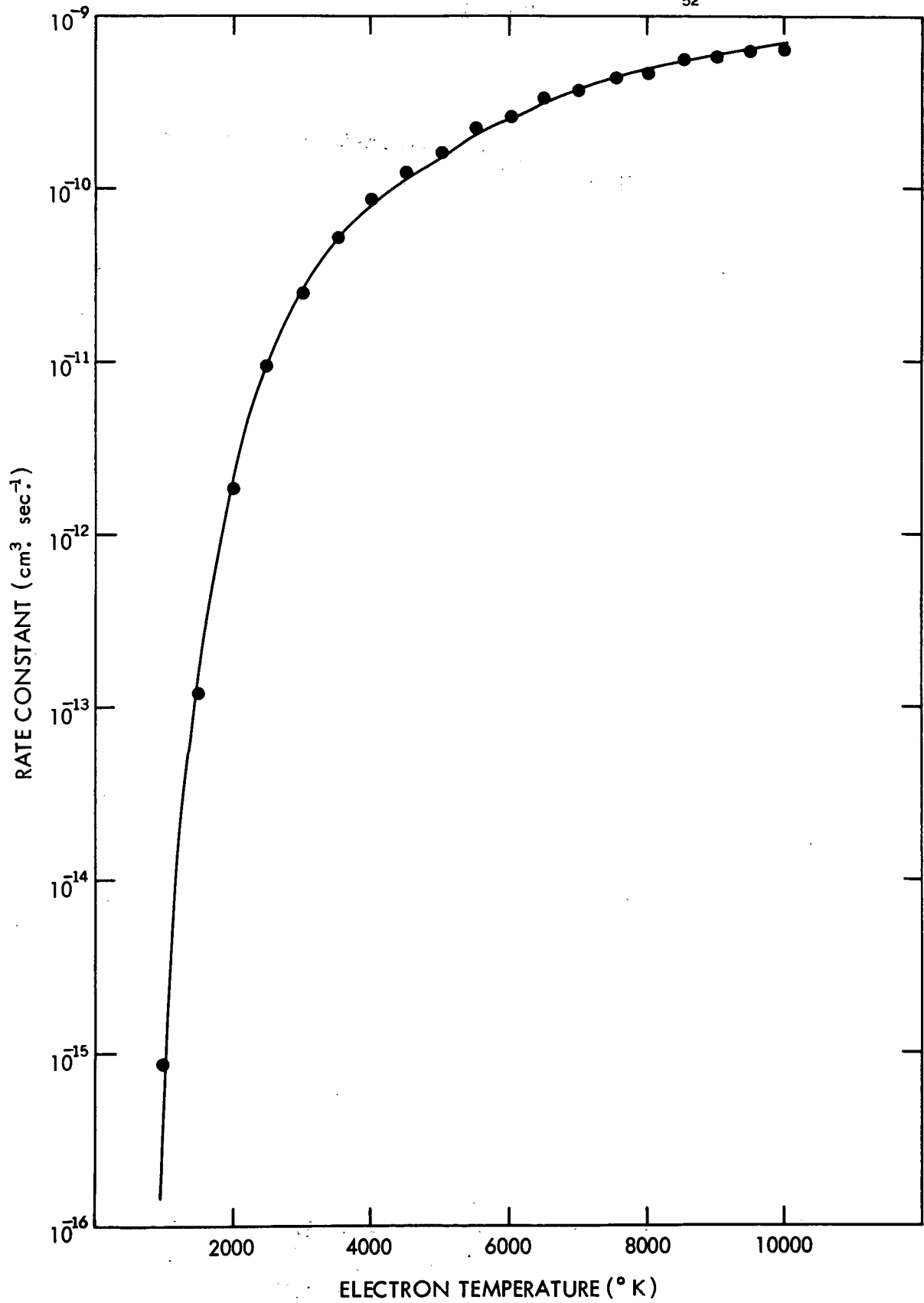
REACTION RATE CONSTANT FOR  $\sigma_{13}$ Figure A1-7. Reaction rate constant calculated from  $\sigma_{13}$

REACTION RATE CONSTANT FOR  $\sigma_{14}$ Figure A1-8. Reaction rate constant calculated from  $\sigma_{14}$

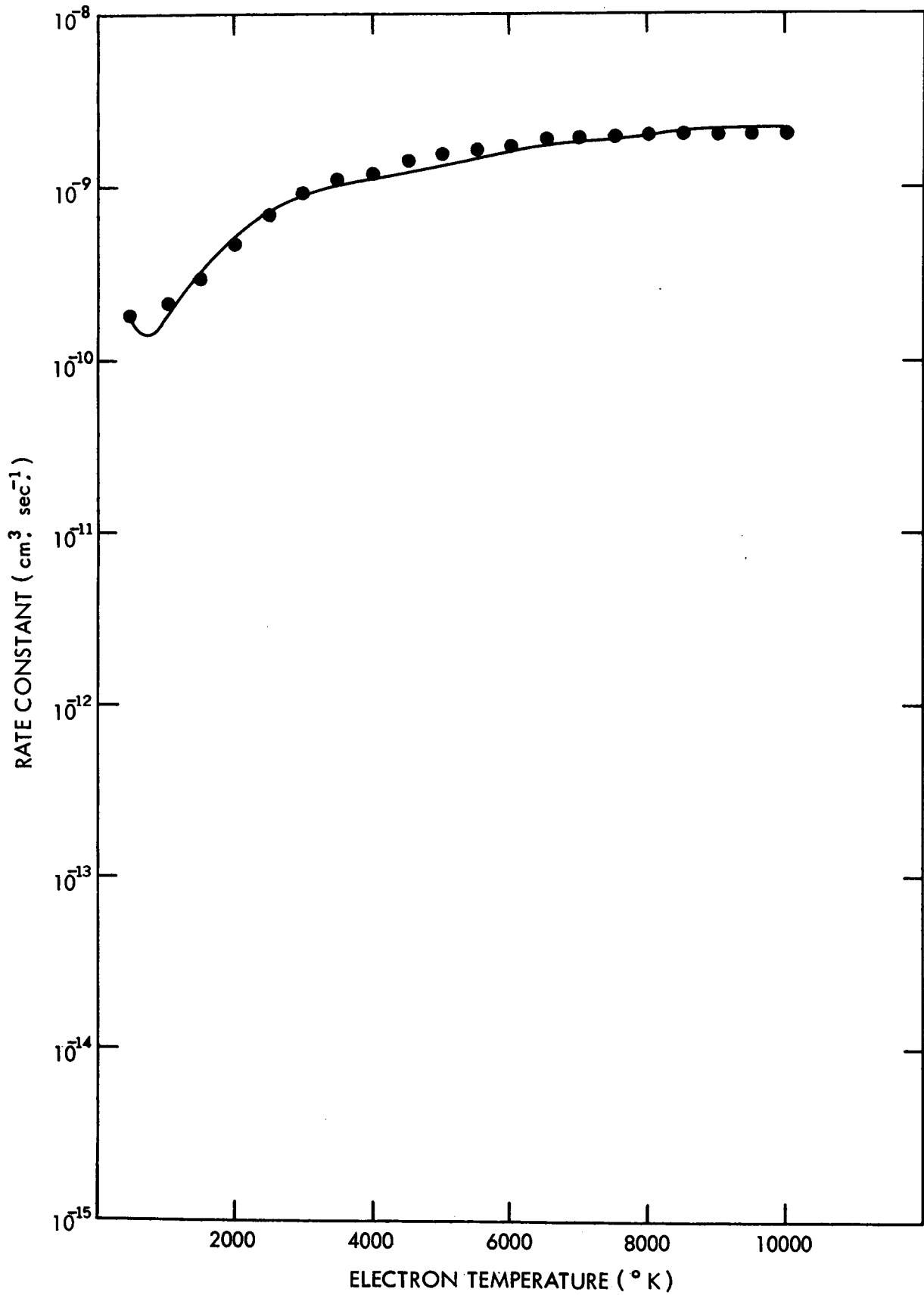
REACTION RATE CONSTANT FOR  $\sigma_{51}$ Figure A1-9. Reaction rate constant calculated from  $\sigma_{51}$

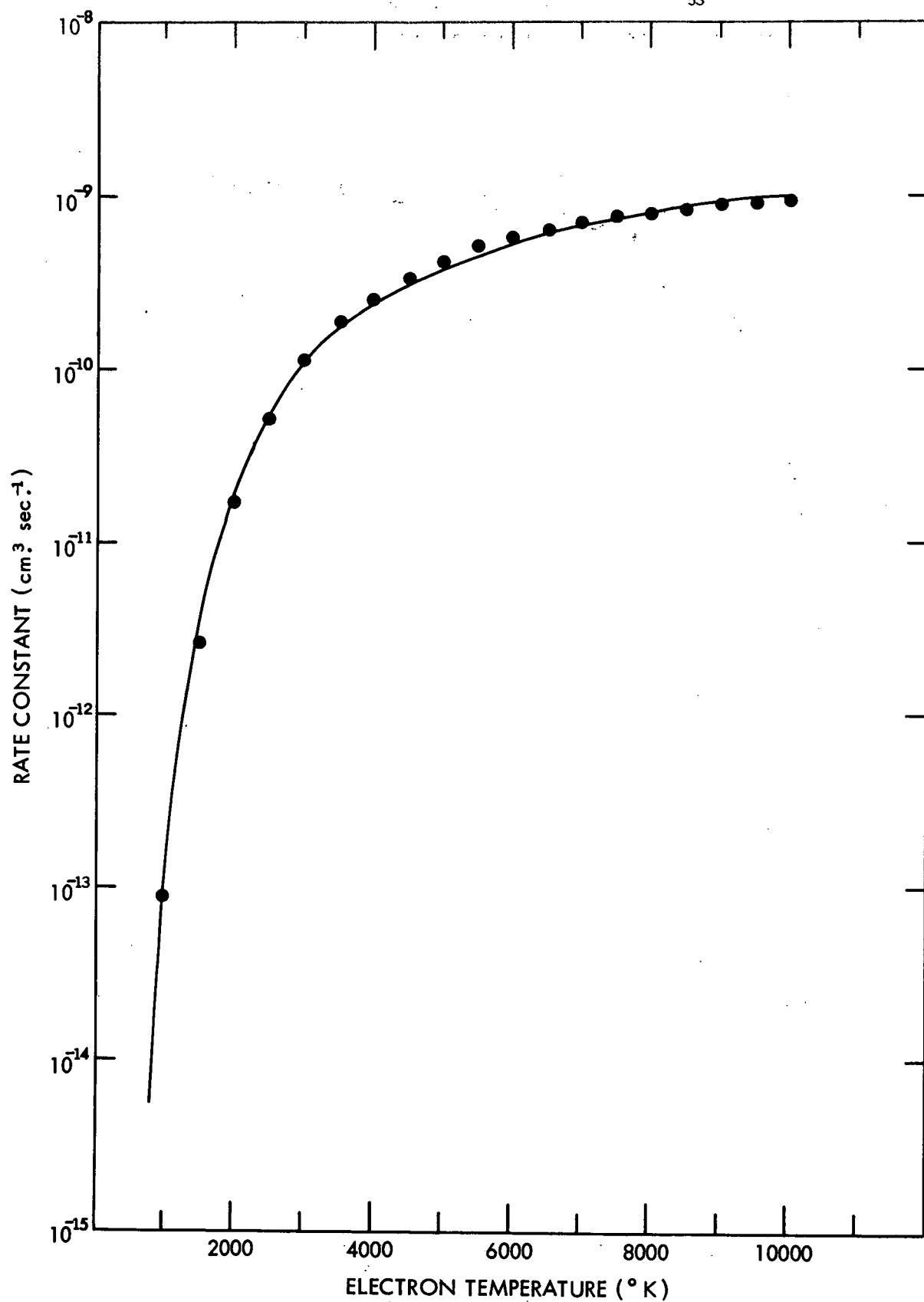
REACTION RATE CONSTANT FOR  $\sigma_{23}$ Figure A1-10. Reaction rate constant calculated from  $\sigma_{23}$

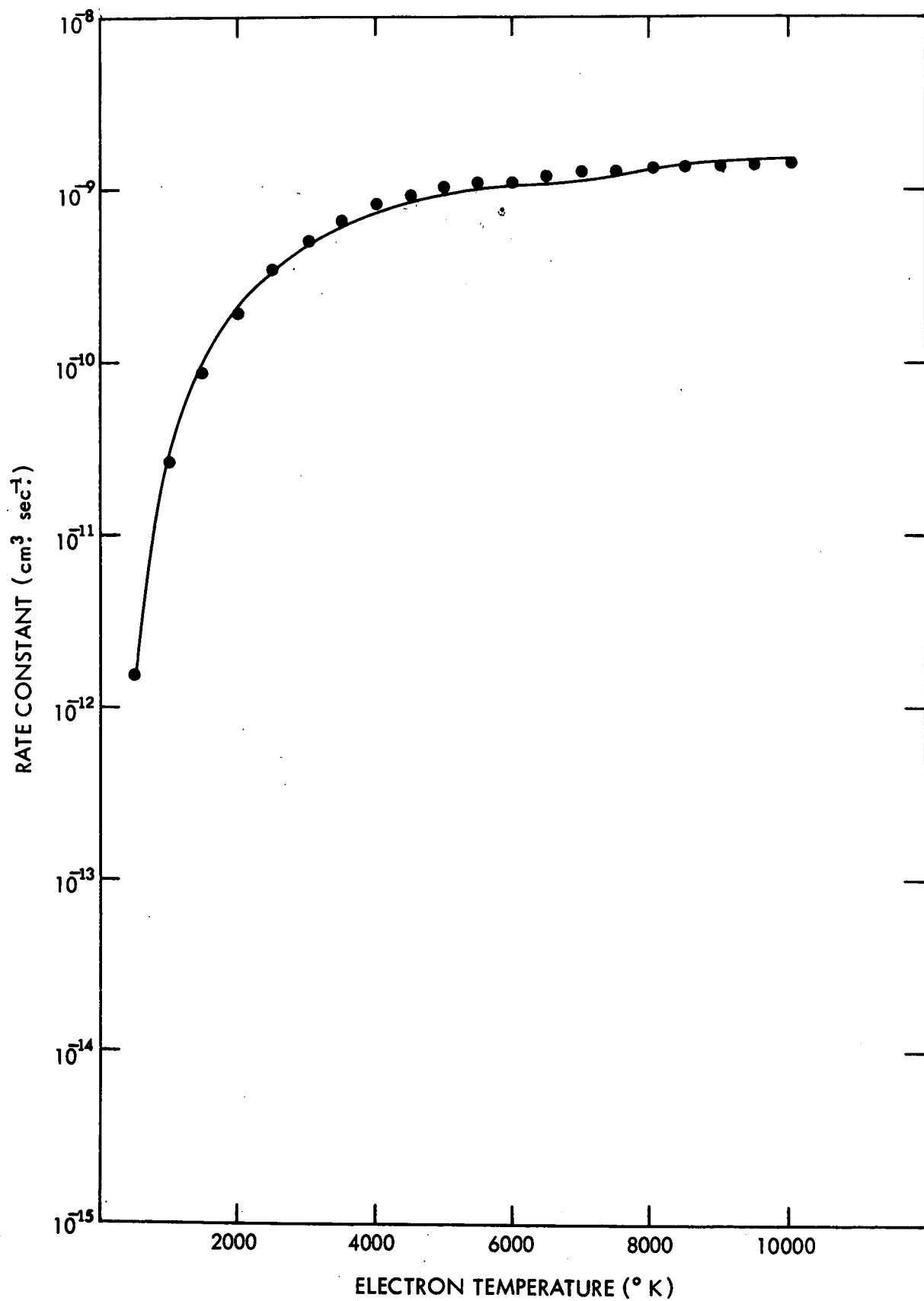
REACTION RATE CONSTANT FOR  $\sigma_{24}$ Figure A1-11. Reaction rate constant calculated from  $\sigma_{24}$

REACTION RATE CONSTANT FOR  $\sigma_{52}$ Figure A1-12. Reaction rate constant calculated from  $\sigma_{52}$



REACTION RATE CONSTANT FOR  $\sigma_{34}$ Figure A1-13. Reaction rate constant calculated from  $\sigma_{34}$

REACTION RATE CONSTANT FOR  $\sigma_{53}$ Figure A1-14. Reaction rate constant calculated from  $\sigma_{53}$

REACTION RATE CONSTANT FOR  $\sigma_{54}$ Figure A1-15. Reaction rate constant calculated from  $\sigma_{54}$

It was found that the reaction rates could be adequately reproduced by a four parameter function of the electron temperature of the form

$$I_{ij} = \text{Exp} \left( P_1 + \frac{P_2}{T_e} + \frac{P_3}{T_e^2} + \frac{P_4}{T_e^3} \right) \quad (\text{A1-22})$$

The four parameters for each cross section of Table (1) are given in Table (2). Equation (A1-22) reproduces the integrated cross section results, over the electron temperature range, to better than 40% in all cases. This was considered acceptable considering the order of magnitude accuracy of the basic cross section calculations. The reaction rates from (A1-22) are also plotted as lines in Figures A1-1 through A1-15. Equations (A1-22) and (A1-21) were used to calculate the reaction rates used in further calculations.

## APPENDIX II

### SIMPLIFICATION OF THE CONTINUITY EQUATIONS

From section 2.4 we have for the continuity equation of the number of  $N_2^*$  in level  $i$

$$\begin{aligned}
 \frac{\partial n_i}{\partial t} + \frac{\partial}{\partial z} (\vec{F}_i)_z = & \sum_{j=0} \{A_{ij} n_j - A_{ji} n_i\} \\
 & + P_{1,0:0,1} \nu_i \sum_{j=0} (j+1) [n_{i-1} n_{j+1} - n_i n_j] \\
 & + P_{1,0:0,1} \nu (i+1) \sum_{j=1} j [n_{i+1} n_{j-1} - n_i n_j] \\
 & + C_{1,0} \nu' n [0] [i n_{i-1} + (i+1) e^{\theta/T} n_{i+1} \\
 & + (i e^{\theta/T} + i+1) n_i]
 \end{aligned} \tag{2-22}$$

These are a set of 6 coupled, non-linear, partial differential equations. The coefficients are functions of altitude through the altitudinal dependence of the model atmosphere and ionosphere parameters.

Each solution to equations (2-22) will be written as a sum of a Boltzmann distributed density,  $n_i$ , and a remainder term,  $\epsilon_i$ , to simplify the coupling between the equations. Thus,

$$n_i = n'_i + \epsilon_i \tag{A2-1}$$

and we require that

$$\sum_{i=0} i n_i = \sum_{i=0} i n'_i \tag{A2-2}$$

$$\sum_{i=0} n_i = \sum_{i=0} n'_i = n \quad (\text{A2-3})$$

Equation (A2-2) and (A2-3), respectively, require the vibrational energy and density of the Maxwell-Boltzmann distributed density to be the energy and density of the solution for the set of equations (2-22). Thus, from equation (A2-1) we have using (A2-2) and (A2-3)

$$\sum_{i=0} i \epsilon_i = 0 \quad (\text{A2-4})$$

$$\sum_{i=0} \epsilon_i = 0 \quad (\text{A2-5})$$

Substituting (A2-1) into the flux term (A2-21) we obtain

$$\vec{F}_i = \vec{F}'_i + \vec{\mathcal{G}}_i \quad (\text{A2-6})$$

where

$$\vec{F}'_i = -D \left[ \nabla n'_i + \frac{n'_i}{H} \hat{k} \right] \quad (\text{A2-7})$$

$$\vec{\mathcal{G}}'_i = -D \left[ \nabla \epsilon_i + \frac{\epsilon_i}{H} \hat{k} \right] \quad (\text{A2-8})$$

Substituting (A2-1) into (2-22) and rearranging terms we have

$$\begin{aligned} \frac{\partial n'_i}{\partial t} + \frac{\partial}{\partial z} (\vec{F}'_i)_z + \frac{\partial \epsilon_i}{\partial t} + \frac{\partial}{\partial z} (\vec{\mathcal{G}}_i)_z = \sum_{j=0} \{A_{ij} (n'_j + \epsilon_j) \\ - A_{ji} (n'_i + \epsilon_i)\} + P_{1,0:0,1} \nu_i \sum_{j=0} (j+1) [n'_{i-1} n'_{j+1} \end{aligned}$$

$$\begin{aligned}
& - n'_i n'_j + \epsilon_{i-1} n'_{j+1} + \epsilon_{j+1} n'_{i-1} - \epsilon_i n'_j \\
& - \epsilon_j n'_i + \epsilon_{i-1} \epsilon_{j+1} - \epsilon_i \epsilon_j] \\
& + P_{1,0:0,1} \nu (i+1) \sum_{j=1}^j [n'_{i+1} n'_{j-1} - n'_i n'_j \\
& + \epsilon_{i+1} n'_{j-1} + \epsilon_{j-1} n'_{i+1} - \epsilon_i n'_j - \epsilon_j n'_i \\
& + \epsilon_{i+1} \epsilon_{j-1} - \epsilon_j \epsilon_i] + C_{1,0} \nu' n [0] [i (n'_{i-1} + \epsilon_{i-1}) \\
& + (i+1) e^{\theta/T} (n'_{i+1} + \epsilon_{i+1}) - (i e^{\theta/T} + i+1) (n'_i + \epsilon_i)] \quad (A2-9)
\end{aligned}$$

We have

$$n'_{i-1} n'_{j+1} - n'_i n'_j = n'_{i+1} n'_{j-1} - n'_i n'_j \quad (A2-10)$$

Using (A2-10) in (A2-9) and rearranging terms we have

$$\begin{aligned}
& \frac{\partial n'_i}{\partial t} + \frac{\partial}{\partial z} (\vec{F}'_i)_z + \frac{\partial \epsilon_i}{\partial t} + \frac{\partial}{\partial z} (\vec{G}'_i)_z = \sum_{j=0} \{A_{ij} (n'_j + \epsilon_j) \\
& + A_{ji} (n'_i + \epsilon_i)\} + P_{1,0:0,1} \nu \left[ i \epsilon_{i-1} \sum_{j=0} (j+1) n'_{j+1} \right. \\
& - (i+1) \epsilon_i \sum_{j=1} j n'_j + i n'_{i-1} \sum_{j=0} (j+1) \epsilon_{j+1} - (i+1) n'_i \sum_{j=1} j \epsilon_j \\
& \left. - i \epsilon_i \sum_{j=0} (j+1) n'_j + (i+1) \epsilon_{i+1} \sum_{j=1} j n'_{j-1} - i n'_i \sum_{j=0} (j+1) \epsilon_j \right]
\end{aligned}$$

$$\begin{aligned}
& + (i+1) n'_{i+1} \sum_{j=0} j \epsilon_{j-1} + i \epsilon_{i-1} \sum_{j=0} (j+1) \epsilon_{j+1} \\
& - (i+1) \epsilon_i \sum_{j=1} j \epsilon_j - i \epsilon_i \sum_{j=0} (j+1) \epsilon_j + (i+1) \epsilon_{i+1} \sum_{j=1} j \epsilon_{j-1} \\
& + C_{1,0} \nu' n [0] [i (n'_{i-1} + \epsilon_{i-1}) + (i+1) e^{\theta/T} (n_{i+1} + \epsilon_{i+1}) \\
& - (i e^{\theta/T} + i+1) (n'_i + \epsilon_i)]
\end{aligned} \tag{A2-11}$$

Using equations (A2-4) and (A2-5) in (A2-11) the 5th, 6th, 9th, 10th, 11th, 12th, 13th, and 14th terms on the right hand side are zero. Thus we have

$$\begin{aligned}
& \frac{\partial n'_i}{\partial t} + \frac{\partial}{\partial z} (\vec{F}'_i)_z + \frac{\partial \epsilon_i}{\partial t} + \frac{\partial}{\partial z} (\vec{G}_i)_z = \sum_{j=0} \{A_{ij} (n'_j + \epsilon_j) \\
& - A_{ji} (n'_i + \epsilon_i)\} + P_{1,0;0,1} \nu \left[ \{i \epsilon_{i-1} - (i+1) \epsilon_i\} \sum_{j=1} j n'_j \right. \\
& \left. + \{(i+1) \epsilon_{i+1} - i \epsilon_i\} \sum_{j=1} j n'_{j-1} \right] + C_{1,0} \nu' n [0] [i (n'_{i-1} + \epsilon_{i-1}) \\
& + (i+1) e^{\theta/T} (n'_{i+1} + \epsilon_{i+1}) - (i e^{\theta/T} + i+1) \\
& (n'_i + \epsilon_i)]
\end{aligned} \tag{A2-12}$$

### A.2.1 The equation for the Boltzmann part of the solution.

Multiply (A2-12) by  $i$  and sum over  $i$  to get



$$\begin{aligned}
\frac{\partial}{\partial t} \sum_{i=0} i n'_i &= \frac{\partial}{\partial z} \left( \sum_{i=0} i \vec{F}'_i \right)_z = \sum_{i=0} \sum_{j=0} i \{A_{ij} (n'_j + \epsilon_j) \\
&\quad - A_{ji} (n'_i + \epsilon_i)\} + P_{1,0;0,1} \nu \left[ \sum_{j=1} j n'_j \left\{ \sum_{i=0} [i^2 \epsilon_{i-1} \right. \right. \\
&\quad \left. \left. - (i+1) \epsilon_i] \right\} + \sum_{j=1} j n'_{j-1} \left\{ \sum_{i=0} [i(i+1) \epsilon_{i+1} - i^2 \epsilon_i] \right\} \right] \\
&\quad + C_{1,0} \nu' n [0] \left[ \sum_{i=0} \{i^2 n'_{i-1} + i(i+1) e^{\theta/T} n'_{i+1} \right. \\
&\quad \left. - i(i e^{\theta/T} + i+1) n'_i\} + \sum_{i=0} \{i^2 \epsilon_{i-1} - i(i+1) \epsilon_i\} \right. \\
&\quad \left. + e^{\theta/T} \sum_{i=0} \{i(i+1) \epsilon_{i+1} - i^2 \epsilon_i\} \right]
\end{aligned} \tag{A2-13}$$

where we have used (A2-4) and

$$\begin{aligned}
\sum_{i=0} i \vec{G}_i &= - \sum_{i=0} i D \left[ \nabla \epsilon_i + \frac{\epsilon_i}{H} \hat{k} \right] \\
&= - D \left[ \nabla \sum_{i=0} i \epsilon_i + \sum_{i=0} i \frac{\epsilon_i}{H} \hat{k} \right] \\
&= 0
\end{aligned} \tag{A2-14}$$

Consider

$$\begin{aligned}
\sum_{i=0} [i^2 \epsilon_{i-1} - i(i+1) \epsilon_i] &= \sum_{i=1} i^2 \epsilon_{i-1} - \sum_{i=0} i^2 \epsilon_i - \sum_{i=0} i \epsilon_i \\
&= \sum_{i=0} (i+1)^2 \epsilon_i - \sum_{i=0} i^2 \epsilon_i
\end{aligned}$$

$$= \sum_{i=0} (2i+1) \epsilon_i \quad (\text{A2-15})$$

$$= 0$$

Also consider

$$\begin{aligned} \sum_{i=0} [i(i+1) \epsilon_{i+1} - i^2 \epsilon_i] &= \sum_{i=0} i(i-1) \epsilon_i - \sum_{i=0} i^2 \epsilon_i \\ &= - \sum_{i=0} i \epsilon_i \\ &= 0 \end{aligned} \quad (\text{A2-16})$$

Using (A2-15) and (A2-16) in (A2-13) we have

$$\begin{aligned} \frac{\partial}{\partial t} \sum_{i=0} i n'_i + \frac{\partial}{\partial z} \left( \sum_{i=0} i \vec{F}'_i \right)_z &= \sum_{i=0} \sum_{j=0} i \{A_{ij} (n'_j + \epsilon_j) \\ &\quad - A_{ji} (n'_i + \epsilon_i)\} + C_{1,0} \nu' [0] \sum_{i=0} \{i^2 n'_{i-1} \\ &\quad + i(i+1) e^{\theta/T} n'_{i+1} - i(i e^{\theta/T} + i+1) n'_i\} \end{aligned} \quad (\text{A2-17})$$

Consider

$$\begin{aligned} \sum_{i=0} \{i^2 n'_{i-1} + i(i+1) e^{\theta/T} n'_{i+1} - i(i e^{\theta/T} + i+1) n'_i\} \\ = \sum_{i=0} \{(i+1)^2 n'_i - i^2 n'_i - i n'_i + e^{\theta/T} \{i(i-1) n'_i - i^2 n'_i\}\} \end{aligned}$$

$$= \sum_{i=0} \{(i+1) - i e^{\theta/T}\} n'_i \quad (\text{A2-18})$$

Therefore equation (A2-17) becomes

$$\begin{aligned} \frac{\partial}{\partial t} \sum_{i=0} i n'_i + \frac{\partial}{\partial z} \left( \sum_{i=0} i \vec{F}'_i \right)_z &= \sum_{i=0} \sum_{j=0} i \{A_{ij} (n'_j + \epsilon_j) \\ &\quad - A_{ji} (n'_i + \epsilon_i)\} + C_{1,0} \nu' n [0] \left[ \sum_{i=0} (i+1) n'_i \right. \\ &\quad \left. - e^{\theta/T} \sum_{i=0} i n'_i \right] \end{aligned} \quad (\text{A2-19})$$

Let  $Z_p$  be the partition function for the Boltzmann distributed part of the solution.

Then,

$$Z_p = \frac{1}{1 - e^{-a}} \quad (\text{A2-20})$$

where

$$a = \frac{\theta}{T_v} \quad (\text{A2-21})$$

and  $T_v$  is the vibrational temperature. Therefore

$$\begin{aligned} \sum_{i=0} i n'_i &= \sum_{i=0} i \frac{n}{Z_p} e^{-a} \\ &= \frac{n}{Z_p} \frac{e^{-a}}{(1 - e^{-a})^2} \\ &= n (Z_p - 1) \end{aligned} \quad (\text{A2-23})$$

Also

$$\begin{aligned}\sum_{i=0} i \vec{F}_i &= -D \left[ \nabla \sum_{i=0} i n'_i + \sum_{i=0} i \frac{n'_i}{H} \hat{k} \right] \\ &= -D \left[ \nabla n (Z_p - 1) + \frac{n (Z_p - 1)}{H} \hat{k} \right]\end{aligned}\quad (\text{A2-24})$$

Consider

$$\begin{aligned}\sum_{i=0} i \sum_{j=0} \{A_{ij} (n'_j + \epsilon_j) - A_{ji} (n'_i + \epsilon_i)\} &= (n'_0 + \epsilon_0) \left\{ \sum_{i=0} i A_{i0} (1 - \delta_{i0}) \right\} \\ &+ (n'_1 + \epsilon_1) \left\{ \sum_{i=0} i A_{i1} (1 - \delta_{i1}) - \sum_{j=0} A_{j1} (1 - \delta_{1j}) \right\} \\ &+ (n'_2 + \epsilon_2) \left\{ \sum_{i=0} i A_{i2} (1 - \delta_{i2}) - \sum_{j=0} 2 A_{j2} (1 - \delta_{j2}) \right\} \\ &+ \dots \\ &+ (n'_k + \epsilon_k) \left\{ \sum_{i=0} i A_{ik} (1 - \delta_{ik}) - \sum_{j=0} k A_{jk} (1 - \delta_{jk}) \right\} \\ &+ \dots \\ &= (n'_0 + \epsilon_0) \left\{ \sum_{i=0} i (1 - \delta_{i0}) A_{i0} + (n'_1 + \epsilon_1) \sum_{i=0} (i - 1) A_{i1} \right\} \\ &+ (n'_2 + \epsilon_2) \left\{ \sum_{i=0} (i - 2) A_{i2} \right\} + \dots \\ &+ (n'_k + \epsilon_k) \left\{ \sum_{i=0} (i - k) A_{ik} \right\} + \dots \\ &= \sum_{i=0} \sum_{j=0} (n'_j + \epsilon_j) (i - j) A_{ij}\end{aligned}\quad (\text{A2-25})$$

Using (A2-23), (A2-24) and (A2-25) in equation (A2-19) we have

$$\begin{aligned}
 & \frac{\partial}{\partial t} n (Z_p - 1) + \frac{\partial}{\partial z} \left\{ -D \left[ \frac{\partial}{\partial z} n (Z_p - 1) + \frac{n (Z_p - 1)}{H} \right] \right\} \\
 &= \sum_{i=0} \sum_{j=0} (n'_j + \epsilon_j) (i - j) A_{ij} \\
 &+ C_{1,0} \nu' n [0] [n (Z_p - 1) + n - e^{\theta/T} n (Z_p - 1)] \quad (A2-26)
 \end{aligned}$$

Let

$$\psi = (Z_p - 1) \quad (A2-27)$$

and use

$$\frac{\partial n}{\partial t} = 0$$

and

$$(Z_p - 1) \frac{\partial n}{\partial z} = - \frac{n (Z_p - 1)}{H}$$

in equation (A2-26) to obtain

$$\begin{aligned}
 n \frac{\partial \psi}{\partial t} + \frac{\partial}{\partial z} \left( -D n \frac{\partial \psi}{\partial z} \right) &= \sum_{i=0} \sum_{j=0} (n'_j + \epsilon_j) (i - j) A_{ij} \\
 &+ C_{1,0} \nu' n [0] n [\psi + 1 - e^{\theta/T} \psi] \quad (A2-28)
 \end{aligned}$$

Using

$$\begin{aligned}
 n'_j &= \frac{n}{Z_p} (e^{-\alpha})^j \\
 &= \frac{n}{\psi + 1} \left( \frac{\psi}{\psi + 1} \right)^j \quad (A2-29)
 \end{aligned}$$

and dividing equation (A2-28) by  $n$  we have

$$\frac{\partial \psi}{\partial t} - \frac{1}{n} \left( \frac{\partial D n}{\partial z} \right) \frac{\partial \psi}{\partial z} - D \frac{\partial \psi^2}{\partial z^2} = \sum_{i=0} \sum_{j=0} \left[ \frac{1}{\psi + 1} \left( \frac{\psi}{\psi + 1} \right)^j + \frac{\epsilon_j}{n} \right] \\ (i - j) A_{ij} + C_{1,0} \nu' n [0] [\psi + 1 - e^{\theta/\tau} \psi] \quad (\text{A2-30})$$

The boundary conditions become for: set 1;

initial condition:  $\psi(z, 0) = 0$

lower boundary:  $\psi(120, t) = 0$

upper boundary:  $\frac{\partial n_i}{\partial z} = -\frac{n_i}{H} \Rightarrow \frac{\partial n'_i}{\partial z} + \frac{\partial \epsilon_i}{\partial z} = -\frac{n'_i}{H} - \frac{\epsilon_i}{H}$

Using (A2-23)

$$\frac{\partial}{\partial z} \sum_{i=p} i n'_i = - \sum_{i=0} i \frac{n'_i}{H}$$

Using (A2-23) and (A2-27) we have

$$\left. \frac{\partial}{\partial z} n \psi \right|_{z=\infty} = - \left. \frac{n \psi}{H} \right|_{z=\infty} \quad (\text{A2-31})$$

Thus,

$$\left. \frac{\partial \psi}{\partial z} \right|_{z=0} = 0$$

set 2;

initial condition:  $\psi(z, 0) = \frac{e^{-\theta/355}}{1 - e^{-\theta/355}} \\ = 7.329241 \times 10^{-5}$

lower boundary:  $\psi(0, t) = 7.329241 \times 10^{-5}$

upper boundary:  $\frac{\partial \psi}{\partial z} = 0$  (A2-32)

It is worthy of note that the only coupling between equation (A2-30) and the other equations is through the  $\epsilon_j/n$  term of the source of  $N_2^*$  due to electron collisions. This fact, and the expectation that  $\epsilon_j/n$  is small with respect to 1 for all  $j$  of interest, will be exploited in the solution of (A2-30).

## A2.2 The equations for the deviation parts of the solution.

Returning to equation (A2-12) for the  $\epsilon_i$ 's and treating the  $n_j$ 's as known quantities we have

$$\begin{aligned}
 \frac{\partial}{\partial t} \epsilon_i + \frac{\partial}{\partial z} (\vec{\mathcal{G}}_i)_z &= \sum_{j=0} \{A_{ij} (n'_j + \epsilon_j) - A_{ji} (n'_i + \epsilon_i)\} - \frac{\partial n'_i}{\partial t} \\
 &- \frac{\partial}{\partial z} (\vec{F}'_i)_z + P_{1,0:0,1} \nu \left[ \{i \epsilon_{i-1} - (i+1) \epsilon_i\} \sum_{j=1} j n_j \right. \\
 &+ \left. \{(i+1) \epsilon_{i+1} - i \epsilon_i\} \sum_{j=1} j n'_{j-1} \right] + C_{1,0} \nu' n [0] [i (n'_{i-1} \\
 &+ \epsilon_{i-1}) + (i+1) e^{\theta/T} (n'_{i+1} + \epsilon_{i+1}) - (i e^{\theta/T} + i+1) \\
 &\cdot (n'_i + \epsilon_i)]
 \end{aligned} \tag{A2-33}$$

Using equations (A2-23) and (A2-27) we have

$$\begin{aligned}
 \frac{\partial}{\partial t} \epsilon_i + \frac{\partial}{\partial z} (\vec{\mathcal{G}}_i)_z &= \sum_{j=0} \{A_{ij} (n'_j + \epsilon_j) - A_{ji} (n'_i + \epsilon_i)\} - \frac{\partial n'_i}{\partial t} \\
 &- \frac{\partial}{\partial z} (\vec{F}'_i)_z + P_{1,0:0,1} \nu [\{i \epsilon_{i-1} - (i+1) \epsilon_i\} n \psi
 \end{aligned}$$

$$\begin{aligned}
& + \{(i+1) \epsilon_{i+1} - i \epsilon_i\} n (\psi + 1)] \\
& + c_{1,0} \nu' n [0] \cdot [i (n'_{i-1} + \epsilon_{i-1}) + (i+1) e^{\theta/T} (n'_{i+1} + \epsilon_{i+1}) \\
& - (i e^{\theta/T} + i+1) (n'_i + \epsilon_i)] \quad (A2-34)
\end{aligned}$$

Rearranging terms in (A2-34) and dividing by  $n'_i$ , we have

$$\begin{aligned}
\frac{1}{n'_i} \frac{\partial}{\partial t} \epsilon_i + \frac{1}{n'_i} \frac{\partial}{\partial z} (\vec{\Theta}'_i)_z &= \sum_{j=0} \left\{ A_{ij} \left( \frac{n''_j}{n'_i} + \frac{\epsilon_j}{n'_j} \frac{n'_j}{n'_i} \right) - A_{ji} \left( 1 + \frac{\epsilon_i}{n'_i} \right) \right\} \\
&- \frac{1}{n'_i} \frac{\partial}{\partial t} n'_i - \frac{1}{n'_i} \frac{\partial}{\partial z} (\vec{F}'_i)_z - \frac{\epsilon_i}{n'_i} [P_{1,0:0,1} \nu n \{(2i+1)\psi \\
&+ i\} + C_{1,0} \nu' n [0] \cdot (i e^{\theta/T} + i+1)] \\
&+ \frac{\epsilon_{i-1}}{n'_{i-1}} \frac{n'_{i-1}}{n'_i} [P_{1,0:0,1} \nu i n \psi + C_{1,0} \nu' n [0] \cdot i] \\
&+ \frac{\epsilon_{i+1}}{n'_{i+1}} \frac{n'_{i+1}}{n'_i} [P_{1,0:0,1} \nu n (i+1) (\psi + 1) + C_{1,0} \nu' n [0] \cdot e^{\theta/T} (i+1)] \\
&+ C_{1,0} \nu' n [0] \left[ i \frac{n'_{i-1}}{n'_i} + (i+1) e^{\theta/T} \frac{n'_{i+1}}{n'_i} - (i e^{\theta/T} + i+1) \right] \quad (A2-35)
\end{aligned}$$

Consider

$$\frac{\partial}{\partial t} \frac{\epsilon_i}{n'_i} = \frac{1}{n'_i} \frac{\partial \epsilon_i}{\partial t} - \frac{\epsilon_i}{(n'_i)^2} \frac{\partial}{\partial t} n'_i$$

thus

$$\frac{1}{n'_i} \frac{\partial \epsilon_i}{\partial t} = \frac{\partial}{\partial t} \frac{\epsilon_i}{n'_i} + \frac{1}{n'_i} \frac{\epsilon_i}{n'_i} \frac{\partial}{\partial t} n'_i \quad (A2-36)$$



Also

$$\nabla \frac{\epsilon_i}{n'_i} = \frac{1}{n'_i} \nabla \epsilon_i - \frac{\epsilon_i}{(n'_i)^2} \nabla n'_i$$

Therefore

(A2-37)

$$\nabla \epsilon_i = n'_i \nabla \frac{\epsilon_i}{n'_i} + \frac{\epsilon_i}{n'_i} \nabla n'_i$$

Therefore

$$\begin{aligned} \frac{1}{n'_i} \frac{\partial}{\partial z} (\vec{y}_i)_z &= \frac{1}{n'_i} \frac{\partial}{\partial z} \left[ -D \left\{ \frac{\partial \epsilon_i}{\partial z} + \frac{\epsilon_i}{H} \right\} \right] \\ &= \frac{1}{n'_i} \frac{\partial}{\partial z} \left[ -D \left\{ n'_i \frac{\partial}{\partial z} \frac{\epsilon_i}{n'_i} + \frac{\epsilon_i}{n'_i} \frac{\partial n'_i}{\partial z} + \frac{\epsilon_i}{H} \right\} \right] \\ &= \frac{1}{n'_i} \frac{\partial}{\partial z} \left[ -D n'_i \frac{\partial}{\partial z} \frac{\epsilon_i}{n'_i} - D \frac{\epsilon_i}{n'_i} \left\{ \frac{\partial n'_i}{\partial z} + \frac{n'_i}{H} \right\} \right] \end{aligned} \quad (A2-38)$$

Let

$$\varphi_i = \frac{\epsilon_i}{n'_i} \quad (A2-39)$$

then (A2-36) and (A2-38) become, respectively,

$$\frac{1}{n'_i} \frac{\partial \epsilon_i}{\partial t} = \frac{\partial}{\partial t} \varphi_i + \frac{1}{n'_i} \varphi_i \frac{\partial}{\partial t} n'_i \quad (A2-40)$$

and

$$\frac{1}{n'_i} \frac{\partial}{\partial z} (\vec{y}_i)_z = \frac{1}{n'_i} \frac{\partial}{\partial z} \left[ -D n'_i \frac{\partial}{\partial z} \varphi_i - D \varphi_i \left\{ \frac{\partial n'_i}{\partial z} + \frac{n'_i}{H} \right\} \right] \quad (A2-41)$$

Using (A2-39), (A2-40), (A2-41) in (A2-35) and rearranging terms we have

$$\begin{aligned} &\frac{\partial}{\partial t} \varphi_i - D \frac{\partial^2}{\partial z^2} \varphi_i - \left[ \frac{1}{n'_i} \frac{\partial}{\partial z} D n'_i + \frac{1}{n'_i} D \left\{ \frac{\partial n'_i}{\partial z} + \frac{n'_i}{H} \right\} \right] \frac{\partial \varphi_i}{\partial z} \\ &+ \left[ \frac{1}{n'_i} \frac{\partial}{\partial t} n'_i - \frac{1}{n'_i} \frac{\partial}{\partial z} \left\{ D \left( \frac{\partial n'_i}{\partial z} + \frac{n'_i}{H} \right) \right\} + \sum_{j=0} A_{ji} (1 - \delta_{ij}) \right. \\ &\left. + P_{i,0;0,1} \nu n \{ (2i+1) \psi + i \} + C_{1,0} \nu' n [0] (i e^{\theta/T} + i + 1) \right] \varphi_i \end{aligned}$$

$$\begin{aligned}
&= \sum_{j=0} \left\{ A_{ij} (1 + \varphi_j) e^{-(j-1)\theta/T_V} - A_{ji} \right\} (1 - \delta_{ij}) - \frac{1}{n'_i} \frac{\partial n'_i}{\partial t} \\
&- \frac{1}{n'_i} \frac{\partial}{\partial z} \left\{ -D \left( \frac{\partial n'_i}{\partial z} + \frac{n'_i}{H} \right) \right\} + \varphi_{i-1} e^{\theta/T} [P_{1,0:0,1} \nu n i \psi \\
&+ C_{1,0} \nu' n [0] i] + \varphi_{i+1} e^{-\theta/T_V} [P_{1,0:0,1} \nu n (i+1) (\psi + 1) \\
&+ C_{1,0} \nu' n [0] e^{\theta/T} (i+1)] + C_{1,0} \nu' n [0] [i e^{\theta/T_V} \\
&+ (i+1) e^{\theta/T - \theta/T_V} - (i e^{\theta/T} + i+1)] \quad (A2-42)
\end{aligned}$$

Consider

$$\begin{aligned}
&\frac{1}{n'_j} \frac{\partial n'_j}{\partial y} \quad \text{where } n'_j = n \frac{\psi^j}{(\psi + 1)^{j+1}} \\
&\frac{1}{n'_j} \frac{\partial n'_j}{\partial y} = \frac{1}{n} \frac{\partial n}{\partial y} + \left\{ \frac{j}{\psi} - \frac{j+1}{\psi+1} \right\} \frac{\partial \psi}{\partial y} \quad (A2-43)
\end{aligned}$$

Thus, if  $y = t$

$$\frac{1}{n'_j} \frac{\partial n'_j}{\partial t} = \left( \frac{j}{\psi} - \frac{j+1}{\psi+1} \right) \frac{\partial \psi}{\partial t} \quad (A2-44)$$

and if  $y = z$

$$\frac{1}{n'_j} \frac{\partial n'_j}{\partial z} = -\frac{1}{H} + \left\{ \frac{j}{\psi} - \frac{j+1}{\psi+1} \right\} \frac{\partial \psi}{\partial z} \quad (A2-45)$$

Using (A2-44) and (A2-45) in (A2-42) and collecting terms we have

$$\begin{aligned}
& \frac{\partial}{\partial t} \varphi_i - D \frac{\partial^2}{\partial z^2} \varphi_i - \left[ \frac{\partial D}{\partial z} + D \left( -\frac{1}{H} + 2 \left\{ \frac{i}{\psi} - \frac{i+1}{\psi+1} \right\} \frac{\partial \psi}{\partial z} \right) \right] \frac{\partial \varphi_i}{\partial z} \\
& + \left[ \left\{ \frac{i}{\psi} - \frac{i+1}{\psi+1} \right\} \frac{\partial \psi}{\partial t} - \frac{\partial \psi}{\partial z} \left\{ \frac{i}{\psi} - \frac{i+1}{\psi+1} \right\} \left\{ \frac{\partial D}{\partial z} + D \left( -\frac{1}{H} \right. \right. \right. \\
& + \left. \left. \left\{ \frac{i}{\psi} - \frac{i+1}{\psi+1} \right\} \frac{\partial \psi}{\partial z} \right) \right\} - D \left\{ \frac{i}{\psi} - \frac{i+1}{\psi+1} \right\} \frac{\partial^2 \psi}{\partial z^2} - D \left( \frac{\partial \psi}{\partial z} \right)^2 \left\{ -\frac{i}{\psi^2} \right. \right. \\
& + \left. \left. \frac{(i+1)}{(\psi+1)^2} \right\} + \sum_{j=0}^n A_{ji} (1 - \delta_{ij}) + P_{1,0:0,1} \nu n \{ (2i+1) \psi + i \} \right. \\
& + C_{1,0} \nu' n [0] (i e^{\theta/T} + i + 1) \left. \right] \varphi_i = \sum_{j=0}^n \left\{ A_{ij} (1 + \varphi_j) e^{-(j-i)\theta/T_v} \right\} (1 - \delta_{ij}) \\
& - \left[ \left( \frac{i}{\psi} - \frac{i+1}{\psi+1} \right) \frac{\partial \psi}{\partial t} - \frac{\partial \psi}{\partial z} \left\{ \frac{i}{\psi} - \frac{i+1}{\psi+1} \right\} \left\{ \frac{\partial D}{\partial z} + D \left\{ -\frac{1}{H} \right. \right. \right. \\
& + \left. \left. \left\{ \frac{i}{\psi} - \frac{i+1}{\psi+1} \right\} \frac{\partial \psi}{\partial z} \right\} + \sum_{j=0}^n A_{ji} (1 - \delta_{ij}) - D \left\{ \frac{i}{\psi} - \frac{i+1}{\psi+1} \right\} \frac{\partial^2 \psi}{\partial z^2} \right. \\
& - D \left( \frac{\partial \psi}{\partial z} \right)^2 \left\{ -\frac{i}{\psi^2} + \frac{i+1}{(\psi+1)^2} \right\} + P_{1,0:0,1} \nu n \{ (2i+1) \psi + i \} \\
& + C_{1,0} \nu' n [0] (i e^{\theta/T} + i + 1) \left. \right] + P_{1,0:0,1} \nu n \{ (2i+1) \psi + i \} \\
& + C_{1,0} \nu' n [0] \left[ i e^{\theta/T_v} + (i+1) e^{\theta/T - \theta/T_v} \right] + \varphi_{i-1} e^{\theta/T_v} \left[ P_{1,0:0,1} \nu n_i \psi \right. \\
& + C_{1,0} \nu' n [0] i \left. \right] + \varphi_{i+1} e^{-\theta/T_v} \left[ P_{1,0:0,1} \nu n (i+1) (\psi+1) \right. \\
& + C_{1,0} \nu' n [0] e^{\theta/T} (i+1) \left. \right]
\end{aligned}$$

The boundary conditions for the  $\epsilon_i$ 's are, by assumption, identical for set 1 and set 2 boundary conditions for  $\psi$ . For

initial condition  $\varphi_i(z, 0) = 0$  for all  $i$

lower boundary  $\varphi_i(120, t) = 0$  for all  $i$

upper boundary 
$$\frac{\partial n_i}{\partial z} = -\frac{n_i}{H}$$

thus,

$$\frac{\partial n_i'}{\partial z} + \frac{\partial \epsilon_i}{\partial z} = -\frac{n_i'}{H} - \frac{\epsilon_i}{H}$$

using (A2-45)

$$n_i' \left[ -\frac{1}{H} + \left\{ \frac{i}{\psi} - \frac{i+1}{\psi+1} \right\} \frac{\partial \psi}{\partial z} \right] + \frac{\partial \epsilon_i}{\partial z} = -\frac{n_i}{H} - \frac{\epsilon_i}{H}$$

thus

$$n_i' \left\{ \frac{i}{\psi} - \frac{i+1}{\psi+1} \right\} \frac{\partial \psi}{\partial z} + \frac{\partial \epsilon_i}{\partial z} = -\frac{\epsilon_i}{H}$$

using equation (A2-32) we obtain

$$\left. \frac{\partial \epsilon_i}{\partial z} \right|_{z=\infty} = -\left. \frac{\epsilon_i}{H} \right|_{z=\infty}$$

now using (A2-37) and (A2-39) we have

$$n_i' \frac{\partial}{\partial z} \varphi_i + \varphi_i \frac{\partial n_i}{\partial z} = -\varphi_i \frac{n_i'}{H}$$

thus, using (A2-45)

$$n_i' \frac{\partial}{\partial z} \varphi_i + \varphi_i n_i' \left\{ -\frac{1}{H} + \left( \frac{i}{\psi} - \frac{i+1}{\psi+1} \right) \frac{\partial \psi}{\partial z} \right\} = -\varphi_i \frac{n_i}{H}$$

again using (A2-32) we have

$$\left[ n'_i \frac{\partial \varphi_i}{\partial z} \right]_{z=\infty} = 0$$

or

$$\left. \frac{\partial \varphi_i}{\partial z} \right|_{z=\phi} = 0 \quad \text{for all } i \quad (\text{A2-47})$$

From equation (A2-46) it is seen that all solutions are coupled through the electronic source term and that only those levels adjacent to the level of interest are coupled through vibration-vibrational or vibrational-translational energy exchange terms. If  $\psi$  is assumed known, then equation (A2-46) represents a set of 6, coupled, linear, partial differential equations for the  $\epsilon_i$  's.

## APPENDIX III

### CONSTRUCTION OF FINITE DIFFERENCE EQUATIONS

To numerically solve equations (A2-30) and (A2-46) we will use the finite difference approximation of Crank and Nicholson (see reference (36)). This particular choice was made because, in a linear problem, the errors are of order two in both the time and space step, and the solutions are expected to be unconditionally stable.

#### A3.1 Finite difference form, the $\psi$ equation.

Equation (A2-30) becomes in six point finite difference form with

$$\begin{aligned}\psi_{\ell}^m &= \psi((\ell - 1)\Delta z, (m - 1)\Delta t) \quad \ell = 1, 2, \dots, L \\ m &= 1, 2, \dots, M\end{aligned}\tag{A3-1}$$

where  $\Delta z$  is the altitudinal space step size and  $\Delta t$  is the time step size

$$\begin{aligned}\frac{\psi_{\ell}^{m+1} - \psi_{\ell}^m}{\Delta t} &- \frac{1}{n_{\ell}} \left( \frac{\partial Dn}{\partial z} \right)_{\ell} \frac{1}{2\Delta z} \{ \psi_{\ell+1}^m - \psi_{\ell-1}^m \} \\ &- \frac{D_{\ell}}{2(\Delta z)^2} \{ \psi_{\ell+1}^{m+1} - 2\psi_{\ell}^{m+1} + \psi_{\ell-1}^{m+1} + \psi_{\ell+1}^m - 2\psi_{\ell}^m + \psi_{\ell-1}^m \} \\ &= \sum_{j=0} \sum_{i=0} \left[ \frac{1}{\psi_{\ell+1}^m + 1} \left( \frac{\psi_{\ell}^m}{\psi_{\ell}^m + 1} \right)^j + \frac{\epsilon_j}{n} \right] (i - j) A_{ij}\end{aligned}\tag{A3-2}$$

and the subscript  $\ell$  and superscript  $m$  mean that the quantities are evaluated at the altitude  $120 + (\ell - 1)\Delta z$  and time  $\sum_1^m (m - 1)\Delta t$ , respectively. The term  $\epsilon_j / n$  has been retained in the source term in (A3-2) for completeness. Solving for the  $m+1$  super-scripted terms in (A3-2) we have

$$\begin{aligned}
& - \frac{D_\ell \Delta t}{2(\Delta z)^2} \psi_{\ell+1}^{m+1} + \left\{ 1 + \frac{D_\ell \Delta t}{(\Delta z)^2} \right\} \psi_\ell^{m+1} - \frac{D_\ell \Delta t}{2(\Delta z)^2} \psi_{\ell-1}^{m+1} \\
& = \left\{ \frac{D_\ell \Delta t}{2(\Delta z)^2} + \frac{1}{n_\ell} \left( \frac{\partial Dn}{\partial z} \right)_\ell \frac{\Delta t}{2\Delta z} \right\} \psi_{\ell+1}^m \\
& + \left\{ 1 - \frac{D_\ell \Delta t}{(\Delta z)^2} \right\} \psi_\ell^m + \left\{ \frac{D_\ell \Delta t}{2(\Delta z)^2} - \frac{1}{n_\ell} \left( \frac{\partial Dn}{\partial z} \right)_\ell \frac{\Delta t}{2\Delta z} \right\} \psi_{\ell-1}^m \\
& + \Delta t \sum_{j=0} \sum_{i=0} \left[ \frac{1}{\psi_\ell^m + 1} \left( \frac{\psi_\ell^m}{\psi_\ell^m + 1} \right)^j + \frac{\ell \epsilon_j^m}{n} \right] (i - j) A_{ij} \quad (A3-3)
\end{aligned}$$

Let

$$A_\ell = \frac{D_\ell \Delta t}{2(\Delta z)^2} \quad (A3-4)$$

$$\begin{aligned}
B_\ell &= 1 + \frac{D_\ell \Delta t}{(\Delta z)^2} \\
&= 1 + 2 A_\ell \quad (A3-5)
\end{aligned}$$

$$\begin{aligned}
D_\ell &= \left\{ A_\ell + \frac{1}{n_\ell} \left( \frac{\partial Dn}{\partial z} \right)_\ell \frac{\Delta t}{\Delta z} \right\} \psi_{\ell+1}^m + \{ 1 - 2A_\ell \} \psi_\ell^m \\
&+ \left\{ A_\ell - \frac{1}{n_\ell} \left( \frac{\partial Dn}{\partial z} \right)_\ell \frac{\Delta t}{2\Delta z} \right\} \psi_{\ell-1}^m \\
&+ \Delta t \sum_{j=0} \sum_{i=0} \left[ \frac{1}{\psi_{\ell+1}^m + 1} \left( \frac{\psi_\ell^m}{\psi_\ell^m + 1} \right)^j + \frac{\ell \epsilon_j^m}{n} \right] (i - j) A_{ij} \quad (A3-6)
\end{aligned}$$

Thus (A3-3) becomes

$$- A_\ell \psi_{\ell+1}^{m+1} + B_\ell \psi_\ell^{m+1} - A_\ell \psi_{\ell-1}^{m+1} = D_\ell^m \quad (A3-7)$$

The boundary conditions become

	set 1	set 2	
$m = 1$	$\psi_\ell^1 = 0$	$\psi_\ell^1 = 7.329241 \text{ E} - 05$	
$\ell = 1$	$\psi_1^m = 0$	$\psi_1^m = 7.329241 \text{ E} - 05$	
(A3-8)	$\ell = L$	$\psi_L^m - \psi_{L-1}^m = 0$	(A3-9)

### A3.2 Finite difference form, the $\varphi_i$ equations.

Let

$$\ell_{\alpha_i^m} = \left[ \frac{\partial D}{\partial z} + D \left( -\frac{1}{H} + 2 \left\{ \frac{i}{\psi} - \frac{i+1}{\psi+1} \right\} \frac{\partial \psi}{\partial z} \right) \right]_{\ell, m} \quad (\text{A3-10})$$

$$\begin{aligned} \ell_{\beta_i^m} = & \left[ \left( \frac{i}{\psi} - \frac{i+1}{\psi+1} \right) \frac{\partial \psi}{\partial t} - \frac{\partial \psi}{\partial z} \left\{ \frac{i}{\psi} - \frac{i+1}{\psi+1} \right\} \left\{ \frac{\partial D}{\partial z} \right. \right. \\ & + D \left( -\frac{1}{H} + \left\{ \frac{i}{\psi} - \frac{i+1}{\psi+1} \right\} \frac{\partial \psi}{\partial z} \right) \left. \right\} - D \left\{ \frac{i}{\psi} - \frac{i+1}{\psi+1} \right\} \frac{\partial^2 \psi}{\partial z^2} \\ & - D \left( \frac{\partial \psi}{\partial z} \right)^2 \left\{ -\frac{i}{\psi^2} + \frac{(i+1)}{(\psi+1)^2} \right\} + \sum_{j=0} A_{ij} (1 - \delta_{ij}) \end{aligned}$$

$$+ P_{1,0;0,1} \nu n \{(2i+1)\psi + i\} + C_{1,0} \nu' n[0] (i e^{\theta/T} + i+1) \Big]_{\ell, m} \quad (\text{A3-11})$$

$$\begin{aligned} \ell_{\gamma_i^m} = & \left[ \sum_{j=0} \left\{ A_{ij} (1 + \varphi_j) e^{-(j-i)\theta/T_V} (1 - \delta_{ij}) - \ell_{\beta_i^m} \right. \right. \\ & + P_{1,0;0,1} \nu n \{(2i+1)\psi + i\} + C_{1,0} \nu' n[0] \left\{ i e^{\theta/T_V} \right. \\ & + (i+1) e^{\theta/T - \theta/T_V} \left. \right\} + \varphi_{i-1} e^{\theta/T_V} [P_{1,0;0,1} \nu n i \psi \\ & + C_{1,0} \nu' n[0] i] + \varphi_{i+1} e^{-\theta/T_V} [P_{1,0;0,1} \nu n (i+1) (\psi+1) \\ & + C_{1,0} \nu' n[0] e^{\theta/T} (i+1)] \left. \right]_{\ell, m} \quad (\text{A3-12}) \end{aligned}$$



Using (A3-10) through (A3-12) and expressing (A2-46) in finite difference

form we have after some rearrangement of terms

$$\begin{aligned}
 & -\frac{D\ell \Delta t}{2(\Delta z)^2} \ell_{+1}^{\varphi_i^{m+1}} + \left[ \frac{D\ell \Delta t}{(\Delta z)^2} + 1 \right] \ell_{\varphi_i^{m+1}} - \frac{D\ell \Delta t}{2(\Delta z)^2} \ell_{-1}^{\varphi_i^{m+1}} \\
 & = \left[ \frac{D\ell \Delta t}{2(\Delta z)^2} + \ell_{\alpha_i^m} \frac{\Delta t}{2\Delta z} \right] \ell_{+1}^{\varphi_i^m} + \left[ 1 - \frac{D\ell \Delta t}{(\Delta z)^2} \right. \\
 & \quad \left. - \ell_{\beta_i^m} \Delta t \right] \ell_{\varphi_i^m} + \left[ \frac{D\ell \Delta t}{2(\Delta z)^2} - \ell_{\alpha_i^m} \frac{\Delta t}{2\Delta z} \right] \ell_{-1}^{\varphi_i^m} \\
 & \quad + \ell_{\gamma_i^m} \Delta t
 \end{aligned} \tag{A3-13}$$

Let

$$\ell_{A_i} = \frac{D\ell \Delta t}{2(\Delta z)^2} \tag{A3-14}$$

$$\ell_{B_i} = 1 + \frac{D\ell \Delta t}{(\Delta z)^2} \tag{A3-15}$$

$$= 1 + 2\ell_{A_i}$$

$$\begin{aligned}
 \ell_{C_i^m} &= \left[ \frac{D\ell \Delta t}{2(\Delta z)^2} + \ell_{\alpha_i^m} \frac{\Delta t}{2\Delta z} \right] \ell_{+1}^{\varphi_i^m} + \left[ 1 - \frac{D\ell \Delta t}{(\Delta z)^2} - \ell_{\beta_i^m} \Delta t \right] \ell_{\varphi_i^m} \\
 & \quad + \left[ \frac{D\ell \Delta t}{2(\Delta z)^2} - \ell_{\alpha_i^m} \frac{\Delta t}{2\Delta z} \right] \ell_{-1}^{\varphi_i^m} + \ell_{\gamma_i^m} \Delta t
 \end{aligned} \tag{A3-16}$$

Thus equation (A3-13) becomes

$$-\ell_{A_i}^{\lambda+1} \varphi_i^{m+1} + \ell_{B_i} \ell_{\varphi_i^{m+1}} - \ell_{A_i} \ell_{-1}^{\varphi_i^{m+1}} = \ell_{C_i^m} \tag{A3-17}$$

The boundary conditions are

$$m = 1 \quad \ell \varphi_i^1 = 0 \quad \text{for all } i$$

$$\ell = 1 \quad {}^1\varphi_i^m = 0 \quad \text{for all } i$$

$$\ell = L \quad {}^L\varphi_i^m - {}^{L-1}\varphi_i^m = 0 \quad \text{for all } i \quad (\text{A3-18})$$

# APPENDIX IV

## COMPUTER PROGRAM LISTINGS

### BOLTSOL

```

C THIS PROGRAM CALCULATES THE                                00000100
C VIBRATIONAL TEMPERATURE, AND NUMBER DENSITY              00000200
C OF VIBRATIONAL QUANTA PRODUCED BY SLOW ELECTRON          00000300
C COLLISIONS FOR VIBRATIONAL NITROGEN.                     00000400
C THE SYMBOLOGY IS THAT CONTAINED IN THE ANALYTICAL       00000500
C FORMULATION OF THE PROBLEM.                               00000600
C THE DIMENSIONS OF PSI WILL CHANGE WITH THE UPPER ALTITUDE 00000700
C LIMIT,ZUPPER,THE STEP SIZE,DELZ.                          00000800
C TIMEX IS THE MAXIMUM TIME AND DELT IS THE TIME STEP.      00000900
C PSI SHOULD BE DIMENSIONED ACCORDING TO PSI(IALT, 2 ) WHEKE 00001000
C MINIMUM VALUE OF IALT IS                                  00001100
C IALT = 1. + (ZUPPER - 120.)/DELZ                          00001200
C IPMOVE IS (ARRAY SIZE)*BYTES*(NUMBER OF ARRAYS).         00001300
C ALL OTHER ARRAYS ARE DIMENSIONED FOR A 10. KM. DELZ.      00001400
C MMTIN GOVERNS THE PRINTER LISTING AND PLOTTING FREQUENCY. 00001500
C TCHANG IS THE TIME AT WHICH THE STEP SIZE IS CHANGED     00001600
C TO DELT2 FROM DELT.                                       00001700
C ITFLAG IS A FLAG TO INDICATE TO THE PROGRAM THAT MORE    00001800
C THAN ONE TIME STEP IS USED.                               00001900
C IFLAG IS RELATED TO ITFLAG AND IS INITIALLY SET TO ZERO. 00002000
C ICFLAG IS A FLAG TO INDICATE TO THE PROGRAM THAT A CORRECTION 00002100
C USING RESULTS FROM PROGRAM BOLTDEV IS TO BE APPLIED TO    00002200
C THE SOURCE TERM OF THIS PROGRAM.                           00002300
C REAL #4 NED,NI,INT,NZ,NE,MBAR,N2Z,NZ1,NZ2,MBAR1,MBAR2,NOZ 00002400
C LOGICAL*1 IMAGE(5151)                                     00002500
C DIMENSION RAID(8),TED(80),ZD(10),NED(45)                 00002600
C ,GAMIZD(70),W(15),X(15),Y(15),ZP(15)                    00002700
C ,ID1(15),ID2(15),Z(89),NOZ(89),KATEOE(89),KATEOD(89)    00002800
C ,TEI(2),TE(89),NZ(6),NE(89),A(89)                       00002900
C ,NZ1(6),NZ2(6),P1(6,6),P2(6,6),P3(6,6),P4(6,6)          00003000
C ,INT(6,6),E(10),B(89),C(89),D1(89),D2(89)               00003100
C ,D3(89),D(89),DI(89),PSI(89,2)                           00003200
C ,EC(89),F(89),TV(90),QUANTA(89),N2Z(89)                  00003300
C ,TZZ(89),ALPSI(90),GRID(8281),CORR(89)                   00003400
C ,ALN2Z(89),ALNE(89),ALQUAN(89),DSOUR(89),DSOURC(89),TV1(1) 00003500
C ,PHI(6,21),EPSIL(6,21),NBOLT(6,21),SUMC(6,6),G(1),N2Z1(1) 00003600
C DATA INPUT.                                              00003700
C READ (5,1,END=90000) RAID                                00003800
C 1 FORMAT (F5.1)                                           00003900
C WRITE (6,2)RAID                                           00004000
C 2 FORMAT ('1',8F6.1)                                       00004100
C READ (5,3,END=90000) TED                                  00004200
C 3 FORMAT (F6.0)                                           00004300
C WRITE (6,4) TED                                           00004400
C 4 FORMAT ('0',10F7.0)                                       00004500

```

```

      READ (5,5,END=90000) ZD
5  FORMAT (F5.0)
      WRITE (6,6) ZD
6  FORMAT ('0',10F6.0)
      READ (5,7,END=90000) NED
7  FORMAT (E11.5)
      WRITE (6,8) NED
8  FORMAT ('0',10E12.5)
      READ (5,10,END=90000) GAMIZD
10 FORMAT (E13.7)
      WRITE (6,11) GAMIZD
11 FORMAT ('0',8E14.7)
      READ (5,12,END=90000) DELZ,ZUPPER,DELT,TIMEX,MMMTIN,ITFLAG
X    ,TCHANG,DELT2,ICFLAG,RATEO
12 FORMAT (F4.0,F5.0,F6.0,F7.0,I4,I2,F7.0,F6.0,I2,E10.2)
      WRITE (6,13) DELZ,ZUPPER,DELT,TIMEX,MMMTIN,ITFLAG,TCHANG,DELT2,
X    ICFLAG,RATEO
13 FORMAT ('0',F4.0,F5.0,F6.0,F7.0,I4,I2,F7.0,F6.0,I2,E10.2)
      READ (5,14,END=90000) DII,TI,NI,ENU,TOO
14 FORMAT (F6.4,F6.0,E13.7,F5.3,F5.0)
      WRITE (6,15) DII,TI,NI,ENU,TOO
15 FORMAT ('0',F6.4,F6.0,E13.7,F5.3,F5.0)
      READ (5,16,END=90000) E
16 FORMAT ((1X,F6.4))
      WRITE (6,17) E
17 FORMAT ('0',10(1X,F6.4))
      READ (5,18,END=90000) (W(N),X(N),Y(N),ZP(N),
C      ID1(N),ID2(N),N=1,15)
18 FORMAT (1X,4E14.6,3X,2I1)
      WRITE (6,19) (W(N),X(N),Y(N),ZP(N),ID1(N),ID2(N),N=1,15)
19 FORMAT ('0',1X,4E14.6,3X,2I1)
      READ (5,20,END=90000) RAI
20 FORMAT (F5.1)
      WRITE (6,21) RAI
21 FORMAT ('0',F5.1)
C RECONSTRUCTION OF THE INTEGRATED CHEN CROSS-SECTIONS
C PARAMETERS.
      WRITE (6,26)
26 FORMAT ('0',2X,'ID',2X,'III',2X,'JJJ',8X,'P1',9X,'P2',
C      13X,'P3',12X,'P4')
      DO 2700 IM=1,15
      III = ID1(IM) + 1
      JJJ = ID2(IM) + 1
      P1(III,JJJ) = W(IM)
      P2(III,JJJ) = X(IM)

```

```

00004600
00004700
00004800
00004900
00005000
00005100
00005200
00005300
00005400
00005500
00005600
00005700
00005800
00005900
00006000
00006100
00006200
00006300
00006400
00006500
00006600
00006700
00006800
00006900
00007000
00007100
00007200
00007300
00007400
00007500
00007600
00007700
00007800
00007900
00008000
00008100
00008200
00008300
00008400
00008500
00008600
00008700
00008800
00008900
00009000

```

```

      P3(III,JJJ) = Y(IM)
      P4(III,JJJ) = ZP(IM)
2700 WRITE (6,27) ID1(IM),ID2(IM),III,JJJ,P1(III,JJJ)
      C      ,P2(III,JJJ),P3(III,JJJ),P4(III,JJJ)
      27 FORMAT ('0',2X,2I1,3X,I1,3X,I1,1P4E14.6)
C TEST OF RAI FOR TABLE RANGE.
      DO 2100 I=1,7
      I1 = I
2100 IF (RAI.GE.RAID(I).AND.RAI.LT.RAID(I+1)) GO TO 2300
      WRITE (6,22)
      22 FORMAT ('1','RAI NOT WITHIN TABLE RANGE')
      WRITE (6,23) RAI
      23 FORMAT ('0',F6.1)
      STOP
2300 CONTINUE
C SET DIAGONAL ELEMENTS OF INTEGRATED CROSS-SECTION MATRIX
C TO ZERO.
      DO 2900 I1K=1,6
      2900 INT(I1K,I1K) = 0.
      IPMOVE = 89*4*1
      IFLAG = 0
      MLOW = 2
      BK = 8.61703E-05
      THETA = 3380.
      MMAX = TCHANG/DELT
      MMIN = 0
      DIFI =(DII*NI)/(TI*0.75)
      CALL JACH2 (Z,T00,TZ,NZ,MBAR,RHOZ,HZ)
C CALCULATION OF TIME INVARIANT COEFFICIENTS AT EACH
C VERTICAL GRID POINT.
      LMAX = 1 + (ZUPPER - 120.)/DELT
      3900 WRITE (6,41)
      41 FORMAT ('0',5X,'DIFF',10X,'A',12X,'B',12X,'C',12X,
      C      'D1',12X,'D2',10X,'D3', 5X,'L')
      DO 2000 L=1,LMAX
      Z(L) = 120. + (L -1)*DELT
C TEST OF Z TO BE WITHIN TABLE RANGES.
      DO 2400 K=1,9
      2400 IF (Z(L).GE.ZD(K).AND.Z(L).LT.ZD(K+1)) GO TO 2500
      WRITE (6,24)
      24 FORMAT ('1','ALTITUDE IS NOT WITHIN TABLE RANGE')
      WRITE (6,25) Z(L)
      25 FORMAT ('0', F5.0)
      STOP
2500 IK = K

```

```

00009100
00009200
00009300
00009400
00009500
00009600
00009700
00009800
00009900
00010000
00010100
00010200
00010300
00010400
00010500
00010600
00010700
00010800
00010900
00011000
00011100
00011200
00011300
00011400
00011500
00011600
00011700
00011800
00011900
00012000
00012100
00012200
00012300
00012400
00012500
00012600
00012700
00012800
00012900
00013000
00013100
00013200
00013300
00013400
00013500

```

```

      IL = K + 1
C CALCULATION OF TEI.
C TEI INDEX IS THE LINE NUMBER.
C OF THE PLOTTED ELECTRON TEMPERATURE DATA.
      DO 2600 LL=1,2
2600 TEI(LL) = GAMIZD(IK + 10*(II-1) + LL - 1)
      C      *(RAI - RAID(II)) + TED((II-1)*10 + IK+LL-1)
C CALCULATION OF BETAZI AND THE ELECTRON TEMPERATURE.
      BETAZI = (TEI(2) - TEI(1))/(ZD(IL) - ZD(IK))
      TE(L) = BETAZI*(Z(L) - ZD(IK)) + TEI(1)
C CALCULATION OF ELECTRON DENSITY.
      DO 100 IT=1,44
      ZTEST1 = 20.*(IT-1) + 120.
      ZTEST2 = ZTEST1 + 20.
      IF ( Z(L).GE.ZTEST1.AND.Z(L).LE.ZTEST2) GO TO 200
100 CONTINUE
      WRITE (6,51)
51 FORMAT ('0','ALTITUDE FOR NE CALCULATION IS OUTSIDE TABLE')
      WRITE (6,52) Z(L)
52 FORMAT ('0',2X,F6.0)
      STOP
200 ITT = IT
      GRADNE = (NED(ITT+1) - NED(ITT))/20.
      NE(L) = GRADNE*(Z(L) - ZTEST1) + NED(ITT)
      ZA = Z(L)
      CALL JACH2(ZA,TOO,TZ,NZ,MBAR,RHOZ,HZ)
      N2Z(L) = NZ(1)
      NOZ(L) = NZ(3)
      SUMNZ = NZ(1) + NZ(3)
      TZZ(L) = TZ
      RATEOD(L) = RATEO*NOZ(L)
      RATEOE(L) = RATEOD(L)*EXP(-THETA/TZZ(L))
C CALCULATION OF DIFFUSION, A AND B COEFFICIENTS.
      DIFF = DIFI*(TZ**0.75)/SUMNZ
      A(L) = (DIFF * DELT)/(2. *((DELZ*1.E+05)**2.))
      B(L) = 1. + 2.*A(L)
      IF(L.EQ.1) GO TO 2000
C CALCULATION OF DERIVATIVE OF PRODUCT OF DIFFUSION
C COEFFICIENT AND MOLECULAR NITROGEN DENSITY
C WITH RESPECT TO ALTITUDE.
      Z1 = Z(L) - 0.5*DELZ
      Z2 = Z(L) + 0.5*DELZ
      CALL JACH2 (Z1,TOO,TZ1,NZ1,MBAR1,RHOZ1,HZ1)
      CALL JACH2 (Z2,TOO,TZ2,NZ2,MBAR2,RHOZ2,HZ2)
      SUMNZ1 = NZ1(1) + NZ1(3)

```

```

00013600
00013700
00013800
00013900
00014000
00014100
00014200
00014300
00014400
00014500
00014600
00014700
00014800
00014900
00015000
00015100
00015200
00015300
00015400
00015500
00015600
00015700
00015800
00015900
00016000
00016100
00016200
00016201
00016300
00016400
00016401
00016402
00016500
00016600
00016700
00016800
00016900
00017000
00017100
00017200
00017300
00017400
00017500
00017600
00017700

```

```

SUMNZ2 = NZ2(1) + NZ2(3)                                00017800
DIFF1 = DIF1*(TZ1**0.75)/SUMNZ1                        00017900
DIFF2 = DIF1*(TZ2**0.75)/SUMNZ2                        00018000
DERIV = (DIFF2*NZ2(1) - DIFF1*NZ1(1))/(DELZ*1.E+05)    00018100
C CALCULATION OF C AND TIME INDEPENDENT PARTIAL D COEFFICIENTS. 00018200
C(L) = (DERIV*DELZ)/(2.*(DELZ*1.E+05)*NZ(1))           00018300
D1(L) = A(L) + C(L)                                     00018400
D2(L) = 1. - 2.*A(L)                                    00018500
D3(L) = A(L) - C(L)                                     00018600
WRITE (6,42) DIFF,A(L),B(L),C(L),D1(L),D2(L),D3(L),L    00018700
42 FORMAT ('0',1P7E13.5,13)                             00018800
2000 CONTINUE                                           00018900
C(1) = C(2)                                             00019000
D1(1) = A(1) + C(1)                                    00019100
D2(1) = 1. - 2.*A(1)                                   00019200
D3(1) = A(1) - C(1)                                    00019300
WRITE (6,61)                                           00019301
61 FORMAT ('1',2X,'ALT',6X,'RATEOE',8X,'RATEOD',5X,'N(0)') 00019302
WRITE (6,62) (Z(ILN),RATEOE(ILN),RATEOD(ILN),NOZ(ILN),ILN=1,LMAX) 00019303
62 FORMAT ('0',0PF5.0,1P3E13.5)                       00019304
IF (IFLAG.EQ.1) GO TO 3950                             00019400
C CALCULATION OF EC AND F COEFFICIENTS FOR INITIAL TIME STEP. 00019500
C LLL IS THE ALTITUDE STEP INDEX.                      00019600
EC(1) = 0.                                             00019700
F(1) = 7.329241E-05                                    00019800
WRITE (6,43)                                           00019900
43 FORMAT ('1',6X,'DI',10X,'EC',10X,'F',10X,'DENOM',10X,'LLL') 00020000
DO 3200 LLL=1,LMAX                                     00020100
C SET DSOURC TO ZERO.                                  00020200
DSOURC(LLI) = 0.                                       00020300
C CALCULATION OF INTEGRATED CHEN CROSS-SECTION VALUES 00020400
C AT ALTITUDE OF INTEREST.                             00020500
BKTE = BK*TE(LLI)                                     00020600
RTE = 1./TE(LLI)                                       00020700
RTE2 = RTE*RTE                                         00020800
RTE3 = RTE2*RTE                                         00020900
DO 2800 IN=1,15                                        00021000
IIJ = ID1(IN) + 1                                     00021100
JJI = ID2(IN) + 1                                     00021200
INT (IIJ,JJI) = EXP(P1(IIJ,JJI) + P2(IIJ,JJI)*RTE     00021300
C + P3(IIJ,JJI)*RTE2 + P4(IIJ,JJI)*RTE3)              00021400
2800 INT(JJI,IIJ) = INT(IIJ,JJI)*EXP(-(E(JJI) - E(IIJ))/BKTE) 00021500
C CALCULATION OF INITIAL SOURCE TERM DI.              00021600
SUMSI = 0.                                             00021700
DO 3400 IIL = 1,6                                     00021800

```

```

SUM = (IIL-1)*INT(IIL,1)*NE(LLL)                                00021900
3400 SUMSI = SUMSI + SUM                                          00022000
    DI(LLL) = SUMSI*DELT + RATEOE(LLL)*DELT*(F(1) + 1. -      00022100
    X      F(1)*EXP(THETA/TZZ(LLL)))                             00022101
C  END CALCULATION OF INITIAL SOURCE TERM AT ALTITUDE DENOTED BY LLL. 00022200
    IF (LTL.EQ.1) GO TO 3200                                       00022300
    DENOM = B(LLL) - A(LLL)*EC(LLL- 1)                             00022400
    EC(LLL)= A(LLL)/DENOM                                           00022500
    F(LLL) = (DI(LLL) + A(LLL)*F(LLL -1))/DENOM                   00022600
    WRITE (6,44) DI(LLL),EC(LLL),F(LLL),DENOM,LLL                00022700
    44 FORMAT ('0',1P4E13.6,I3)                                     00022800
3200 CONTINUE                                                    00022900
C  CALCULATION OF INITIAL PSI.                                     00023000
    MMM = 1                                                         00023100
    LLMAX = LMAX - 1                                                00023200
    PSI(LLMAX-1,1) = F(LLMAX-1)/(1.-EC(LLMAX-1))                 00023300
    DO 3500 NNN=2,LLMAX                                           00023400
    NNNN = LMAX - NNN                                              00023500
    PSI(NNNN,1) = EC(NNNN)*PSI(NNNN+1,1) + F(NNNN)               00023600
    NNNNA = NNNN + 1                                              00023700
    TV(NNNNA) = THETA/ALOG((PSI(NNNNA, 1 )+1.)/PSI(NNNNA, 1 ))  00023800
    QUANTA(NNNNA) = N2Z(NNNNA)*PSI(NNNNA, 1 )                    00023900
3500 CONTINUE                                                    00024000
    PSI(LMAX,1) = PSI(LMAX - 1,1)                                  00024100
    PSI(LMAX+1,1) = PSI(LMAX,1)                                    00024200
    TV(LMAX ) = THETA/ALOG((PSI(LMAX , 1 )+1.)/PSI(LMAX , 1 ))  00024300
    TV(1) = 0.                                                     00024400
    QUANTA(1) = 0.                                                 00024500
    QUANTA(LMAX ) = N2Z(LMAX )*PSI(LMAX , 1 )                     00024600
C  WRITE RESULTS ON OUTPUT TAPE.                                   00024700
    WRITE (10) (Z(ILN),TZZ(ILN),TE(ILN),TV(ILN),N2Z(ILN),NE(ILN), 00024800
    C    QUANTA(ILN),PSI(ILN, 1 ),DI(ILN),D(ILN),MMM,DELZ,        00024900
    X    MMAX,DELT,IFLAG,ILN=1,LMAX)                               00025000
    WRITE (6,34)                                                    00025100
34  FORMAT ('1',2X,'ALT',          2X,'T',6X,'TE',              00025200
    C    4X,'TV', 4X,'N(N2)', 8X,'NE', 12X,'QUANTA',              00025300
    C    9X,'PSI', 5X,'SOURCE INT',5X,'SOURCE',5X,'ELEC SOURCE', 00025400
    X    2X,'CORRECTION')                                           00025500
    WRITE (6,35) MMM,MMAX,DELT,IFLAG,ICFLAG,MMMIN                00025600
35  FORMAT ('0',6X,I4,6X,I4,6X,F6.0,6X,I2,I2,I4)                  00025700
    WRITE (6,28) (Z(IKN),TZZ(IKN),TE(IKN),TV(IKN),N2Z(IKN),NE(IKN) 00025800
    C    ,QUANTA(IKN),PSI(IKN, 1 ),DI(IKN),D(IKN),DSOUR(IKN),    00025900
    X    DSOUR(IKN),IKN=1,LMAX)                                       00026000
28  FORMAT (' ',OPF5.0,OP3F6.0,1P8E13.5)                           00026100
C  CALCULATION OF COEFFICIENTS AND PSI FOR OTHER TIME STEPS.     00026200

```



```

C MMT IS AN INDEX CONTROLLING THE AMOUNT OF PRINTED OUTPUT.
C MMT IS THE TIME STEP INDEX.
      MMT = 2
      IF (ICFLAG.EQ.0) GO TO 3950
      READ (11,END=90001,ERR=90002) MMIN,DELT1,LBOUND,DELZ1,DELZ2,
X     LINC,(G(1),N2Z1(1),TV1(1),(I,PHI(I,ILN),EPSIL(I,ILN),
X     NBOLT(I,ILN),I=1,6,1),ILN=1,LMAX)
3950 DO 3600 MMM=MLOW,MMAX
      DO 3700 LLLL=1,LMAX
      IF (LLLL.EQ.1) D(1)=D1(1)*PSI(2, 1 )+DI(1)
      IF (LLLL.EQ.1) GO TO 3700
C  CALCULATION OF INTEGRATED CHEN CROSS-SECTION VALUES
C  AT ALTITUDE OF INTEREST.
      BKTE = BK*TE(LLLL)
      RTE = 1./TE(LLLL)
      RTE2 = RTE*RTE
      RTE3 = RTE2*RTE
      DO 3801 IJK=1,15
      INI = ID1(IJK) + 1
      INJ = ID2(IJK) + 1
      INT(INI,INJ) = EXP(P1(INI,INJ) + P2(INI,INJ)*RTE
      + P3(INI,INJ)*RTE2 + P4(INI,INJ)*RTE3)
3801 INT(INJ,INI) = INT(INI,INJ)*EXP(-(E(INJ) - E(INI))/BKTE)
C  CALCULATION OF D COEFFICIENT AT ALTITUDE LLLL.
      SUMST = 0.
      DO 3901 IIII=1,6
      DO 3901 JJJJ=1,6
      SUMS = 1./((PSI(LLLL, 1 ) + 1.)*((PSI(LLLL, 1 ) )/
C  (PSI(LLLL, 1 )+1.))*((JJJJ-1))*((IIII-JJJJ)
C  *INT(IIII,JJJJ)*NE(LLLL)
3901 SUMST = SUMST + SUMS
      IF (ICFLAG.EQ.0) GO TO 1500
1100 IF(MMM-MMMIN)1500,1200,90003
1200 SUMT = 0.
      DO 1300 II=1,6
      DO 1300 JJ=1,6
      SUMC(II,JJ) = INT(II,JJ)*NE(LLLL)*EPSIL(JJ,LLLL)*(II-JJ)
1300 SUMT = SUMT + SUMC(II,JJ)
      CORR(LLLL) = SUMT/N2Z(LLLL)
      DSOURC(LLLL) = CORR(LLLL)*DELT
      IF (LLLL.EQ.LMAX) GO TO 1000
      GO TO 1600
1000 READ (11,END=90001,ERR=90002) MMIN,DELT1,LBOUND,DELZ1,DELZ2,
X     LINC,(G(1),N2Z1(1),TV1(1),(I,PHI(I,ILN),EPSIL(I,ILN),
X     NBOLT(I,ILN),I=1,6,1),ILN=1,LMAX)

```

```

GO TO 1600
1500 DSOURC(LLLL) = 0.
1600 CONTINUE
DSOUR(LLLL) = SUMST*DELT + DSOURC(LLLL)
D(LLLL) = D1(LLLL)*PSI(LLLL+1, 1 ) + D2(LLLL)*PSI(LLLL, 1 )
C + D3(LLLL)*PSI(LLLL-1, 1 ) + DSOUR(LLLL)
X + RATEDE(LLLL)*DELT*(PSI(LLLL,1) + 1.
X - PSI(LLLL,1)*EXP(THETA/TZZ(LLLL)))
DENOM1 = B(LLLL) - A(LLLL)*EC(LLLL-1)
EC(LLLL) = A(LLLL)/DENOM1
F(LLLL) = (D(LLLL) + A(LLLL)*F(LLLL-1))/DENOM1
3700 CONTINUE
C CALCULATION OF PSI, VIBRATIONAL TEMPERATURE, ETC.
PSI(LMAX-1, 2 ) = F(LMAX-1)/(1.-EC(LMAX-1))
PSI(LMAX, 2 ) = PSI(LMAX-1, 2 )
PSI(LMAX+1, 2 ) = PSI(LMAX, 2 )
DO 4000 INN=2,LMAX
NNNNN = LMAX - INN
PSI(NNNNN, 2 ) = EC(NNNNN)*PSI(NNNNN+1, 2 ) + F(NNNNN)
NNNNM = NNNNN + 1
TV(NNNNM) = THETA/ALOG((PSI(NNNNM, 2 )+1.)/PSI(NNNNM, 2 ))
4000 QUANTA(NNNNM) = N2Z(NNNNM)*PSI(NNNNM, 2 )
TV(LMAX ) = THETA/ALOG((PSI(LMAX , 2 )+1.)/PSI(LMAX , 2 ))
TV(1) = 0.
QUANTA(1) = 0.
QUANTA(LMAX ) = N2Z(LMAX )*PSI(LMAX , 2 )
C WRITE RESULTS ON OUTPUT TAPE.
WRITE (10) (Z(ILN),TZZ(ILN),TE(ILN),TV(ILN),N2Z(ILN),NE(ILN),
C QUANTA(ILN),PSI(ILN, 2 ),DI(ILN),D(ILN),MMM,DELZ,
X MMAX,DELT,IFLAG,ILN=1,LMAX)
C TEST FOR PRINTING AND PLOTTING.
IF(MMM.NE.MMMT) GO TO 3600
MMMT = MMMT + MMMTIN
WRITE (6,34)
WRITE (6,35) MMM,MMAX,DELT,IFLAG,ICFLAG,MMMIN
WRITE (6,28) (Z(IKN),TZZ(IKN),TE(IKN),TV(IKN),N2Z(IKN),NE(IKN)
C ,QUANTA(IKN),PSI(IKN, 2 ),DI(IKN),D(IKN),DSOUR(IKN),
C DSOURC(IKN),IKN=1,LMAX)
C CONSTRUCTION OF PRINTER PLOTTER ARRAYS.
DO 4100 IMN=2,LMAX
ALPSI(IMN) = ALOG10(PSI(IMN, 2 ))
ALN2Z(IMN) = ALOG10(N2Z(IMN))
ALQUAN(IMN) = ALOG10(QUANTA(IMN))
4100 ALNE(IMN) = ALOG10(NE(IMN))
C PRINTER PLOTTING.

```

WRITE (6,29)	00035100
29 FORMAT ('1',46X,'TEMPERATURES VERSUS ALTITUDE')	00035200
XR = 1000.	00035300
XL = 0.	00035400
YT = 10000.	00035500
YB = 0.	00035600
NUMPR1 = LMAX + 1	00035700
NUMPR2 = LMAX	00035800
CALL PLOT2 (GRID,XR,XL,YT,YB)	00035900
CALL PLOT3 ('T',Z,TZZ,NUMPR1)	00036000
CALL PLOT3 ('V',Z,TV,NUMPR1)	00036100
CALL PLOT4 (20,'TEMPERATURE DEG. K')	00036200
WRITE (6,30)	00036300
30 FORMAT('0',59X,'ALTITUDE (KM.)')	00036400
WRITE (6,31)	00036500
31 FORMAT ('1',51X,'PSI VERSUS ALTITUDE')	00036600
YT = 0.0	00036700
YB = -5.0	00036800
CALL PLOT2 (GRID,XR,XL,YT,YB)	00036900
CALL PLOT3 ('*',Z,ALPSI,NUMPR2)	00037000
CALL PLOT4 (3,'PSI')	00037100
WRITE (6,30)	00037200
YT = +9.0	00037300
YB = +4.0	00037400
WRITE (6,32)	00037500
32 FORMAT ('1',46X,'QUANTA AND ELECTRON DENSITIES')	00037600
CALL PLOT2 (GRID,XR,XL,YT,YB)	00037700
CALL PLOT3 ('E',Z,ALNE,NUMPR2)	00037800
CALL PLOT3 ('Q',Z,ALQUAN,NUMPR2)	00037900
CALL PLOT4 (23,'NUMBER DENSITY CM**-3')	00038000
WRITE (6,30)	00038100
3600 CALL CMOVE(IPMOVE,PSI(1,2),1,PSI(1,1),1)	00038200
CONTINUE	00038300
C TEST FOR CHANGE OF TIME STEP.	00038400
MLOW = MMAX + 1	00038500
IF (ITFLAG.EQ.1.AND.IFLAG.EQ.0) GO TO 3800	00038600
END FILE 10	00038700
STOP	00038800
C SET UP DO LOOP INDICIES FOR SECOND TIME INCREMENT STEP SIZE.	00038900
3800 DELT = DELT2	00039000
MMAX = (TIMEX - TCHANG)/DELT2 + MLOW - 1	00039100
IFLAG = ITFLAG	00039200
GO TO 3900	00039300
90000 WRITE (6,33)	00039400
33 FORMAT ('1','END OF FILE ENCOUNTERED ON CARD READER')	00039500

```
      STOP
90001 WRITE (6,84)
      84 FORMAT ('1','END OF FILE ENCOUNTERED ON INPUT TAPE')
      STOP
90002 WRITE (6,85)
      85 FORMAT ('1','IO ERROR ENCOUNTERED ON INPUT TAPE')
      STOP
90003 WRITE (6,86)
      86 FORMAT ('1','MMMIN IS LESS THAN MMM')
      STOP
      END
```

```
00039600
00039700
00039800
00039900
00040000
00040100
00040200
00040300
00040400
00040500
00040600
```

0416 CA

## BOLTDEV

```

C THIS PROGRAM CALCULATES THE DEPARTURES IN NUMBER DENSITY      00000100
C FROM A BOLTZMAN DISTRIBUTION OF VIBRATIONAL QUANTA             00000200
C PRODUCED BY AN ELECTRONIC SOURCE.                               00000300
C THE SYMBOLOGY IS THAT CONTAINED IN THE ANALYTICAL             00000400
C FORMULATION OF THE PROBLEM.                                     00000500
C THE DIMENSIONS OF PSI WILL CHANGE WITH THE UPPER ALTITUDE     00000600
C LIMIT,ZUPPER,THE STEP SIZE,DELZ,THE MAXIMUM TIME,TIMEX,        00000700
C AND THE TIME STEP SIZE,DELT.                                     00000800
C PHI SHOULD BE DIMENSIONED ACCORDING TO PHI(6,IALT) WHERE        00000900
C MINIMUM VALUE OF IALT IS                                         00001000
C  $IALT = 1. + (ZUPPER - 120.)/DELZ$                                00001100
C ALL OTHER ARRAYS ARE DIMENSIONED FOR A 10. KM. DELZ.           00001200
C MMT IS AN INDEX CONTROLLING THE AMOUNT OF PRINTED OUTPUT.      00001300
C MMTIN GOVERNS THE PRINTER LISTING AND PLOTTING FREQUENCY.      00001400
C ISTART IS THE TIME STEP FROM BOLTSOL RESULTS AT WHICH THE      00001500
C CALCULATIONS OF DEVIATIONS IS STARTED.                          00001600
C LINC CONTROLS THE ALTITUDE INCREMENT FOR THE DEVIATION         00001700
C PART OF THE PROGRAM, EQUIVALENT DELZ =LINC*DELZ               00001800
C DELZ IS THE ALTITUDE INCREMENT FOR THE BOLTZMAN PART           00001900
C OF THE PROBLEM.                                                 00002000
C DELT IS THE TIME INCREMENT FOR THE BOLTZMAN PART               00002100
C OF THE PROBLEM.                                                 00002200
C EDELT IS THE EQUIVALENT TIME STEP FOR THE DEVIATION            00002300
C PART OF THE PROBLEM.                                           00002400
C TINC IS THE NUMBER OF DELT INCREMENTS IN EDELT.                00002500
C LBOUND IS THE LOWER BOUNDARY FOR THE DEVIATION CALCULATION.    00002600
C REAL *4 NED,NI,INT,NZ,NE,MBAR,NZZ,NZ1,NZ2,MBAR1,MBAR2,NU,NBOLT 00002700
C X ,NOZ                                                           00002701
C INTEGER TINC,TINC2                                              00002800
C LOGICAL*1 IMAGE(5151)                                           00002900
C DIMENSION Z(89),RAID(8),TED(80),ZD(10),NED(45)                 00003000
C X ,GAMIZD(70), NZ(6),NE(89),A(89),NOZ(89)                      00003100
C X ,W(15),X(15),Y(15),ZP(15),ID1(15)                            00003101
C X ,ID2(15),TEI(2),TE(89),P1(6,6)                                00003102
C X ,P2(6,6),P3(6,6),P4(6,6),INT(6,6)                            00003103
C X ,NZ1(6),NZ2(6),GRADT(89),HPRESS(89)                          00003200
C X ,E(10),B(89),MMAX1(3),DELT1(3),IFLAG(3),                     00003300
C X NZZ(89), MMM(3),DI(89),PSI(30,3),RATEOE(89),RATEOD(89)       00003400
C X ,TZZ(89),GRID(8281),SUME1A(89),SUME2A(89)                    00003500
C X ,DERIVD(89),DIFF(89),H(89),DPSIZ(89),DPSIT(89)               00003600
C X ,D2PSIZ(89),ALPHA(6,89),BETA(6,89),GAMMA(6,89)              00003700
C X ,NU(89),P1001(89),TV(30,3) ,QUANTA(30,1),D(30,1)            00003800
C X ,PHI(6,89),C1(6,89),C2(6,89),C3(6,89),C(6,89),F(6,89)       00003900
C X ,EC(6,89),ALPHI1(89),ALPHI2(89),ALPHI3(89),ALPHI4(89),       00004000
C X ALPHI5(89),ALPHI6(89),EPSIL(6,89),NBOLT(6,89),REPSIL(6,89) 00004100

```

C DATA INPUT.	00004200
READ (5,1,END=90000) RAID	00004201
1 FORMAT (F5.1)	00004202
WRITE (6,2)RAID	00004203
2 FORMAT ('1',8F6.1)	00004204
READ (5,3,END=90000) TED	00004205
3 FORMAT (F6.0)	00004206
WRITE (6,4) TED	00004207
4 FORMAT ('0',10F7.0)	00004208
READ (5,5,END=90000) ZD	00004209
5 FORMAT (F5.0)	00004210
WRITE (6,6) ZD	00004211
6 FORMAT ('0',10F5.0)	00004212
READ (5,7,END=90000) NED	00004213
7 FORMAT (E11.5)	00004214
WRITE (6,8) NED	00004215
8 FORMAT ('0',10E12.5)	00004216
READ (5,10,END=90000) GAMIZD	00004217
10 FORMAT (E13.7)	00004218
WRITE (6,11) GAMIZD	00004219
11 FORMAT ('0',8E14.7)	00004220
READ (5,12,END=90000) DELZ,ZUPPER,DELT,TIMEX,MMMTIN,LINC,TINC	00004700
X ,LBOUND,TINC2,RATEO	00004800
12 FORMAT (F4.0,F5.0,F6.0,F7.0,I4,4I3,E10.2)	00004900
WRITE (6,13)DELZ,ZUPPER,DELT,TIMEX,MMMTIN,LINC,TINC	00005000
X ,LBOUND,TINC2,RATEO	00005100
13 FORMAT ('0',F4.0,F5.0,F6.0,F7.0,I4,4I3,E10.2)	00005200
READ (5,14,END=90000) DII,TI,NI,ENU,TOO	00005300
14 FORMAT (F6.4,F6.0,E13.7,F5.3,F5.0)	00005400
WRITE (6,15) DII,TI,NI,ENU,TOO	00005500
15 FORMAT ('0',F6.4,F6.0,E13.7,F5.3,F5.0)	00005600
READ (5,16,END=90000) E	00005700
16 FORMAT ((1X,F6.4))	00005800
WRITE (6,17) E	00005900
17 FORMAT ('0',10(1X,F6.4))	00006000
READ (5,18,END=90000) (W(N),X(N),Y(N),ZP(N),	00006001
C ID1(N),ID2(N),N=1,15)	00006002
18 FORMAT (1X,4E14.6,3X,2I1)	00006003
WRITE (6,19) (W(N),X(N),Y(N),ZP(N),ID1(N),ID2(N),N=1,15)	00006004
19 FORMAT ('0',1X,4E14.6,3X,2I1)	00006005
READ (5,20,END=90000) RAI	00006006
20 FORMAT (F5.1)	00006007
WRITE (6,21) RAI	00006008
21 FORMAT ('0',F5.1)	00006009
READ (5,22) ISTART	00006100

```

22 FORMAT (I4)                                00006200
   WRITE (6,23) ISTART                        00006300
23 FORMAT ('0',I4)                            00006400
   CALL JACH2(Z,TOO,TZ,NZ,MBAR,RHOZ,HZ)        00006500
C RECONSTRUCTION OF THE INTEGRATED CHEN CROSS-SECTIONS 00006501
C PARAMETERS.                                00006502
   WRITE (6,26)                               00006503
26 FORMAT ('0',2X,'ID',2X,'III',2X,'JJJ',8X,'P1',9X,'P2',
C       13X,'P3',12X,'P4')                  00006504
   DO 2700 IM=1,15                            00006505
     III = ID1(IM) + 1                        00006506
     JJJ = ID2(IM) + 1                        00006507
     P1(III,JJJ) = W(IM)                     00006508
     P2(III,JJJ) = X(IM)                     00006509
     P3(III,JJJ) = Y(IM)                     00006510
     P4(III,JJJ) = ZP(IM)                    00006511
2700 WRITE (6,27) ID1(IM),ID2(IM),III,JJJ,P1(III,JJJ),
X       P2(III,JJJ),P3(III,JJJ),P4(III,JJJ) 00006512
27 FORMAT ('0',2X,2I1,2(3X,I1),1P4E14.6)    00006513
   DIFI =(DII*NI)/(TI*0.75)                  00006514
C IPMOV AND IMMOV ARE (ARRAY SIZE)*BYTES*(NUMBER OF ARRAYS) 00006515
   IPMOV = 30*4*2                             00006600
   IMMOV = 1*4*2                               00006700
   BK = 8.61703E-05                           00006800
   THETA = 3380.                              00006900
   ISTAR = ISTART - 1                          00007000
   LMAX = 1. + (ZUPPER - 120.)/DELZ            00007100
C SET PHI(I,L),EC(I,LBOUND),AND F(I,LBOUND) TO ZERO. 00007200
C SET REPSIL(I,LBOUND) AND DIAGONAL ELEMENTS OF THE 00007300
C INTEGRATED CHEN CROSS-SECTION MATRIX TO ZERO.    00007400
   DO 3000 IJ = 1,6                            00007401
     DO 3001 K=1,LBOUND                        00007402
       EC(IJ,K) = 0.                          00007500
3001 F(IJ,K) = 0.                              00007600
       REPSIL(IJ,LBOUND) = 0.                 00007700
       INT(IJ,IJ) = 0.                        00007800
       DO 3000 LL = 1,LMAX,LINC                00007901
3000 PHI(IJ,LL) = 0.                          00008000
C READ TAPE CONTAINING BOLTZMAN PART SOLUTION.      00008100
   READ ( 10,END=90001,ERR=90002) (Z(ILN),TZZ(ILN),TE(ILN),
X       TV(ILN,1),NZZ(ILN),NE(ILN),QUANTA(ILN,1), 00008200
X       PSI(ILN,1),DI(ILN),D(ILN,1),MMM(1),DELZ1, 00008300
X       MMAX1(1),DELT1(1),IFLAG(1),ILN=1,LMAX) 00008400
   IF (ISTAR - MMM(1)) 90003,3600,4100        00008500
3600 DO 3700 M=2,3                            00008600
                                           00008700
                                           00008800

```

```

3700 READ ( 10,END=90001,ERR=90002) (Z(ILN),TZZ(ILN),TE(ILN),
X      TV(ILN,M),N2Z(ILN),NE(ILN),QUANTA(ILN,1),
X      PSI(ILN,M),DI(ILN),D(ILN,1),MMM(M),DELZ1,
X      MMAX1(M),DELT1(M),IFLAG(M),ILN=1,LMAX)
      MMT = ISTAR + 1
      GO TO 6000
4100 DO 1000 JK=3,ISTAR
1000 READ (10,END=90001,ERR=90002)
      MMT = ISTAR + 1
      DO 4200 LM=1,3
4200 READ ( 10,END=90001,ERR=90002) (Z(ILN),TZZ(ILN),TE(ILN),
X      TV(ILN,LM),N2Z(ILN),NE(ILN),QUANTA(ILN,1),
X      PSI(ILN,LM),DI(ILN),D(ILN,1),MMM(LM),DELZ1,
X      MMAX1(LM),DELT1(LM),IFLAG (LM),ILN=1,LMAX)
      GO TO 6000
3900 DO 3901 J=1,TINC
      CALL CMOVE (IPMOV,PSI(1,2),1,PSI(1,1),1)
      CALL CMOVE (IPMOV,TV(1,2),1,TV(1,1),1)
      CALL CMOVE(IMMOV,MMM(2),1,MMM(1),1)
      CALL CMOVE(IMMOV,MMAX1(2),1,MMAX1(1),1)
      CALL CMOVE(IMMOV,DELT1(2),1,DELT1(1),1)
      CALL CMOVE(IMMOV,IFLAG(2),1,IFLAG(1),1)
      READ ( 10,END=90001,ERR=90002) (Z(ILN),TZZ(ILN),TE(ILN),
X      TV(ILN,3),N2Z(ILN),NE(ILN),QUANTA(ILN,1),
X      PSI(ILN,3),DI(ILN),D(ILN,1),MMM(3),DELZ1,
X      MMAX1(3),DELT1(3),IFLAG(3),ILN=1,LMAX)
      IF (IFLAG (3).EQ.1.AND.IFLAG (2).EQ.0) GO TO 6000
3901 CONTINUE
      GO TO 3800
C  CALCULATION OF A,B AND OTHER TIME INVARIANT TERMS.
6000 DELT = DELT1(3)
      IF (IFLAG(3).EQ.1) TINC = TINC2
      EDELT = DELT*TINC
      DO 2500 II=1,LMAX,LINC
      CALL JACH2 (Z(II),TOO,TZ,NZ,MBAR,RHOZ,HZ)
      HPRESS(II) = HZ*MBAR/28.
      NOZ(II) = NZ(3)
      SUMNZ = NZ(1) + NZ(3)
      DIFF(II) = DIFI*(TZ**0.75)/SUMNZ
      A(II) = (DIFF(II)*EDELT)/(2.*((DELZ*LINC*1.E+05)**2.))
      B(II) = 1. + 2*A(II)
      T05=TZ**0.5
      NU(II) = 1.48209E-11*T05
      P1001(II) = 2.6003E-06*TZ*EXP(91.5/TZ)
      RATEOD(II) = RATEO*NOZ(II)

```



```

      RATEOD(II) = RATEOD(II)*EXP(-THETA/TZZ(II))
C  CALCULATION OF DERIVATIVES OF DIFF.,TEMP. AND DENSITY SCALE HEIGHT.
      IF (II.EQ.1) GO TO 2500
      Z1 = Z(II) - 0.5*DELZ
      Z2 = Z(II) + 0.5*DELZ
      CALL JACH2(Z1,T00,TZ1,NZ1,MBAR1,RHOZ1,HZ1)
      CALL JACH2 ( Z2,T00,TZ2,NZ2,MBAR2,RHOZ2,HZ2)
      GRADT(II) = (TZ2 - TZ1)/DELZ
      H(II) = HPRESS(II)/(1 + HPRESS(II) * GRADT(II)/TZZ(II))
      SUMNZ1 = NZ1(1) + NZ1(3)
      SUMNZ2 = NZ2(1) + NZ2(3)
      DIFF1 = DIFI*(TZ1**0.75)/SUMNZ1
      DIFF2 = DIFI*(TZ2**0.75)/SUMNZ2
      DERIVD(II) = (DIFF2 - DIFF1)/(DELZ*1.E+05)
2500 CONTINUE
      GRADT(1) = GRADT(2)
      H(1) = HPRESS(1)/(1 + HPRESS(1) * GRADT(1)/TZZ(1) )
      DERIVD(1) = DERIVD(2)
      LINCPI = LINC + LBOUND
      LLMAX = LMAX - LINC
      MMAX = MMAX1(3) - 1
3800 DO 4000 L = LINCPI,LLMAX,LINC
C  CALCULATION OF DERIVATIVES OF PSI WITH RESPECT TO
C  ALTITUDE AND TIME.
      DPSIZ(L) = (PSI(L+1,2) - PSI(L-1,2))/(2.*(DELZ*1.E+05))
      D2PSIZ(L) = (PSI(L+1,2) - 2.*PSI(L,2) + PSI(L-1,2))/
X      ((DELZ*1.E+05)**2 )
      DELTS = DELT1(1) + DELT1(3)
      DPSIT(L) = (PSI(L,3 ) - PSI(L, 1))/(2.*DELTS)
C  CALCULATION OF INTEGRATED CHEN CROSS-SECTION VALUES
C  AT ALTITUDE OF INTEREST.
      BKTE = BK*TE(L)
      RTE = 1./TE(L)
      RTE2 = RTE*RTE
      RTE3 = RTE2*RTE
      DO 2800 IN=1,15
      IIJ = ID1(IN) + 1
      JJI = ID2(IN) + 1
      INT (IIJ,JJI) = EXP(P1(IIJ,JJI) + P2(IIJ,JJI)*RTE
C      + P3(IIJ,JJI)*RTE2 + P4(IIJ,JJI)*RTE3)
2800 INT(JJI,IIJ) = INT(IIJ,JJI)*EXP(-(E(JJI) - E(IIJ))/BKTE)
      DO 4000 I=1,6
      BRAKET = (I-1)/PSI(L,2) - I/(PSI(L,2) + 1.)
      ALPHA(I,L) = DERIVD(L) + DIFF(L)*(-1./(H(L)*1.E+05) + 2.*BRAKET
X      *DPSIZ(L))

```

```

C  CALCULATION OF SOURCE TERMS.                                00016200
C  CALCULATION OF SUMMATIONS FOR USE IN BETA AND GAMMA.        00016201
    SUMA1 = 0.                                                    00016202
    SUMA2 = 0.                                                    00016203
    DO 5000 IIL=1,6                                              00016204
    SUM1 = INT(I,IIL)*NE(L)                                       00016205
    SUMA1 = SUMA1 + INT(IIL,I)*NE(L)                             00016206
    SUM2 = SUM1*(1. + PHI(IIL,L))*EXP( (I - IIL)*THETA/TV(L,2)) 00016207
5000 SUMA2 = SUMA2 + SUM2                                         00016208
    BETA(I,L) = BRAKET*DPSIT(L) - DPSIZ(L)*BRAKET*(DERIVD(L) + 00016900
X    DIFF(L)*(-1./(H(L)*1.E+05) + BRAKET*DPSIZ(L)))             00017000
X    - DIFF(L)*BRAKET*D2PSIZ(L) - DIFF(L)*(DPSIZ(L)**2 )*(-(I-1)/ 00017100
X    (PSI(L,2)**2 ) + I/((PSI(L,2) + 1.))**2 ))                00017200
X    + SUMA1 + P1001(L)*NU(L)*N2Z(L)*((2.*I - 1.)*PSI(L,2) + I -1.) 00017300
X    + RATEOE(L)*((I-1)*EXP(THETA/TZZ(L)) + (I-1) + 1.))      00017301
    IF (I.EQ.1) GO TO 7000                                       00017400
    IF (I.EQ.6) GO TO 8000                                       00017500
    GAMMA (I,L) = SUMA2 - BETA(I,L) + P1001(L)*NU(L)*N2Z(L)*(( 00017600
X    2.*I - 1.)*PSI(L,2) + I - 1. + (I-1.)*PSI(L,2)*PHI(I-1,L) 00017700
X    *EXP(THETA/TV(L,2)) + I*(PSI(L,2) + 1.)*PHI(I+1,L)         00017800
X    *EXP(-THETA/TV(L,2)))                                       00017900
X    + RATEOE(L)*((I-1)*EXP(THETA/TV(L,2))*(PHI(I-1,L) + 1.) + 00017901
X    I*EXP(THETA/TZZ(L) - THETA/TV(L,2))*(PHI(I+1,L) + 1.))    00017902
    GO TO 4500                                                    00018000
7000 GAMMA(I,L) = SUMA2 - BETA(I,L) + P1001(L)*NU(L)*N2Z(L)*(( 00018100
X    2.*I - 1.)*PSI(L,2) + I - 1. + I*(PSI(L,2) + 1.)*PHI(2,L) 00018200
X    *EXP(-THETA/TV(L,2)))                                       00018300
X    + RATEOE(L)*EXP(THETA/TZZ(L) - THETA/TV(L,2))*(PHI(2,L) + 1.) 00018301
    GO TO 4500                                                    00018400
8000 GAMMA(I,L) = SUMA2 - BETA(I,L) + P1001(L)*NU(L)*N2Z(L)*(( 00018500
2 X    2.*I - 1.)*PSI(L,2) + I - 1. + (I - 1.)*PSI(L,2)*PHI(I-1,L) 00018600
X    *EXP(THETA/TV(L,2)))                                       00018700
X    + RATEOE(L)*((I-1)*EXP(THETA/TV(L,2))*(PHI(I-1,L) + 1.)) 00018701
4500 CONTINUE                                                    00018800
    C1(I,L) = A(L) +ALPHA(I,L)*EDEL T/(2.*DELZ*LINC*1.E+05)    00018900
    C2(I,L) = 1. - 2.*A(L) -BETA(I,L)*EDEL T                   00019000
    C3(I,L) = A(L) -ALPHA(I,L)*EDEL T/(2.*DELZ*LINC*1.E+05)    00019100
    C(I,L) = C1(I,L)*PHI(I,L+LINC)+C2(I,L)*PHI(I,L)+ C3(I,L)    00019200
X    *PHI(I,L-LINC)+GAMMA(I,L)*EDEL T                           00019300
C  CALCULATION OF EC(I,L) AND F(I,L) COEFFICIENTS.             00019400
    DENOM = B(L) - A(L)*EC(I,L-LINC)                             00019500
    EC(I,L) = A(L)/DENOM                                         00019600
    F(I,L) = (C(I,L) + A(L)*F(I,L-LINC))/DENOM                  00019700
4000 CONTINUE                                                    00019800
C  CALCULATION OF PHI.                                          00019900

```

```

      IF (LBOUND.EQ.1) GO TO 4300
      DO 4301 IL=1,6
      NBOLT(IL,LBOUND) = N2Z(LBOUND)*(1./(PSI(LBOUND,2) + 1.))*
X      ((PSI(LBOUND,2)/(PSI(LBOUND,2) + 1.))* (IL - 1))
4301 EPSIL(IL,LBOUND) = 0.
      GO TO 4400
4300 NBOLT(1,1) = N2Z(1)
      NBOLT(2,1) = 0.
      NBOLT(3,1) = 0.
      NBOLT(4,1) = 0.
      NBOLT(5,1) = 0.
      NBOLT(6,1) = 0.
      EPSIL(1,1) = 0.
      EPSIL(2,1) = 0.
      EPSIL(3,1) = 0.
      EPSIL(4,1) = 0.
      EPSIL(5,1) = 0.
      EPSIL(6,1) = 0.
4400 DO 4600 II=1,6
      PHI(II,LLMAX) = F(II,LLMAX)/(1. - EC(II,LLMAX))
      PHI(II,LMAX) = PHI(II,LLMAX)
      NBOLT(II,LLMAX) = N2Z(LLMAX)*(1./(PSI(LLMAX,2) + 1.))
X      *((PSI(LLMAX,2)/(PSI(LLMAX,2) + 1.))* (II-1))
      NBOLT(II,LMAX) = N2Z(LMAX)*(1./(PSI(LMAX,2) + 1.))
X      *((PSI(LMAX,2)/(PSI(LMAX,2) + 1.))* (II - 1))
      EPSIL(II,LLMAX) = PHI(II,LLMAX)*NBOLT(II,LLMAX)
      EPSIL(II,LMAX) = PHI(II,LMAX)*NBOLT(II,LMAX)
      LLLMAX = LMAX - 2*LINC
      DO 4700 LL=LINCPI,LLLMAX,LINC
      NN = LMAX - LINC + LBOUND - LL
      PHI(II,NN) = EC(II,NN)*PHI(II,NN+LINC)+F(II,NN)
      NBOLT(II,NN) = N2Z(NN)*(1./(PSI(NN,2) + 1.))
X      *((PSI(NN,2)/(PSI(NN,2) + 1.))* (II-1))
4700 EPSIL(II,NN) = PHI(II,NN)*NBOLT(II,NN)
4600 CONTINUE
C  WRITE RESULTS TO TAPE
      WRITE (11) MMM(3),DELT1(3),LBOUND,DELZ,DELZ1,LINC,(Z(ILN),
X      N2Z(ILN),TV(ILN,2),(I,PHI(I,ILN),EPSIL(I,ILN),
X      NBOLT(I,ILN),I=1,6,1),ILN=LBOUND,LMAX,LINC)
      IF (MMN(2).NE.MMMT) GO TO 3500
      DO 5200 NN=LBOUND,LMAX,LINC
      SUME1 = 0.
      SUME2 = 0.
      DO 5100 IK=1,6
      SUME = EPSIL(IK,NN)

```

```

SUMEI = EPSIL(IK,NN)*(IK-1)                                00024400
SUME1 = SUME1 + SUMEI                                      00024500
5100 SUME2 = SUME2 + SUMEI                                  00024600
    SUME1A(NN) = SUME1                                      00024700
    SUME2A(NN) = SUME2                                      00024800
    IF (NN.EQ.LBOUND) GO TO 5200                            00024900
    DO 5200 IK=1,6                                           00025000
    REPSIL(IK,NN) = SUME1A(NN)/EPSIL(IK,NN)                 00025100
5200 CONTINUE                                                00025200
    MMT = MMT + MMTIN                                       00025400
91  FORMAT ('1',2X,'C1(I,L)',2X,'C2(I,L)',2X,'C3(I,L)',5X,'C(I,L)', 00025500
X      2X,'GAMMA(I,L)',1X,'ALPHA(I,L)',1X,'BETA(I,L)', 00025600
X      4X,'A(L)',4X,'B(L)',5X,'EC(I,L)',4X,'F(I,L)') 00025700
    DO 4900 IJK=1,6                                         00025800
    WRITE (6,91)                                             00025900
    WRITE (6,92)(C1(IJK,L),C2(IJK,L),C3(IJK,L),C(IJK,L),GAMMA(IJK,L), 00026000
X      ALPHA(IJK,L),BETA(IJK,L),A(L),B(L),EC(IJK,L),F(IJK,L), 00026100
X      L=LINCP1,LLMAX,LINC)                                00026200
92  FORMAT (' ',1P11E10.3)                                  00026300
    WRITE (6,93)                                             00026400
93  FORMAT ('0',2X,'DPSIT',5X,'DERIVD',4X,'DPSIZ',5X,'D2PSIZ',8X 00026500
X      , 'DIFF',5X,'H',8X,'P1001',4X,'NU') 00026600
    WRITE (6,94) (DPSIT(L),DERIVD(L),DPSIZ(L),D2PSIZ(L),DIFF(L),H(L) 00026700
X      ,P1001(L),NU(L),L=LINCP1,LLMAX,LINC) 00026800
94  FORMAT (' ',1P8E10.3)                                   00026900
    WRITE (6,37)                                             00027000
37  FORMAT ('0',2X,'MMM',1X,'LEVEL',3X,'DELT',3X,'EDELT') 00027100
    WRITE (6,35) MMM(3),IJK,DELT,EDELT                     00027200
35  FORMAT ('0',2X,I4,3X,I3,3X,F5.0,3X,F5.0)               00027300
    WRITE (6,34)                                             00027400
34  FORMAT ('0',2X,'ALT',2X,'T',4X,'TV', 00027500
X      9X,'N(N2)',8X,'PSI',11X,'PHI',8X,'SUM EPSILON', 00027600
X      3X,'SUM I*EPSILON',3X,'EPSILON',4X,'BOLTDEN',3X,'REPSIL') 00027700
4900 WRITE (6,36) (Z(IKN),TZZ(IKN),TV(IKN,2), 00027800
X      N2Z(IKN),PSI(IKN,2),PHI(IJK,IKN),SUME1A(IKN), 00027900
X      SUME2A(IKN),EPSIL(IJK,IKN),NBOLT(IJK,IKN),REPSIL(IJK,IKN), 00028000
X      IKN=LBOUND,LMAX,LINC)                                00028100
36  FORMAT (' ',0PF5.0,0P2F6.0,1P5E14.6,1P3E12.3)         00028200
C  CONSTRUCITON OF PRINTER PLOTTER ARRAYS.                 00028300
    DO 4800 JJ=LBOUND,LMAX                                00028400
    ALPHI1(JJ) = PHI(1,JJ)                                  00028500
    ALPHI2(JJ) = PHI(2,JJ)                                  00028600
    ALPHI3(JJ) = PHI(3,JJ)                                  00028700
    ALPHI4(JJ) = PHI(4,JJ)                                  00028800
    ALPHI5(JJ) = PHI(5,JJ)                                  00028900

```

4800 ALPHI6(JJ) = PHI(6,JJ)	00029000
C PRINTER PLOTTING.	00029100
WRITE (6,29)	00029200
29 FORMAT ('1',43X,'DEVIATION VERSUS ALTITUDE')	00029300
XR = 1000.	00029400
XL = 0.	00029500
YT = +14.	00029600
YB = -6.	00029700
NUMPR1 = LMAX + 1	00029800
CALL PLOT2(GRID,XR,XL,YT,YB)	00029900
CALL PLOT3('1',Z,ALPHI1,NUMPR1)	00030000
CALL PLOT3('2',Z,ALPHI2,NUMPR1)	00030100
CALL PLOT3('3',Z,ALPHI3,NUMPR1)	00030200
CALL PLOT3('4',Z,ALPHI4,NUMPR1)	00030300
CALL PLOT3('5',Z,ALPHI5,NUMPR1)	00030400
CALL PLOT3('6',Z,ALPHI6,NUMPR1)	00030500
CALL PLOT4(3,'PHI')	00030600
WRITE (6,30)	00030700
30 FORMAT ('0',59X,'ALTITUDE (KM.)')	00030800
3500 IF (MMM(2).LT.MMMAX) GO TO 3900	00030900
END FILE 11	00031000
STOP	00031100
90000 WRITE (6,33)	00031200
33 FORMAT ('1','END OF FILE ENCOUNTERED ON CARD READER')	00031300
STOP	00031400
90001 WRITE (6,84)	00031500
84 FORMAT ('1','END OF FILE ENCOUNTERED ON INPUT TAPE')	00031600
STOP	00031700
90002 WRITE (6,85)	00031800
85 FORMAT ('1','IO ERROR ENCOUNTERED ON INPUT TAPE')	00031900
STOP	00032000
90003 WRITE (6,86)	00032100
86 FORMAT ('1','ISTART IS LESS THAN OR EQUAL TO THE FIRST TIME	00032200
X STEP AVAILABLE')	00032300
STOP	00032400
END	00032500

## REACTRAT

```

C   THIS PROGRAM CALCULATES THE REACTION RATES FOR ION-ATOM          00000100
C   INTERCHANGE BETWEEN O PLUS AND N2.                               00000200
C   THE POPULATION OF THE VIBRATIONALLY EXCITED LEVELS              00000300
C   OF N2 AND THE VIBRATIONAL TEMPERATURE COME FROM                 00000400
C   THE OUTPUT TAPE OF PROGRAM BOLTDEV.                               00000500
C   REAL * 4 NI, N2Z, NBOLT,KBOLT,KEFF,KVIBL,NLTOT,KPRIM            00000600
C   LOGICAL * 1 IMAGE(5151)                                           00000700
C   DIMENSION Z(89), N2Z(89),PHI(6,89),TV(89),EPSIL(6,89)          00000800
C   X ,NBOLT(6,89),KBOLT(89), KEFF( 89),RATIOK(21),KVIBL(6)         00000900
C   X ,ILEVEL(6),TAUN (89),ALKBOL(21),ALKEFF(21),II(6),NLTOT(6,89) 00001000
C   X ,TAUB(89),TAUE(89),ALTAUB(21),ALTAUE(21),ALTAUN(21)          00001100
C   X ,ARRAY(21),ARRAY1(21),GRID(8281)                               00001200
C DATA INPUT                                                         00001300
C   READ (5,12,END=90000) DELZ,ZUPPER,DELT,TIMEX,MMMTIN,LINC,TINC. 00001400
C   X ,LBOUND,TINC2                                                  00001500
C 12 FORMAT (F4.0,F5.0,F6.0,F7.0,I4,4I3)                             00001600
C   WRITE (6,13)DELZ,ZUPPER,DELT,TIMEX,MMMTIN,LINC,TINC            00001700
C   X ,LBOUND,TINC2                                                  00001800
C 13 FORMAT ('O',F4.0,F5.0,F6.0,F7.0,I4,4I3)                         00001900
C   READ (5,14,END=90000) DII,TI,NI,ENU,TOO                         00002000
C 14 FORMAT (F6.4,F6.0,E13.7,F5.3,F5.0)                             00002100
C   WRITE (6,15) DII,TI,NI,ENU,TOO                                  00002200
C 15 FORMAT ('O',F6.4,F6.0,E13.7,F5.3,F5.0)                         00002300
C   READ (5,16,END=90000) (ILEVEL(N),KVIBL(N),N=1,6)               00002400
C 16 FORMAT (6(I2,E9.1))                                             00002500
C   WRITE (6,17) (ILEVEL(N),KVIBL(N),N=1,6)                         00002600
C 17 FORMAT(' ',I2,E9.1)                                             00002700
C   LMAX = 1. + (ZUPPER - 120.)/DELZ                                00002800
C   READ (5,18,END=90000) INCRMT,KPRIM,IPR                           00002900
C 18 FORMAT(I6,E9.1,I6)                                              00003000
C   WRITE (6,19) INCRMT,KPRIM,IPR                                    00003100
C 19 FORMAT (' ',I6,1PE9.1,I6)                                       00003200
C   READ (10,END=90001,ERR=90002) MMM,DELT1,LBOUND,DELZ            00003300
C   X ,DELZ1,LINC,(Z(ILN),N2Z(ILN),TV(ILN),(II(I),                00003400
C   X   PHI(I,ILN),EPSIL(I,ILN),NBOLT(I,ILN),I=1,6,1),ILN=        00003500
C   X   LBOUND,LMAX,LINC)                                           00003600
C   ITEST = MMM                                                       00003700
C   JMAX = INCRMT - 1                                                 00003800
C   DO 1000 M=1,10000,INCRMT                                         00003900
C   DO 1500 L=LBOUND,LMAX,LINC                                       00004000
C   SUM1 = 0.                                                         00004100
C   SUM2 = 0.                                                         00004200
C   DO 2000 J=1,6                                                     00004300
C   NLTOT(J,L) = NBOLT(J,L) + EPSIL(J,L)                            00004400
C   A = (KVIBL(J) - KPRIM)*NBOLT(J,L)                               00004500

```

```

      B = KVIBL(J)*EPSIL(J,L)                                00004600
      SUM1 = SUM1 + A                                          00004700
2000  SUM2 = SUM2 + B                                          00004800
      TAUINV = SUM1 + KPRIM*N2Z(L)                             00004900
      TAUB(L) = 1./TAUINV                                     00005000
      TAUE(L) = 1./(TAUINV + SUM2)                             00005100
      TAUN (L) = 1./(1.3E-12*N2Z(L))                          00005200
      KBOLT(L) = KPRIM + SUM1/N2Z(L)                          00005300
      KEFF(L) = KBOLT(L) + SUM2/N2Z(L)                        00005400
      RATIOK(L) = KEFF(L)/KBOLT(L)                            00005500
      ALTAUB(L) = ALOG10(TAUB(L))                             00005600
      ALTAUE(L) = ALOG10(TAUE(L))                             00005700
      ALTAUN(L) = ALOG10(TAUN (L))                            00005800
      ALKBOL(L) = ALOG10(KBOLT(L))                            00005900
      ALKEFF(L)= ALOG10(KEFF(L))                              00006000
1500  CONTINUE                                                00006100
C    WRITE RESULTS TO TAPE.                                   00006200
      WRITE (11) MMM,DELT1,LBOUND,DELZ,DELZ1                 00006300
      X    ,LINC,(Z(ILN),N2Z(ILN),TV(ILN),TAUB(ILN),         00006400
      X    TAUE(ILN),KBOLT(ILN),KEFF(ILN),RATIOK(ILN),       00006500
      X    (II(I), NBOLT(I,ILN),EPSIL(I,ILN),NLTOT(I,ILN),  00006600
      X    I=1,6,1),ILN=LBOUND,LMAX,LINC)                   00006700
      IF (MMM.NE.ITEST) GO TO 5000                            00006800
      ITEST = ITEST + IPR                                     00006900
      WRITE (6,20)                                             00007000
20  FORMAT ('1',1X,'MMM IS ')                                00007100
      WRITE (6,21) MMM                                         00007200
21  FORMAT ('+',9X,I6)                                         00007300
      WRITE (6,50)                                             00007400
50  FORMAT ('0',2X,'ALT',4X,'TV',4X,'N(N2)',9X,'KBOLT'9X,   00007500
      X    'KEFF',11X,'RATIOK',7X,'TAUN',10X,'TAUB',11X,'TAUE') 00007600
      WRITE (6,51) (Z(ILN),TV(ILN),N2Z(ILN),KBOLT(ILN),KEFF(ILN), 00007700
      X    RATIOK(ILN),TAUN(ILN),TAUB(ILN),TAUE(ILN),ILN=LBOUND,LMAX,LINC) 00007800
51  FORMAT ('0',OPF5.0,OPF6.0,1P7E14.6)                     00007900
C    PRINTER PLOT.                                           00008000
      XR = 1000.                                              00008100
      XL = 0.                                                  00008200
      YT = 11.                                                 00008300
      YB = 1.                                                  00008400
      NUMPRI = LMAX + 1                                       00008500
      DO 3000 N=1,6                                           00008600
      DO 3100 LL=LBOUND,LMAX,LINC                             00008700
      IF (LL.GE.2) GO TO 3105                                  00008800
      ARRAY(LL) = 1.                                          00008900
      ARRAY1(LL) = 1.                                         00009000

```

	GO TO 3100	00009100
3105	ARRAY(LL) = ALOG10(NBOLT(N,LL))	00009200
	ARRAY1(LL) = ALOG10(NLTOT(N,LL))	00009300
3100	CONTINUE	00009400
	WRITE (6,22)	00009500
22	FORMAT ('1',40X,'DENSITIES VERSUS ALTITUDE FOR')	00009600
	WRITE (6,23) N	00009700
23	FORMAT ('+',71X,I2)	00009800
	CALL PLOT2(GRID,XR,XL,YT,YB)	00009900
	CALL PLOT3('*',Z,ARRAY,NUMPR1)	00010000
	CALL PLOT3('+',Z,ARRAY1,NUMPR1)	00010100
	CALL PLOT4(27,'LOG NUMBER DENSITY (CM**-3)')	00010200
	WRITE (6,24)	00010201
24	FORMAT ('0',59X,'ALTITUDE (KM.)')	00010300
3000	CONTINUE	00010400
	WRITE (6,25)	00010500
25	FORMAT ('1',40X,'REACTION RATES VERSUS ALTITUDE')	00010600
	YT = -9.	00010700
	YB = -14.	00010800
	CALL PLOT2(GRID,XR,XL,YT,YB)	00010900
	CALL PLOT3('*',Z,ALKBOL,NUMPR1)	00011000
	CALL PLOT3('+',Z,ALKEF,NUMPR1)	00011100
	CALL PLOT4(35,'LOG REACTION RATE (CM**3 SEC**-1)')	00011200
	WRITE (6,24)	00011300
	YT = 1.5	00011400
	YB = 0.5	00011500
	WRITE (6,26)	00011600
26	FORMAT ('1',40X,'RATIO OF REACTION RATES')	00011700
	CALL PLOT2(GRID,XR,XL,YT,YB)	00011800
	CALL PLOT3('*',Z,RATIOK,NUMPR1)	00011900
	CALL PLOT4(20,'RATIO OF KEFF/KBOLT')	00012000
	WRITE (6,24)	00012100
	YT = 5.	00012200
	YB = 0.	00012300
	WRITE (6,27)	00012400
27	FORMAT ('1',40X,'ELECTRON LOSS TIME CONSTANT')	00012500
	CALL PLOT 2(GRID,XR,XL,YT,YB)	00012600
	CALL PLOT3('*',Z,ALTAUB,NUMPR1)	00012700
	CALL PLOT3('+',Z,ALTAUE,NUMPR1)	00012800
	CALL PLOT3('N',Z,ALTAUN,NUMPR1)	00012900
	CALL PLOT4(24,'LOG TIME CONSTANT (SEC.)')	00013000
5000	IF (INCR TM.EQ.1) GO TO 5500	00013100
	DO 5500 JJ=1,JMAX	00013200
	READ (10,END=90001,ERR=90002)	00013300
5500	CONTINUE	00013400



```

      READ (10,END=90001,ERR=90002) MMM,DELT1,LBOUND,DELZ
X      ,DELZ1,LINC,(Z(ILN),N2Z(ILN),TV(ILN),(II(I),
X      PHI(I,ILN),EPSIL(I,ILN),NBOLT(I,ILN),I=1,6,1),ILN=
X      LBOUND,LMAX,LINC)
1000 CONTINUE
      END FILE 11
      STOP
90000 WRITE (6,33)
      33 FORMAT ('1','END OF FILE ENCOUNTERED ON CARD READER')
      STOP
90001 WRITE (6,84)
      84 FORMAT ('1','END OF FILE ENCOUNTERED ON INPUT TAPE')
      STOP
90002 WRITE (6,85)
      85 FORMAT ('1','IO ERROR ENCOUNTERED ON INPUT TAPE')
      STOP
      END

```

```

00013500
00013600
00013700
00013800
00013900
00014000
00014100
00014200
00014300
00014400
00014500
00014600
00014700
00014800
00014900
00015000
00015100

```

0152 CA